Inaugural dissertation

for

obtaining the doctoral degree

of the

Combined Faculty of Mathematics, Engineering and Natural Sciences

of the

Ruprecht - Karls - University

Heidelberg

Presented by

M.Sc. Jiaxin Zhong

born in: Guangdong, China

Oral examination: 25 July 2023

Stress-induced degradation of inulin in *Cichorium intybus*: Exploring the transcriptional regulation of Fructan 1-exohydrolases

Referees: Prof. Dr. Thomas Rausch

Prof. Dr. Rüdiger Hell

Abstract

The preservation of the polyfructan inulin, a valuable commercial product obtained from chicory during the harvest season is severely hampered by its degradation due to low temperatures in late autumn. The degradation process is primarily attributed to the activity of fructan exohydrolases (1-FEH1, 1-FEH2a, and 1-FEH2b). However, the upregulation mechanism of *1-FEH* genes in response to cold has remained poorly understood. This thesis endeavors to explore the roles of different transcription factors responsible for regulating the expression of *1-FEH* genes and seeks to uncover the underlying transcription regulatory network allowing *1-FEH* genes to respond to environmental cues. Thus, the overall aim of this thesis is to shed light on the complex transcriptional regulation of *1-FEH* genes and thereby to provide direction for future chicory breeding efforts.

The primary objective of the initial part of this thesis was to investigate the variation in expression levels of the three isoforms of *1-FEH*s in mature taproots and young seedlings subjected to a detailed time course of cold treatment. The qRT-PCR results indicate that *1-FEH1* exhibited a prolonged and consistent cold-induced up-regulation whereas *1-FEH2a* and *1-FEH2b* were rapidly but only transiently up-regulated within the initial 24 hours following exposure to low temperatures; interestingly, expression of *1-FEH* genes was also affected by heat stress and water deficiency. A co-expression analysis conducted in this study identified a set of cold-inducible transcription factors, namely CiNAC5, CiDREB1A/C/D, and CiDREB2A. Further investigations using the dual luciferase assay, promoter deletion analysis, electrophoretic mobility shift assay (EMSA) and yeast-two-hybrid revealed that i) CiNAC5 specifically activates the promoter region (-353 to ATG) of *p1-FEH1*; ii) CiDREB2A was identified as a key regulator of *1-FEH2b*, which responds to a range of stress conditions by binding to the DRE *cis*-element located on the *1-FEH2b* promoter; iii) CiDREB2B has been found to bind to CiMYB5 (yeast-two-hybrid), resulting in a synergistic upregulation of *1-FEH2b* (dual luciferase assay) and offering an explanation for the strong up-regulation of *1-FEH2b* under heat stress; iv) the identification of a single nucleotide polymorphism (SNP) located on the DRE *cis*-element within the promoter region of *p1-FEH2a* was observed, which resulted in the inability of the promoter to be recognized and activated by CiDREB1 and CiDREB2.

Furthermore, this thesis established a CRISPR RNP delivery system and a chicory protoplast regeneration method, which will facilitate future research on the individual functions of *1-FEH1* and *1-FEH2*. By identifying the transcription factors involved in regulating *1-FEH* genes, this thesis offers valuable insights into the mechanisms underlying the regulation of *1-FEH*s and may have significant implications for the commercial production of inulin in chicory.

Zusammenfassung

Inulin, ein wertvolles, aus Zichorien gewonnenes Produkt, unterliegt während der Erntesaison bei niedrigen Temperaturen einem starken Abbau. Dieser Abbauprozess wird in erster Linie auf die Aktivität von Fructan-Exohydrolasen (1-FEH1, 1-FEH2a und 1-FEH2b) zurückgeführt. Der Mechanismus der Hochregulierung von *1-FEH*s als Reaktion auf Kälte ist jedoch noch unzureichend aufgeklärt. In dieser Arbeit sollen Transkriptionsfaktoren untersucht werden, die für die Regulation von *1-FEH*s verantwortlich sind. Außerdem soll die Reaktion des zugrundeliegenden Transkriptionsregulationsnetzwerks von *1-FEH*s auf Umweltreize verstanden werden. Ziel dieser Arbeit ist es, die Regulation von *1-FEH*s aufzuklären und so auch Ansätze für die zukünftige Züchtung von Chicorée zu geben.

Das Hauptziel des ersten Teils dieser Arbeit bestand darin, die Unterschiede der Expressionsniveaus der drei Isoformen von *1-FEH*s in reifen Speicherwurzeln und jungen Sämlingen während Kältebehandlung zeitlich detailliert zu untersuchen. Die qRT-PCR-Ergebnisse zeigen, dass *1-FEH1* eine lang anhaltende und konsistente Reaktion auf Kälte zeigt, während *1-FEH2a* und *1-FEH2b* innerhalb der ersten 24 Stunden nach der Kälte-Exposition schnell aber nur vorübergehend hochreguliert werden. Darüber hinaus wurde eine Reaktion der *1-FEH*s auf Hitzestress und Wassermangel beobachtet. Die in dieser Studie durchgeführte Ko-Expressionsanalyse identifizierte eine Reihe von kälteinduzierbaren Transkriptionsfaktoren, nämlich CiNAC5, CiDREB1A/C/D und CiDREB2A. Weitere Untersuchungen unter Verwendung eines dualen Luziferase-Assays, einer Promotor-Deletionsanalyse, Electrophoretic Mobility Shift Assay (EMSA) und Hefe-Zwei-Hybrid-System ergaben, dass i) CiNAC5 spezifisch die Promotorregion (-353 bis ATG) von *p1-FEH1* aktiviert; ii) CiDREB2A als ein Schlüsselregulator von *1-FEH2b* identifiziert wurde, der auf eine Reihe von Stressbedingungen reagiert, indem er an das DRE *cis*-Element am *1-FEH2b*-Promotor bindet; iii) wurde festgestellt, dass CiDREB2B mit CiMYB5 interagiert, was zu einer synergistischen Hochregulierung von *1-FEH2b* als Reaktion auf Hitzestress führt; iv) wurde ein Einzelnukleotid-Polymorphismus (SNP) identifiziert, der sich auf dem DRE *cis*-Element innerhalb der Promotorregion von *p1-FEH2a* befindet, was dazu führte, dass der Promotor nicht erkannt und von CiDREB aktiviert werden konnte.

Darüber hinaus wurden im Rahmen dieser Arbeit ein CRISPR-RNP-Übertragungssystem und eine Methode zur Regeneration von Chicorée-Pflanzen aus Protoplasten entwickelt, die die künftige Erforschung der individuellen Funktionen von *1-FEH1* und *1-FEH2* erleichtern werden. Durch die Identifizierung der Transkriptionsfaktoren, die an der Regulierung von *1-FEH*s beteiligt sind, bietet diese Arbeit wertvolle Einblicke in die Mechanismen, die der Regulierung von *1-FEH*s zugrunde liegen, und könnte einen erheblichen Beitrag für die kommerzielle Produktion von Inulin aus Chicorée haben.

Table of Contents

1 Introduction

1.1 Fructan

1.1.1 Fructan structure and metabolism in plants

Fructan is a type of oligosaccharide or polysaccharide in which fructosyl units are polymerized to one molecular sucrose by β (2→1) linkage or β (2→6) linkage (Yoshida 2021). Instead of using starch as long-term reserve carbohydrates, fructan is accumulated as principal stored forms of energy in 15% of higher plants (Hendry 1993), such as in *Asparagaceae*, *Asteraceae*, *Boraginaceae*, *Campanulaceae*, *Liliaceae*, and *Triticeae*. Fructan is mainly synthesized in the vacuole by fructosyltransferase. Furthermore, fructan is found to be present in the apoplast, as well as in phloem and xylem tissues (Livingston III and Henson 1998; Silva et al. 2015; Wang and Nobel 1998). According to the position between fructose and glucose and the type of linkage between fructosyl residues, fructan can be classified into the following groups (Fig. 1.1).

Inulin is a linear fructan consisting of fructosyl units bound to the fructose portion of sucrose via a β (2→1) linkage. It is found in chicory roots (*Cichorium intybus*), Jerusalem artichoke tubers (*Helianthus tuberosus*) as well as globe artichoke inflorescence (*Cynara cardunculus*) (Redondo-Cuenca et al. 2021). The biosynthesis of inulin starts with the 1-SST (sucrose: sucrose 1-fructosyltransferase) which transfers fructose from one molecular of sucrose to another and generates 1-kestose and one glucose. The elongation of inulin is facilitated by 1-FFT (fructan: fructan 1-fructosyltransferase) by transferring fructose from a fructan to another fructan, which modifies the degree of polymerization (DP) of inulin. Inulin degradation is caused by the activity of 1-FEH (fructan 1-exohydrolase) which removes a terminal fructose from a fructan and produces sucrose as a final product. Neo-inulin is similar to inulin and consists of fructose polymerization via β (2→1) linkage and additionally contains a fructose bound to the glucose in sucrose via β (2→6) linkage. This type of fructan is found in Aloe vera (*Aloe barbadensis*) (Salinas et al. 2016). Neo-inulin can be catalyzed by 6G-FFT (fructan: fructan 6G-fructosyltransferase) which transfers a fructose to the glucose portion of sucrose or 1-kestose.

Levan-type of fructan is generally referring to a fructan in which fructose polymerized by a β (2→6) linkage bound to the fructose in sucrose. The β (2→6) linkage fructose is extended by 6-SFT (sucrose: fructan 6-fructosyltransferase) in fructan. Linear levan can be identified in plants belonging to the *Poaceae* family, such as wheat (*Triticum aestivum*) and barley (*Hordeum vulgare*), as well as in temperate grasses such as orchardgrass (*Dactylisglomerata*) and perennial ryegrass (*Lolium perenne*) (Yoshida 2021). Many plants produce levan as main frame but at the same time with β (2→1) linked fructose as side chain, to accumulate complex branched fructan in the tissue. This branched type of levan that contains both β (2→1) and β (2→6) linkage is known as graminan, which can be found in tissues of winter wheat (*Triticum aestivum*) (Kawakami and Yoshida 2012).

Agavin is a new class of neofructans which was first described in *Agava tequilana* (Mancilla-Margalli and Lopez 2006) and commonly found in *Agave* species (Pérez-López and Simpson 2020). This type of fructan is so far the most complex forms of plant fructan that have been discovered, as it comprises three possible linkages of neo-type fructan.

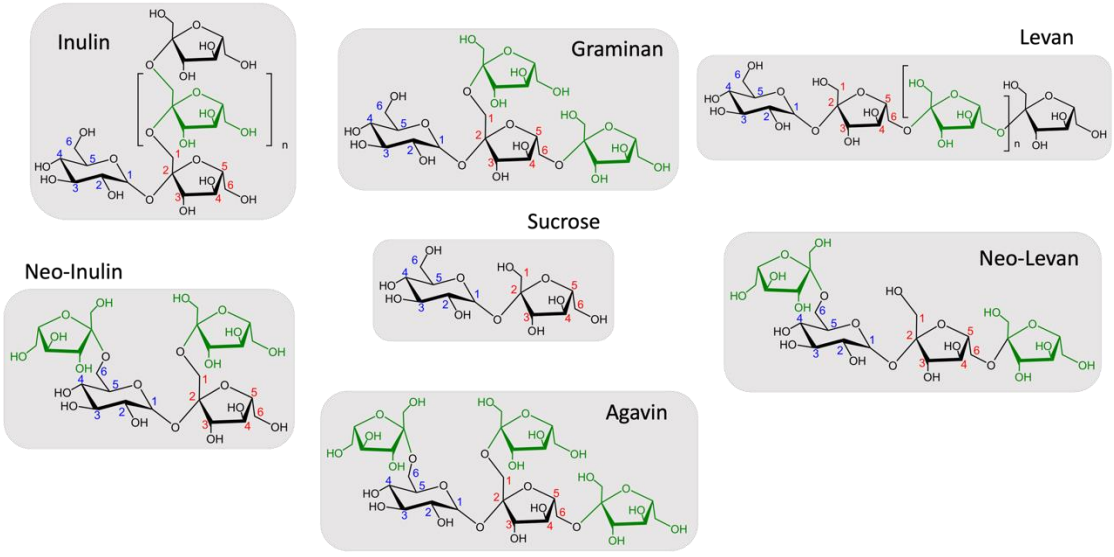

Figure 1.1 Fructan structure. Fructan is classified based on the type of linkage between fructosyl residues and sucrose. Inulin type fructan contains β (2→1) linkage of fructosyl units. Levan type fructan contains β (2→6) linkage of fructosyl units. Neo-type fructan consist of fructose bounds to the glucose in sucrose via β (2→6) linkage.

1.1.2 Fructan metabolism in response to abiotic stress

Plants are well known to accumulate soluble sugar content to increase freezing tolerance when exposed to cold stress (Tarkowski and Van den Ende 2015). Many overwintering plants in northern regions accumulate fructan under cold conditions as a source of energy for winter survival and degrade fructan for germination and regeneration in spring (Yoshida 2021). In Perennial ryegrass, researchers found fructan composition changed and low-DP fructan induced during cold acclimatation, with the observation of fructan accumulation and depolymerization simultaneously (Abeynayake et al. 2015). Fructan contributes to freezing tolerance by inserting between polar headgroups and increasing the stability of biomembranens. Inulin-type of fructan might insert into lipid bilayers and make hydrogen bonds with the phosphate groups to prevent crystallization and damage of the membrane (Valluru et al. 2008). In addition to their cold tolerance contribution, fructan also play an important role in plant response to osmotic stress. By overexpressing fructan synthetase genes, tobacco (*Nicotiana tabacum*) exhibited enhanced PEG-simulated drought stress tolerance (Sun et al. 2020). In wheat (*Triticum aestivum*), a greater fructan content has been found in a higher drought-resistance cultivar, where fructan synthesis occurs during early stages of drought stress while degradation occurs later (Hou et al. 2018). Previous results suggested that fructan played a crucial role in wheat seedlings against drought stress, presumably through the increasement of reactive oxygen species (ROS) scavenging and the maintenance of lipid peroxidation status (Nemati et al. 2018; Peshev et al. 2013). Implementing exogenous nitric oxide on *Lolium perenne* induced fructan synthesis enzyme activity and increased fructan content, which possibly leaded to maintaining ROS homeostasis and mitigating oxidative stress under water stress condition (Rigui et al. 2019). As a part of the antioxidant system, fructan was converted into less harmful fructan radical in the process of scavenging aggressive •OH and •OOH radicals (Bolouri-Moghaddam et al. 2010). The association between fructan and ROS is relevant to plant antipathogenic activity. Fructan prime ROS dynamic and strengthen *Botrytis cinerea* resistance in *Arabidopsis* and chicory (Versluys et al. 2022; Van Rensburg et al. 2020). In snow mold-resistant wheat cultivars, it has been observed a higher accumulation and slower metabolize fructan in comparison with snow mold-susceptible cultivars (Kawakami and Yoshida 2012).

1.1.3 Crosstalk between fructans and phytohormones

Previous studies have shown that fructan metabolism varied at different stages of plant development and in response to various environments. Sequence analysis of fructan active enzymes promoters revealed the presence of several *cis*-elements which were considered to mediate auxin or abscisic acid (ABA) response (Michiels et al. 2004; Zhang et al. 2015; Nagaraj et al. 2001). These results have provided a prospect of correlation between developmental signaling and fructan metabolism. This relationship of fructan and growth regulator was rather complex and likely related to the degree of polymerization, structure and position of fructan (Márquez-López et al. 2022).

Auxin is an important type of regulator for plant growth and development. Exogenous auxin increased fructan accumulation in callus of *Symphytum officinale* (Haafl et al. 1991) and plant of *Agave tequilana* (Barreto et al. 2010). Moreover, increasing fructan synthesis enzyme activities were observed in *Lolium perenne* with the treatment of auxin (Gasperl et al. 2016). Recent research in chicory revealed that auxin increased fructan content at low concentration and promoted fructan degradation at high concentration (Mohammadi et al. 2021). On the other hand, ABA levels in the wheat stem were remarkably enhanced under drought condition and significantly relevant to FEH activities (Yang et al. 2004). Under water stress, ABA presumably enhanced fructan hydrolysis in wheat by strongly induced the gene expression and enzymatic activities of 1-FEH and 6-FEH (Xu et al. 2016; Zhang et al. 2020). In perennial ryegrass (*Lolium perenne*), ABA content increased after 1-week cold acclimatation, while the DP of fructan decreased. Additionally, the freezing tolerant genotype presented high content of ABA with low rate of ethylene emission and low degree of fructan polymerization (Jurczyk et al. 2021). According to former discoveries, ethylene played a negative role in fructan biosynthesis. In young chicory seedling, treatment of 1-aminocyclopropane-1-carboxylic acid (ACC, ethylene precursor) repressed expression of *1-SST* and *1-FFT* but increased expression of *1-FEH* (Wei et al. 2016). A redistribution of fructan within the onion bulb was observed with the supplement of ethylene, which delayed sprout emergence and suppressed sprout growth (Ohanenye et al. 2019).

1.2 Chicory: A valuable source of inulin for commercial applications

1.2.1 *Cichorium intybus*

Chicory (*Cichorium intybus* L.) is a perennial plant belonging to the *Asteraceae* family, native to Eurasia and widely cultivated today throughout the world. (Cichota et al. 2020). This species is allogamous for reproduction due to the disorder of a sporophytic self-incompatibility system and the flower morphology is not conducive to self-fertilization in the absence of pollinator (Patella et al. 2019; Barcaccia et al. 2016). Humans have selected chicory cultivars for centuries to produce medical or nutritional compounds, and most currently as livestock feed (Nwafor et al. 2017). According to their purpose and usage, chicory can be divided into four cultigroups: The 'industrial' or 'root' chicory, cultivated in northwestern Europe, India, South Africa and Chile. The utilization of its taproot is mainly for the extraction of inulin and the production of coffee substitute. The 'Brussels' or 'witloof' chicory, cultivated in the same European area, is used to produce etiolated buds or chicons by forcing. The 'leaf' chicory, mainly known as 'Radicchio' in northern Italy, is commonly used as fresh salads or cooked according to the regional tradition. The 'forage' chicory is initially found along roadsides and is considered as weed in many countries. Its use dates back to the mid-1970s to increase the supply of forage for livestock (Cadalen et al. 2010; Barcaccia, et al. 2016).

1.2.2 Inulin function in plants and for humans

The discovery of Inulin dated back to the early 1800s, when inulin was first found in the roots of elecampane (*Inula helenium*) (Shoaib et al. 2016). Inulin is a highly abundant storage fructan in many plants of the *Asteraceae* family such as chicory (*Cichorium intybus*), Jerusalem artichoke (*Helianthus tuberosus*), cardoon (*Cynara cardunculus*) and elecampane (*Inula helenium*) (Redondo-Cuenca et al. 2021). In chicory root, the inulin content could reach 42-76% of dry weight, which made chicory the main source for commercial inulin extraction in industry (Shoaib et al. 2016). In plant, inulin not only serves as storage carbohydrate, but also play an important role in osmotic or freezing stress response. Attributed to the flexible structures, inulin can insert much deeper than levan into membranes and interact with C=O groups to stabilize membrane, preventing cell membrane damage from dehydration and crystallization (Valluru et al. 2008).

The unique property of inulin provides its multiple function in pharmaceutical and food industries. Inulin has been used in drug delivery as a versatile polymer and its membrane stabilization ability was used to stabilize therapeutic proteins (Afinjuomo et al. 2021). In addition, inulin is a suitable dietary fiber and offers prebiotic action in both human and animal, by enhancing the growth and functionality of *Bifidobacterium* bacteria, which further produce short-chain fatty acids in the colon (Tawfick et al. 2022). On the other hand, the low caloric value (1.5 kcal/g or 6.3 kJ/g) of inulin makes it an ideal supplement for food. Inulin dissolves in water to form a creamy and gelatinous structure that can replace fat in foods such as yogurt and ice cream, thereby reducing the fat content (Guven et al. 2005; Akalın et al. 2008).

In manufacturing industry, inulin-rich plants are abundant bioresources to produce FDCA (2,5-furandi-carboxylic acid), which is utilized as a fundamental material for sustainable plastic production (Heo et al. 2021). Furthermore, inulin-rich feedstocks are exploited for the production of bio-renewable fuel such as bioethanol, acetone and butanol (Singh et al. 2022; Lee et al. 2022). Inulin is also used as ingredient in cosmetics due to its antimicrobial protective effect on skin and a great stability of the emulsions formed by the inulin surfactant (Tripodo and Mandracchia 2019; Niziol-Lukaszewska et al. 2019).

1.2.3 Inulin metabolism in chicory

Inulin as the main commercial product from chicory root, its application and value depend on the degree of polymerization, which is affected by the field condition and chicory harvest time. According to the inulin mean polymer length (mDP), yield, gene expression and activity of inulin metabolism related enzymes, the cultivation of chicory in western Europe can be defined into three phases (Van Arkel et al. 2012).

Phase I: During the early stages of taproot development, the biosynthesis of inulin in chicory was catalyzed by two fructosyltransferase 1-SST and 1-FFT. During growing season, the expression of *1-SST* increased sharply at the same time of taproot thickening. Meanwhile, the high photosynthesis rate and the initiation of inulin metabolism resulted in high amounts of storage carbohydrates. The highest level of mDP was reached during this phase, which lasted until mid-September. Phase II: In this period, the temperature dropped below than 10 °C, which induced the gene expression of *1-FEH1*. The yield of inulin continued increasing while the mDP

gradually decreased, which might be the result of the combination of residual polymerization of 1-SST and 1-FFT, and the hydrolysis of 1-FEH1. Phase III: As the temperature continued decreasing, the induction of *1-FEH* leaded to mDP decrease. A high amount of fructose was observed between December and January, which was due to the activities of 1-FEHs degrading inulin by releasing the terminal fructose from the fructan chain.

1.2.4 Chicory fructan 1-exohydrolases play different roles in inulin degradation

Three isoforms of fructan 1-exohydrolases have been identified in chicory, which hydrolyzed the β (2→1) linkages in inulin rather than the β (2→6) linkages in levan (De Roover et al.1999a; Van den Ende et al. 2001). However, several research have revealed the protein properties and functional difference between 1-FEH1 and 1-FEH2. Evolutionary analysis suggested that 1-FEH1 had been evolved from a cell-wall invertase-like ancestor that later obtained a vacuolar targeting signal. *1-FEH1* is highly expressed in cold-induced roots, but only low expression was found in forced roots, which contrasts with *1-FEH2* that is highly expressed in forced roots. In addition, high concentration of sucrose showed more pronounced inhibition on 1-FEH2a than 1-FEH1 (De Roover et al. 1999a), indicating that 1-FEH2 was predominantly responsible to break down fructan when sucrose concentration decreased in vascular during the time of forcing. A strong induction of *1-FEH2* was observed after defoliation treatment in young chicory, while *1-FEH1* was not responsible to defoliation. These results suggested that 1-FEH2 played an important role in chicory survival strategy and was induced when energy demands greatly increased (De Roover et al. 1999b; Van den Ende et al. 2001). The reason for the induction of *1-FEH1* in mature field-grown chicory roots during autumn is still unknown as there appears to be no significant energy demand at that time. More investigation is required to comprehend the mechanisms and reasons behind the evolution of fructan exohydrolases from cell-wall invertases, their specific locations within the plant, and the ways in which they are regulated during various developmental phases.

1.2.5 The regulation of fructan active enzymes (FAZYs)

It has been demonstrated in chicory taproot and wheat kernels that the enzyme activities of fructan active enzymes (FAZYs) are correlated to the gene expression

levels (Van Laere and Van den Ende 2002; Cimini et al. 2015), suggesting that FAZY are mainly regulated at the transcriptional level. Fructan synthesis genes are induced by sugar supplementation and nitrogen deprivation (Kusch, Greiner, et al. 2009; Xue et al. 2011), while fructan exohydrolases genes are induced by low temperature (Michiels et al. 2004) and defoliation (Ende et al. 2001). In chicory, the gene expression and the enzyme activity of 1-SST are corresponded to plant developmental stage (Van Arkel et al. 2012). Another research revealed that drought induced *1-SST* gene expression as well as enzyme activity in roots and leaves of chicory seedlings (Van Laere et al. 2000). Additionally, oligofructans slightly decreased under ACC and cold treatment, correlating with reduced expression of *1-SST* and *1-FFT* (Wei et al. 2016). In previous research, several transcription factors have been identified to be regulators of FAZY. The transcription factor CiMYB17 was involved in the complex regulation of FAZY genes expression in chicory, particularly after the exposure of abiotic stress (Wei et al. 2017). In *Triticum aestivum*, TaMYB13-1 acted as a positive regulator of fructosyltransferase genes and regulated fructan biosynthesis by directly binding to the promoter of fructosyltransferase genes (Kooiker et al. 2013; Xue et al. 2011).

1.3 Potential plant transcription factors relevant for inulin metabolism

1.3.1 AP2/ERF

The AP2/ERF (APETALA2/ethylene-responsive element binding factors) transcription factors are a large group of factors that are mainly found in plants (Feng et al. 2020). Transcription factors from the AP2/ERF family contain either one or two AP2 domains, each consisting of 58 residues, which was function to bind DNA (Agarwal et al. 2017). These domains were first identified in the APETALA2 protein, a floral homeotic protein from *Arabidopsis*. The AP2/ERF super family is generally classified into four major subfamilies: DREB (Dehydration Responsive Element-Binding protein), ERF (Ethylene-Responsive-Element-Binding Factor), AP2 (APETALA2) and RAV (Related to ABI3/VP) (Mizoi et al. 2012). It has been reported that AP2/ERF transcription factors played a crucial role in regulating various aspects of plant development and stress response. In rice (*Oryza sativa*), the AP2/ERF transcription factor LATE FLOWERING SEMI-DWARF (LFS) suppressed the long-day-specific floral repressor gene and therefore induced

flowering under long photoperiodic conditions (Shim et al. 2022). Another research identified the *DUO-B1* gene in wheat (*Triticum aestivum*), which encoded an AP2/ERF transcription factor that regulated spike structure in bread wheat (Wang et al. 2022). AP2/ERFs also participated in the process of fruits ripening by regulating cell wall-modifying genes to remodel cell wall structure and regulating chlorophyl degradation to de-green the fruit color (Zhai et al. 2022). An RNA sequencing study revealed that the expression of AP2-domain-containing regulators were significantly induced in the initial imbibition of seed germination in rice (He et al. 2020). In maize, an AP2/ERF transcription factor, ZmRAP2.7, was demonstrated to be involved in brace roots development (Li et al. 2019). Additionally, recent research identified an AP2-type transcription factor family protein NARROW AND DWARF LEAF1 (NDL1), which mediated leaf development and maintenance of the shoot apical meristem (Kusnandar et al. 2022). Moreover, several members of the AP2/ERF transcription factor superfamily have been identified as playing a role in the response to various stress, including cold, heat, drought, and salinity (Xie et al. 2022; Park et al. 2021; Yu et al. 2022).

1.3.2 DREB

Dehydration responsive element binding (DREB) factors comprise one of the subfamilies of AP2/ERF super family which contains a single AP2 domain. According to Nakano et al. (2006), DREB subfamily could be further divided into six subgroups named as A-1 to A-6. The study of DREBs has provided valuable insights into the molecular mechanisms of plant abiotic stress responses. In *Arabidopsis*, it has been demonstrated that the core sequence of DRE (A/GCCGAC) was essential for highly specific interactions with the DREB proteins (Sakuma et al. 2002). Previous genetic and molecular analyses have found that DREB1 proteins, also known as C-repeat binding factors (CBF), were crucial factors involved in cold acclimation, by regulating *cis*-element on promoters of a subset of cold-regulated (COR) genes (Gilmour et al. 1998; Liu et al. 2019). The expression of *DREB1* was closely linked to temperature fluctuations and regulated by calcium signals (Hiraki et al. 2019). The induction of *DREB1* genes during cold stress was orchestrated by multiple factors, including CALMODULIN BINDINGTRANSCRIPTION ACTIVATOR3 (CAMTA3) and CAMTA5, which showed different cold-signaling pathways function in the responses to rapid and gradual decreases in temperature (Kidokoro et al. 2017a). Two

DREB1 genes, *CiDREB1A* and *CiDREB1B* were cloned from chicory and their expression were induced by low temperature in an ABA-independent stress signaling pathway (Liang et al. 2014).

On the other hand, DREB2 acts as a master regulator of drought and salinity stress responses in many plant species. The overexpression of maize *ZmDREB2A* increased thermotolerance in transgenic plants and upregulated genes related to the heat shock and detoxification, suggesting that ZmDREB2A has a double function in response to both osmotic and heat stress (Qin et al. 2007). Expression of OsDREB2A transcription factor confers significant tolerance to osmotic, salt and dehydration stresses during simulated stress conditions with enhanced growth performance in rice (*Oryza sativa*) (Mallikarjuna et al. 2011). Subsequent analysis of the expression of other members of the DREB2 subgroup and homologous genes in other plant species demonstrated that a DREB2-type genes can also be induced by low temperatures (Mizoi et al. 2013).

1.3.3 R2R3-MYB

MYB transcription factors are characterized by the MYB domain which is a highly conserved DNA-binding domain. This domain typically consists of one to four imperfect amino acid sequence repeats (R) which is about 50 to 53 amino acids and encodes three α-helices. The second and third helices form a helix–turn–helix (HTH) structure that interposes in the major groove of specific DNA sequence motif (Du et al. 2009). According to the number of adjacent repeats, MYB proteins can be divided into four classes: MYB-related, R2R3-MYB, R1R2R3-MYB, and 4R-MYB proteins (Jiang and Rao 2020). The N-terminal of R2R3-MYB protein contains the highly conserved MYB domain for DNA-binding, while located at the C-terminal is an activation or repression domain, which is highly variable and provided structurally and functionally differences (Dubos et al. 2010; Chen et al. 2019). Most MYB proteins are function as transcription factors, among which the R2R3-MYB were involved in multiple aspects of plant development and responses to abiotic and stresses (Wang et al. 2021). It has been reported in *Arabidopsis* that R2R3-MYB transcription factor AtMYB15 interacted with ICE1 and regulated the expression of *CBF3* responding to low temperature (Agarwal et al. 2006). In rice, an overexpression of *OsMYB2* has been shown to enhance the expression of stress-

related genes, such as *OsDREB2A*, and improve the plant's tolerance towards salt, cold, and dehydration (Yang et al. 2012). Another R2R3-MYB transcription factor, AtMYB44, has been identified in *Arabidopsis*, demonstrating that overexpression of *AtMYB44* leaded to the reduced expression of genes encoding protein phosphatases 2C (PPC2) and thereby enhanced the tolerance of abiotic stresses, such as dehydration, low temperature, and salinity (Jung et al. 2008).

Previous research revealed the association between MYB transcription factors and fructan metabolism. In *Triticum aestivum*, TaMYB13 bound to a (A/G/T)TT(A/T/C)GGT core sequence presenting in the promoters of wheat *Ta1-SST* and *Ta6-SFT* genes and contributed to the fructan accumulation (Kooiker et al. 2013; Xue et al. 2011). Wei et al. (2017a) used TaMYB13 as query and identified CiMYB17 in chicory. CiMYB17 activated the promoter of genes related to fructan synthesis and degradation, indicating that CiMYB17 was involved in the complex regulation of fructan metabolism. Moreover, CiMYB3 and CiMYB5 enhanced promoter activities of *1-FEH*s by recognition the MYB-core motifs (C/TNGTTA/G) and regulated fructan degradation in response to abiotic stress and hormonal cues (Wei et al. 2017b).

1.3.4 NAC

Plant specific proteins NAC [No apical meristem (NAM), *Arabidopsis* transcription activation factor (ATAF), Cup-shaped cotyledon (CUC)] are a major transcription factor family function as regulators in stress tolerance and plant development (Puranik et al. 2012). In general, NAC proteins contain a highly conserved NAC-domain located at the N-terminal for interaction with DNA and a diverse C-terminal for transcriptional activation, repression, and protein interaction. There is growing evidence that NAC transcription factors play an important role in the stress response of many species. Under low temperatures, the less growth of *Arabidopsis* drove a slow accumulation of a membrane-associated NAC transcription factor NTL8, which altered the *VERNALIZATION INSENSITIVE 3* cold induction profile in the long-term process of vernalization (Zhao et al. 2020). In addition, three NAC proteins identified in *Arabidopsis*, ANAC019, ANAC055 and ANAC072, were upregulated by drought, high salinity and abscisic acid, and bound specifically to the *CATGTG* motif (Tran et al. 2004). In pepper (*Capsicum annuum* L.), CaNAC064 was found as a regulator of

cold stress tolerance and interacted with low temperature-induced haplo-proteinase proteins (Hou et al. 2020). In rice, the NAC transcription factor, OsNAC6, activated genes encoding peroxidases and responded to various stresses such as cold, drought, high salinity, wounding, and blast disease (Nakashima et al. 2007). Overexpression of the gene *TaNAC29* in wheat enhanced plant's tolerance to salt stress as well as improved physiological traits such as greener leaves, reduced H_2O_2 accumulation, and strengthened cell membrane stability (Xu et al. 2015).

In addition to stress response, NAC transcription factors are involved in the process of plant development. Overexpression of *TaRNAC1*, a predominantly root-expressed NAC transcription factor from wheat, significantly increased root length at the early growth stage, and increased 70% dry weight biomass of mature root (Chen et al. 2018). In maize, two endosperm-specific NAC transcription factors, ZmNAC128 and ZmNAC130, were demonstrated to regulate the transcription of *Bt2* (*brittle2*) and its protein level and affect the starch accumulation (Zhang et al. 2019). However, limited research has been conducted to demonstrate the association between NAC transcription factors and carbohydrate metabolism, warranting further investigation.

1.3.5 WRKY

WRKY transcription factors are one of the largest groups transcription regulators in plant, which function as repressors and activators. These transcription factors are characterized by a DNA binding domain in the N-terminal, which is 60 residues in length containing WRKY amino acid sequence, as well as a zinc-finger in the C-terminal (Rushton et al. 2010). The conserved WRKY domain recognize a specific DNA sequence called the W-box (TTGACC/T), which is the minimal element required for many WRKY proteins to specifically bind to DNA (Ciolkowski et al. 2008). Over the past decade, studies on WRKY have shown that it was common for WRKY transcription factor to regulate different aspects of plant. In *Nicotiana tabacum*, the expression of *tWRKY3* and *tWRKY4* rapidly increased not only after tobacco mosaic virus infection but also by salicylic acid induction, and further enhanced the resistance to the pathogen (Chen et al. 2000). However, another WRKY protein CaWRKY1 in *Capsicum annuum*, has been reported as a negative regulator, which turned off the systematic acquired resistance once the pathogen stress diminished (Oh et al. 2008). SUSIBA2 (sugar signaling in barley) is a WRKY

protein found in barley, which has been reported to bind the W-box and the SURE (sugar response) *cis*-elements (Sun et al. 2003). Expression of barley SUSIBA2 in rice increased the starch yield and reduced the methane emissions, providing a sustainable approach for increased starch content food production (Su et al. 2015). Later research revealed the mechanism of a dual-promoter gene encoding SUSIBA1 and SUSIBA2 orchestrating the coordinated regulation of starch and fructan synthesis in barley (Jin et al. 2017).

1.4 Biotechnology

The utilization of plant genetic engineering is a pivotal component in enhancing crop productivity, improving quality, and strengthening resistance against abiotic and biotic stressors in agricultural production. To produce a chicory cultivar possessing elevated inulin content, one strategy involves the inactivation of *1-FEH* genes to prevent inulin degradation. Serval genome editing methodologies have been developed, encompassing Zinc finger nucleases (ZFNs) and the utilization of DNA-binding transcription activator-like (TAL) effectors derived from the plant bacterial pathogen *Xanthomonas*. Despite their significant impact and valuable contributions, both platforms possess distinctive drawbacks and necessitate considerable resources for customization to fulfill specific requirements, with their integration into plant systems remaining a challenging endeavor. In recent years, research focus has primarily shifted towards the CRISPR/Cas system as a genome editing tool. The implementation of CRISPR/Cas offers plant breeders the capability to precisely introduce targeted sequence variations, representing a transformative resource for the expedited improvement of agricultural crops. The present chapter aims to provide an overview of the development of CRISPR/Cas9 technology and its applications in plant systems.

1.4.1 CRISPR/Cas9

CRISPR/Cas (Clustered Regularly Interspaced Short Palindromic Repeats /CRISPR-associated protein) is an adaptive immune system of bacteria against the infection of bacteriophage (Heler et al. 2014). The system allows the host to record the foreign genetic element by integrating a short DNA fragment from invader into the host chromosome, and thereby to prevent the second infection (Amitai and Sorek 2016). According to the current classification of CRIPSR-*cas* loci (Makarova et al. 2015),

CIRSPR system can be grouped by six distinct types, among which type II utilizes a single endonuclease, Cas9, containing HNH-like and RuvC domain for DNA recognition and cleavage (Shmakov et al. 2015). In most CRISPR system, a conserved DNA sequence known as a short protospacer adjacent motif (PAM) is require for DNA target selection and degradation (Leenay et al. 2016). The Cas9 enzyme from *Streptococcus pyogenes* recognizes 5'-NGG-3' PAM sequence and cleavages the 3' end of the target DNA (Jinek et al. 2012). After the first invasion, foreign sequences are carried by CRISPR arrays and form the 5' end of mature CRISPR RNAs (crRNAs) after transcription (Brouns et al. 2008). A small noncoding *tans*-activating crRNA (tracrRNA) base pair with the crRNA and form dual-RNA structure (Deltcheva et al. 2011). During the second invasion, the dual-RNA generate hybridization with DNA of the same former invader, which guide the Cas9 nuclease to cleave the foreign DNA containing an adjacent PAM and a complementary 20-nucleotide target sequence (Jinek et al. 2012). This silencing process can be utilized by researchers to modified specific site in genome by altering the guide RNA within the crRNA. To simplify the system, a single guide RNA (sgRNA) combining crRNA and tracrRNA retains the function of Cas9 to cleave the target site and generates a double-strand break (DSB) (Jinek et al. 2012). The DSB is subsequently repaired by either the error-prone nonhomologous end joining (NHEJ) mechanism, leading to small random indels at the cleavage site (Lieber 2010), or the homology-directed repair (HDR) pathway, resulting in precise sequence insertion at the DSB location via a homologous repair template (McVey et al. 2016; Ran et al. 2013).

1.4.2 Application of CRISPR/Cas9 in agricultural plants

Crops are important sources for human's consumption. The world's growing population requires innovative breeding technologies to increase agricultural productivity and meet the growing demand for agricultural products. Traditional cross-breeding methods take 8-10 years to introduce desirable alleles, which is not only time consuming, but also limited by the reduced genetic variability (Chen et al. 2019). CRISPR/Cas9 genome editing system as a potential breeding technology can precisely modified target sequence in the genome and shorten the time to achieve desirable varieties. Over the past decade, the usage of CRISPR/Cas9 has been reported in rice (*Oryza sativa*) and wheat (*Triticum aestivum*) (Shan et al. 2013). The application of CRISPR/Cas9 can improve crops' traits in multiple aspects. One

common strategy is using CRISPR/Cas9 to knock out negative regulator that affected yields by introducing indels in the genes. For instance, loss-of-function mutation in grain weight–related genes *Grain Weight 2* (*GW2*), *Grain Weight 5* (*GW5*) and *Thousand- Grain Weight 6* (*TGW6*), significantly increased grain weight in rice due to trait pyramiding (Xu et al. 2016). Additionally, CRISPR/Cas9 guided null mutation in *GRAIN NUMBER 1a* (*Gn1a*), *DENSE AND ERECT PANICLE* (*DEP1*), and *Grain Size* (*GS3*) improved yield-related traits (Li et al. 2016). Mutation of the *Waxy1* gene in maize using CRISPR/Cas9 increased the amount of amylopectin in seed starch (Gao et al. 2020). Moreover, CRISPR/Cas9 can knock out disease-susceptibility genes to confer crops' resistance to biotic stresses. CRISPR/Cas9-mediated knockout of *MILDEW RESISTANT LOCUS O* (*Mlo*) increased resistance to powdery mildew in bread wheat and tomato (Wang et al. 2014; Nekrasov et al. 2017). Another strategy of using of CRISPR/Cas9 is to knock in or replace specific genome sequence via HDR pathway to generate new allelic variant that do not exist naturally and facilitate the breeding process. Maize ARGOS8 is a negative regulator of ethylene responses. Using CRISPR/Cas9 to knock in *GOS2* promoter to replace the native promoter of *ARGOS8,* increased the gene transcript level and improved maize grain yield under drought stress conditions (Shi et al. 2017).

1.4.3 Deliver CRISPR/Cas9 reagent into plants

The traditional approach for stable expression of CRISPR/Cas9 DNA is to use *Agrobacterium*-mediated transformation or particle bombardment to deliver a DNA cassette including Cas proteins, gRNA and marker gene for selection. This method allows the integration of CRISPR constructs into the genome of plants, which may lead to side effects and increase the off-target rate. In addition, the insertion sites of CRISPR constructs are usually unpredictable. Although it is possible to get rid of CRISPR constructs by genetic segregation and generate transgene-free mutant plants, this method is limited for asexually propagated crops. An alternative approach is transient expression of CRISPR/Cas9, in which the selection step for regenerated plants using harborside or antibiotic is eliminated. Without the selection pressure, the regenerated plants with modification have chance to grow without the foreign DNA construct in the genome. Similarly, transfecting CRISPR construct into protoplast to edit genomic DNA does not require integration of the CRISPR cassette into plant genome. Consequently, the genome modified protoplast can further be regenerated

into full plants, while the plasmid will be depredated during the regeneration process. This method has been successfully achieved in chicory with mutation frequency 4.5% in the protoplast (Bernard et al. 2019). However, vector containing the CRISPR/Cas9 cassette can be inserted at a non-negligible frequency into the plant genome after transient transformation. In tobacco, Lin et al. (2018) reported that Cas9 DNA had been found in 17.2 % of mutant plants after using protoplast transient transfection. To avoid the disadvantage of plasmid-based CRISPR/Cas9 system and establish a DNA-free genome editing method, there is a growing interest in using ribonucleoprotein (RNP) delivered into plant cells by protoplast transfection. The RNP complex and sgRNA can be pre-assembled *in vitro* with reaction buffer. Subsequently, RNP complex can be delivered into plant protoplast by polyethylene glycol (PEG)-mediated cell transfection, particle bombardment, electroporation, or lipofection (Fig. 1.2). Woo et al. (2015) were first utilized RNP for genome editing into plant protoplasts of *Arabidopsis thaliana*, tobacco, lettuce, and rice and achieved regenerated plants with 46% mutation frequency.

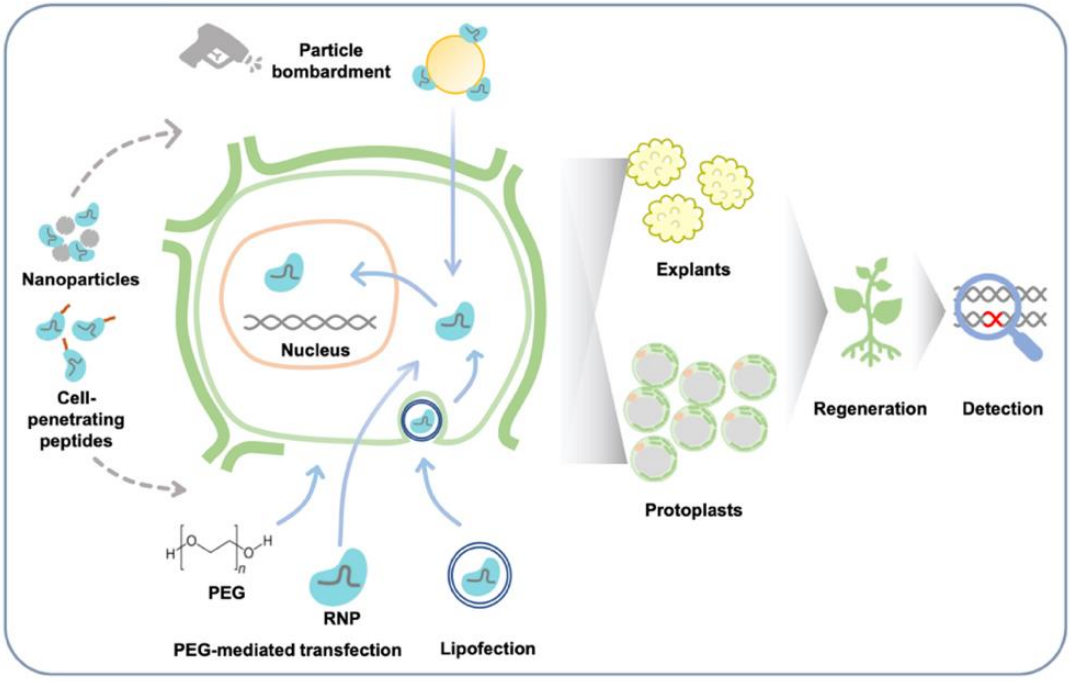

Figure 1.2 CRISPR/Cas9 RNP-mediated genetic engineering in plants (Zhang et al. 2021). RNP can be dilivered into protoplast by particle bombardment, polyethylene glycol (PEG)-mediated transfection, lipofection, nanoparticles and cell-penetratingpeptides. Transformed cells and tissues are used for plant regeneration and edit detection.

2 Aims

Although the fructan 1-exohydrolases have been identified in chicory and well-studied with their cold induction during harvest season, the specific functions of these three isoforms, 1-FEH1, 1-FEH2a and 1-FEH2b, remained unclear. Additionally, limited information was available on the transcription factors that regulate their expression. The overall aim of this thesis is to investigate the differential regulation pathways of *1-FEH* genes and to identify the transcriptional regulators involved in stress signaling of *1-FEH* genes. Another goal of this thesis is to establish a robust and practical protoplast-based transfection system for genetic engineering of inulin yield and quality using biotechnological methods. The strategies and experimental procedures applied in this thesis include:

(1) Promoter analysis is conducted on *1-FEH1*, *1-FEH2a*, and *1-FEH2b* based on the identified *cis*-elements on their respective promoters and screen potential transcription factor families.

(2) Putative transcription factors are identified in a chicory RNAseq database by querying with published sequences from other plant species.

(3) Co-expression analysis is conducted through quantitative real-time PCR (qRT-PCR) to investigate the relationship between putative transcription factors and genes related to fructan metabolism in response to various abiotic stresses.

(4) Dual luciferase assay (DLA) is performed in chicory mesophyll protoplasts to investigate the transcription factor activation on *1-FEH* promoter regions.

(5) Electrophoretic mobility shift assay (EMSA) is employed to identify the specific binding sites of the transcription factors on the promoter region of interest.

(6) Yeast-two-hybrid and luciferase complementation assay (LCA) are used to study the interaction between transcription factors.

(7) An approach is developed to introduce site-specific mutations in target genes of chicory via CRISPR ribonucleoprotein (RNP) delivery and protoplast regeneration.

3 Results

3.1 Identification of CiDREB and CiNAC transcription factors in *Cichorium intybus*

3.1.1 Bioinformatic analysis of promoter sequence predicts possible binding sites for CiDREBs and CiNACs

To address the question whether abiotic stress responding transcription factors CiDREB and CiNAC are involved in the regulation of *1-FEH* genes expression, I scanned the promoter sequence to approximately 1kb upstream from the start codon of *1-FEH1*, *1-FEH2a* and *1-FEH2b* in JASPAR database (jaspar.genereg.net). Based on the conserved binding sites of AtDREB or AtNAC from *Arabidopsis thaliana*, I screened the promoter of *1-FEH* for the presence of *cis*-elements containing the core motifs of DRE (Dehydration Response Element) or NACBS (NAC Binding Site). Compared to *p1-FEH2a* and *p1-FEH2b*, *p1-FEH1* contains two times more putative NACBS, with one NACBS rather close to the TATA box (Fig. 3.1).

Table 1 Prediction of DRE on promoter sequence of 1-FEHs

Promoter	Putative DRE element and position
p1-FEH1 (1195 bp)	ATGTCGTT (-811), ATGTCGGACG (-717), ATGTGGAC (-353), TGTGGGTG (-188)
p1-FEH2a (1147 bp)	ATGCCGTCAT (-487), TGGCCAACTT (-192), AATTCGGTAG (-136)
p1-FEH2b (1740 bp)	TGTCGGTC (-781), TGGCCAACTT (-186), AAGTCGGTAG (-138)

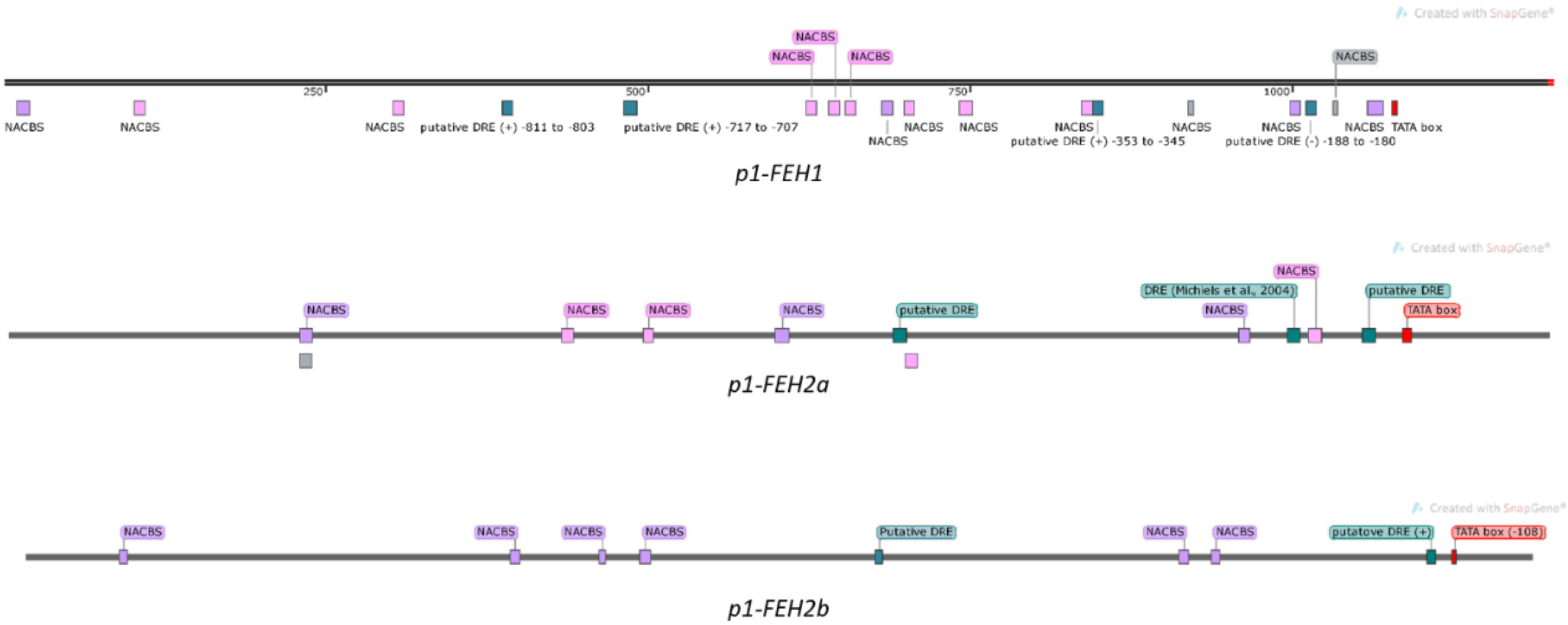

Figure 3.1 Promoter analysis of *1-FEH1*, *1-FEH2a* and *1-FEH2b*. Putative NAC binding sites are indicated in pink/purple boxes on the promoter region. Putative DRE elements are indicated in green boxes. TATA boxes are highlighted with red boxes. Figure was generated by SnapGene.

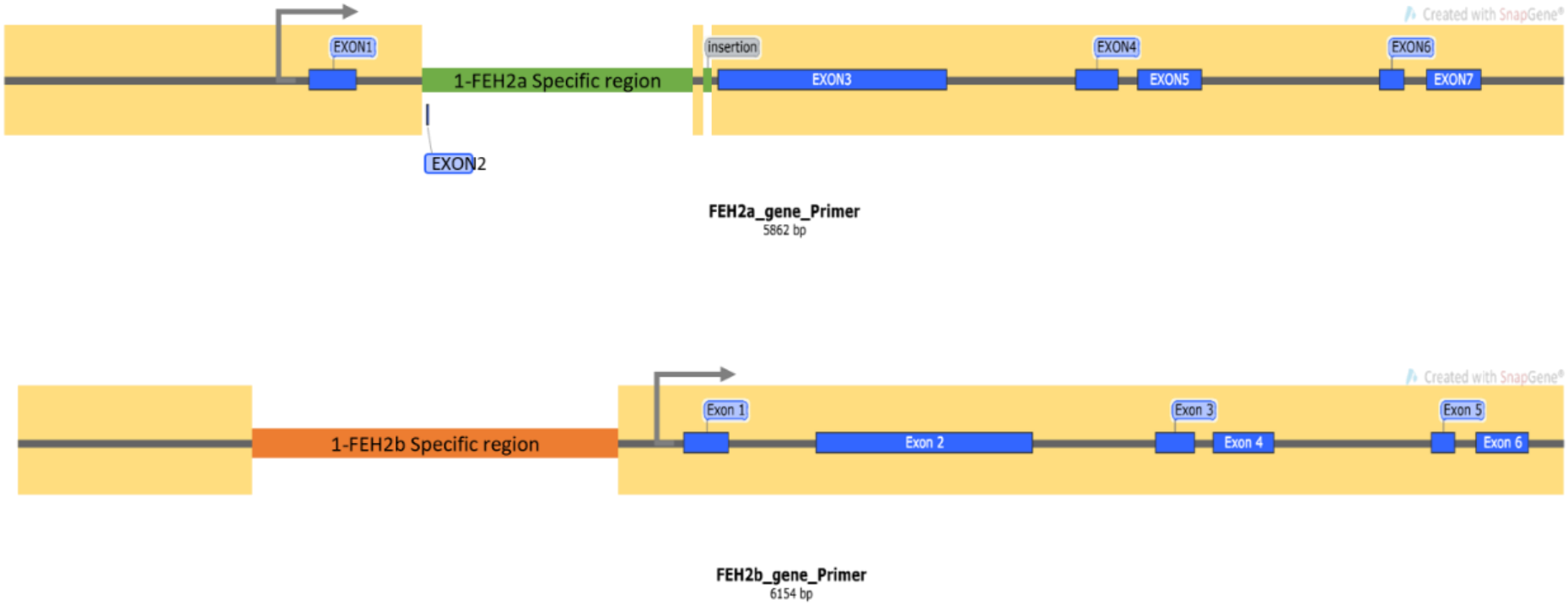

Figure 3.2 Schematic comparison of genomic sequences between *1-FEH2a* and *1-FEH2b*. Homologous regions are annotated in yellow. *1-FEH2a* specific region is indicated in green. *1-FEH2b* specific sequence is located in the promoter region, which is indicated in orange.

Previous promoter deletion analysis of *p1-FEH2a* demonstrated that the -172 to -278 region was critical for *1-FEH2a* cold induced expression, presumably due to the presence of potential cold-responsive ABRE (GACACGTA) and/or CRT/DRE elements (TGGCCAACTT). Further deletion down to -172 decreased the promoter activity in plants under cold treatment (Michiels *et al.* 2004). There are more DRE elements found on *p1-FEH2a* and *p1-FEH2b*, which are listed on table 1. Interestingly, both *p1-FEH2a* and *p1-FEH2b* display a DRE element upstream near the TATA box, but with one base pair different on the core motif.

Notably, *1-FEH2a* and *1-FEH2b* share highly conserved sequence of promoter, except that *p1-FEH2b* contains a long insertion located on -1716 to -246 upstream from ATG. Although *1-FEH2a* and *1-FEH2b* coding sequences show 96.05% similarity, *1-FEH2a* contains an insertion around 1kb between exon 1 and exon 3, which contains a distinct exon 2 coding three additional amino acids compared to *1-FEH2b* (Fig. 3.2).

3.1.2 Identification and cloning of CiDREB isoforms in chicory

In previous research, Liang *et al.* (2013) used homologous regions of reported *CBF/ DREB1* genes from other plants as queries, and identified two genes coding *CiDREB1A* and *CiDREB1B* in chicory. However, primers used to clone *CiDREB1B* coding sequence resulted in amplification of four close isoforms named *CiDREB1C-F* (Wei, Dissertation, 2017). By using *LsDREB2A* from *Lactuca sativa* as query sequence and tBLASTn searching in chicory database, Wei (2017) identified two additional *CiDREB2* genes and designated them as *CiDREB2A* and *CiDREB2B*.

Alignment of CiDREB1 and CiDREB2 protein sequences revealed a conserved AP2 domain containing 57 amino acids (Fig. 3.3A). To predict the potential function and to clarify the phylogenetic relationship of identified CiDREB candidates, I used MEGA7 to conduct the evolutionary analyses of CiDREB among AtDREB from *Arabidopsis thaliana*. Classified in subgroup 1 family, CiDREB1A/1C/1D showed similarity to DWARF AND DELAYED FLOWERING (AtDDF1, AT1G12610.1; AtDDF2, AT1G63030.1) which showed increased tolerance to high levels of salt by overexpression in *Arabidopsis* (Magome et al. 2004). This subgroup 1 family is considered as involved in cold response, including cold inducible transcription factors CBF1 (AT4G25490.1), CBF2 (AT4G25470.1), and CBF3 (AT4G25480.1).

CiDERB2A and CiDREB2B were classified in subgroup 2 family (Fig. 3.3B), which included AtDREB2A and AtDREB2B that were involved in response to drought (Mizoi et al. 2012).

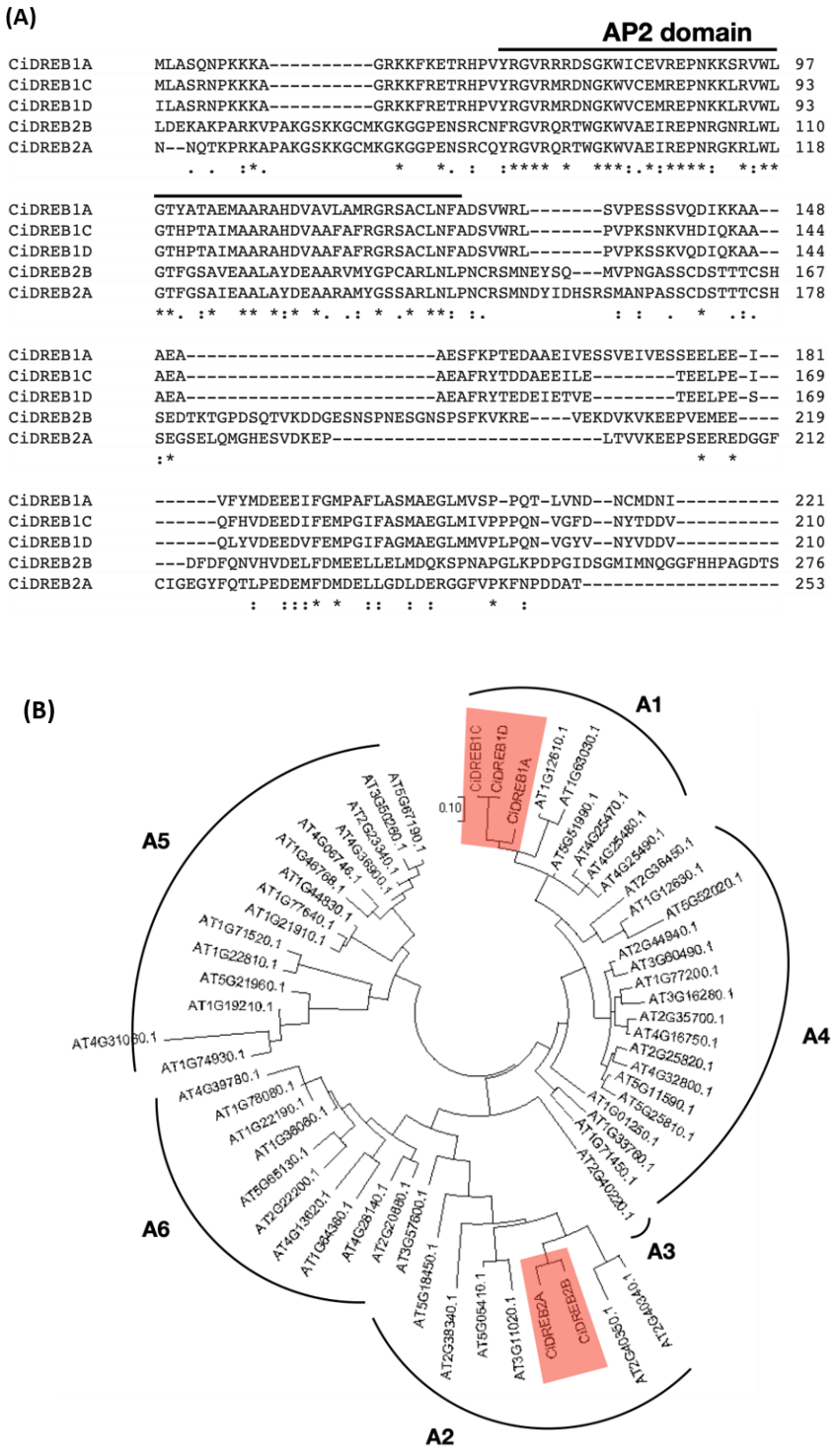

Figure 3.3 Protein sequence analysis of CiDREB. (A) Comparison of the predicted amino acid sequences of CiDREB identified in chicory. Multiple amino acid sequence alignments were performed by MEGA7. The AP2 DNA-binding domain was anaylized by NCBI conserved domain search

(https://www.ncbi.nlm.nih.gov) and indicated by a black line. Asterisks, colons and full stops indicate positions that have an identical, conserved and weakly conserved residue, respectively. **(B)** Molecular Phylogenetic analysis of CiDREB transcription factors among AtDREB from *Arabidopsis thaliana* by Maximum Likelihood method. Evolutionary analyses were conducted in MEGA7.

The open reading frames of *CiDREB1A/1C/1D* and *CiDREB2A/2B* contain a conserved NLS (Nuclear Localization Signal) peptide. To determine their subcellular localization, I generated pART-based construct *CaMV35S:CiDREB2B:EGFP* which was subsequently transfected into chicory root protoplasts. As control, *CaMV35S:EGFP* were transfected independently. Fusion protein CiDREB2B:EGFP signals were found in the nucleus (Fig. 3.4) as confirmed by DAPI staining (4', 6-diamino-2-phenylindole, dihydrochloride), while EGFP signal without transcriptional fuses to the transcription factors was distributed in the whole cell. All the observation concluded that CiDREB2B located in the nucleus where most transcription factors function.

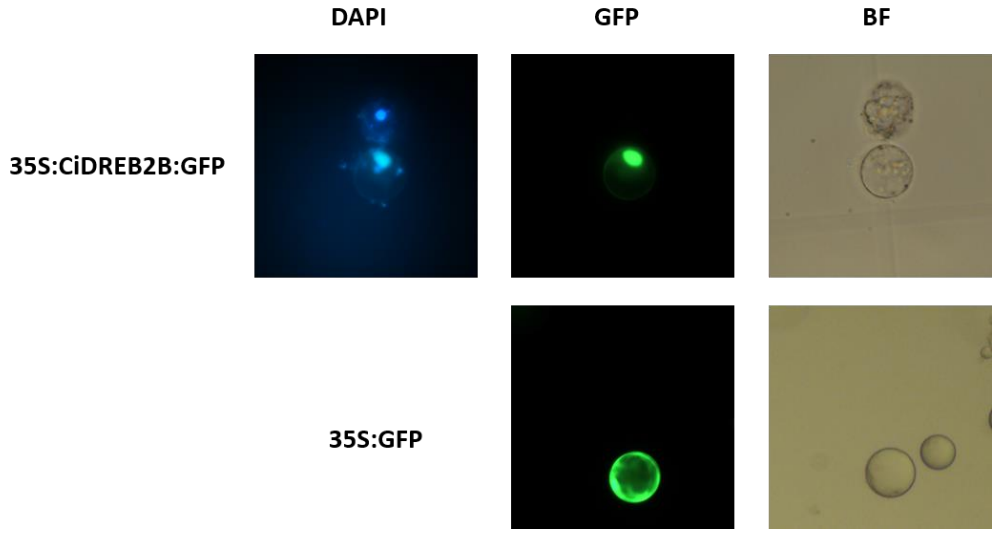

Figure 3.4 Subcellular localization of CiDREB2B in chicory root protoplasts. GFP signal indicates the transient transformation of *CaMV35S:CiDREB2B:GFP*, which is co-localized with DAPI staining (bule). Free GFP is expressed in the whole cell.

3.1.3 Identification and cloning of CiNAC isoforms in chicory

In search for putative CiNAC transcription factors in chicory, I used the conserved NAC domain of *Arabidopsis* as a query to nBLASTt in the chicory RNA database. Eight CiNACs were successfully cloned and were named as CiNAC1-8 after the order in which they were found. Alignment of CiNAC protein sequences showed that they contained bipartite conserved NAC domain (Fig. 3.5). In the evolutionary

analyses of CiNAC among AtNAC from *Arabidopsis thaliana*, I found that CiNAC5 is close to AtANAC017 (AT1G3190.1, Fig. 3.6) that has been reported as a transcription factor related to mitochondrial respiratory capacity and retrograde signaling trigger by reductive stress (Fuchs et al. 2022).

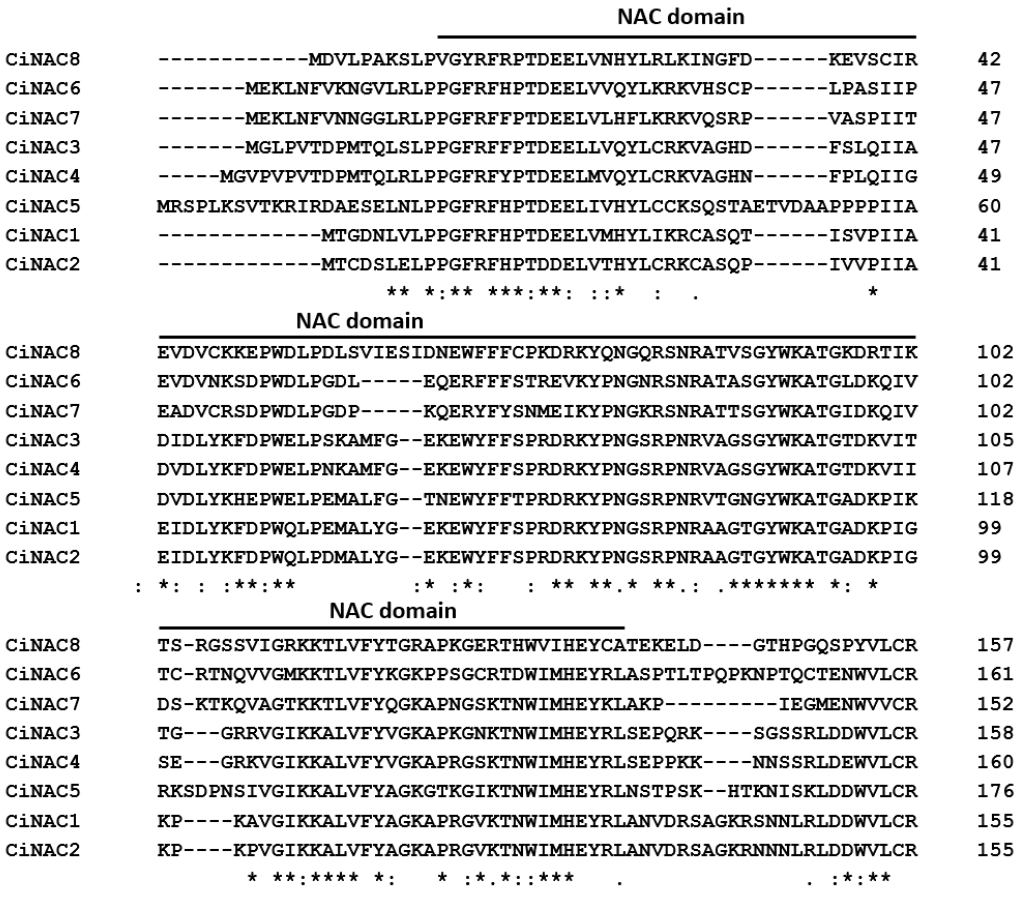

Figure 3.5 Comparison of the deduced amino acid sequences of CiNAC1-8 identified in chicory. Multiple amino acid sequence alignments were performed by MEGA7. The NAC domain was analyzed by NCBI conserved domain search (https://www.ncbi.nlm.nih.gov/Structure/cdd/wrpsb.cgi) and indicated by a black line. Asterisks, colons and full stops indicate positions that have an identical, conserved and weakly conserved residue, respectively.

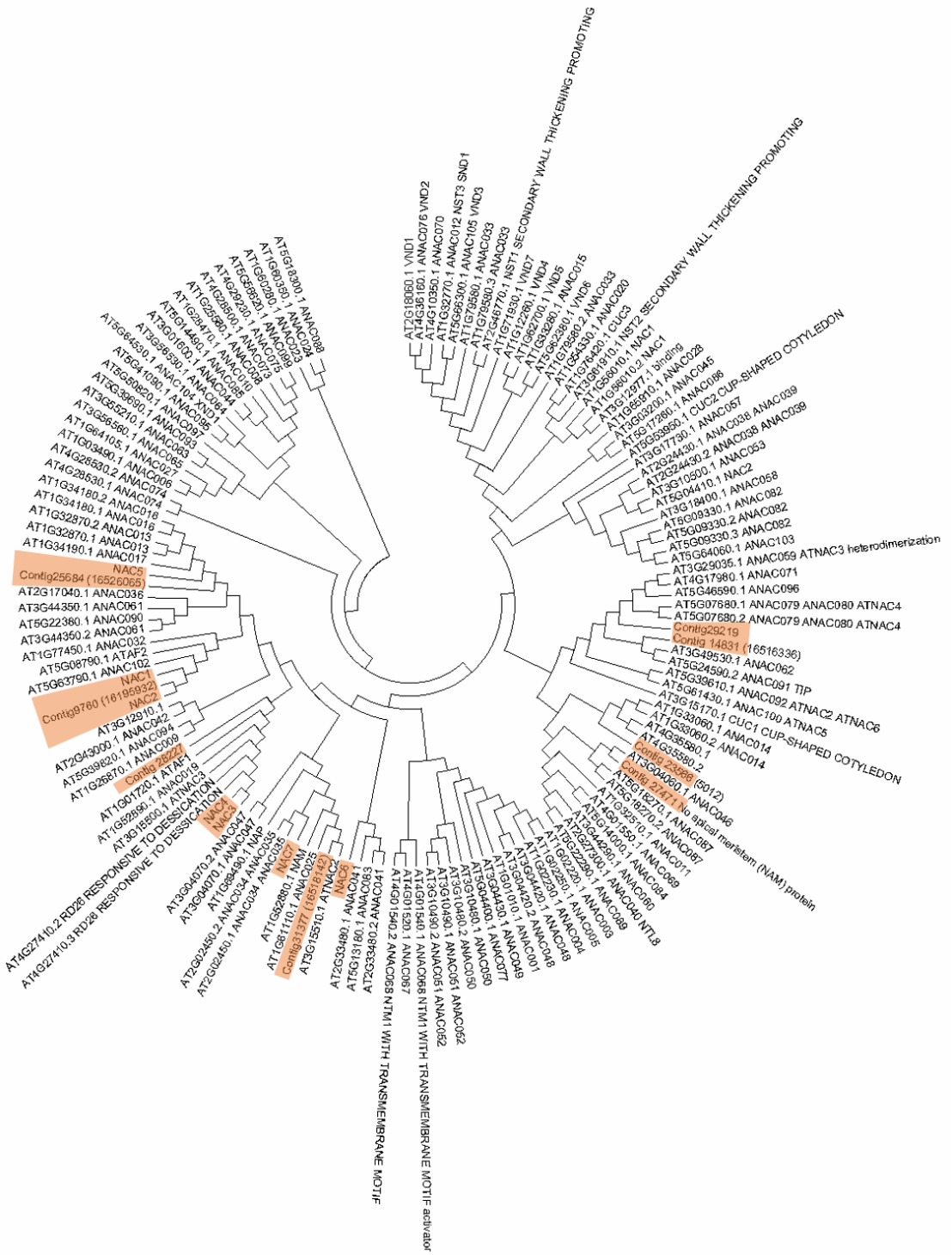

Figure 3.6 Molecular Phylogenetic analysis of CiNAC transcription factors among AtNAC from *Arabidopsis thaliana* by Maximum Likelihood method. Evolutionary analyses were conducted in MEGA7. CiNAC identified in chicory are highlight in orange.

3.2 Transcription factors (TF) co-expressed with *1-FEH* target genes in response to low temperature: Search for TF candidates involved in the regulation of *1-FEH* expression

3.2.1 *1-FEH2a* and *1-FEH2b* show strong but transient induction in tissue slices of mature taproot under cold treatment

To address the expression profile of *1-FEH*s and transcription candidates in mature plants, three-month-old chicory were used in this thesis. Chicory taproot slice tissue were incubated in water and treated with room temperature (25 °C) or cold condition (4°C±1). Compared to room temperature control, *1-FEH2a* and *1-FEH2b* had strong induction after 24 hours under cold treatment, while the expression level of *1-FEH1* slightly fluctuated within the three-day-experiment (Fig. 3.7).

Like *AtCBF* genes from the DREB subgroup 1 family, *CiDREB1A/1C/1D* were cold inducible, with the transcript levels increasing after 3 hours at low temperature followed by a decrease after 6 hours (Fig. 3.8), which indicated an early cold response in advance of the cold induction of *1-FEH2a* and *1-FEH2b*.

The expression of *CiDREB2A* exhibited a moderate induction following 24 hours of cold treatment, while *CiDREB2B* expression remained undetected at both room temperature and under cold conditions (Fig. 3.8). Among several CiNAC transcription factor candidates, I observed that *CiNAC5* and *CiNAC8* was upregulated in response to cold treatment (Fig. 3.8 and Fig. S1). The induction of CiNAC5 due to cold stress was observed after 3 hours and peaked after 24 hours, after which its expression returned to the control level after 72 hours of cold treatment. Likewise, *CiNAC8* induced under low temperature in the first 24 hour, followed by a decrease in expression level after 72 hours (Fig. S1). However, the transcript levels of *CiNAC8* in the first hour were unexpectedly higher in room temperature than under cold treatment, which probably was due to effect of wounding during tissue slice preparation. *CiNAC6* slightly increased along cold treatment and decreased at room temperature, while no cold induction was observed for *CiNAC1* (Fig. S1).

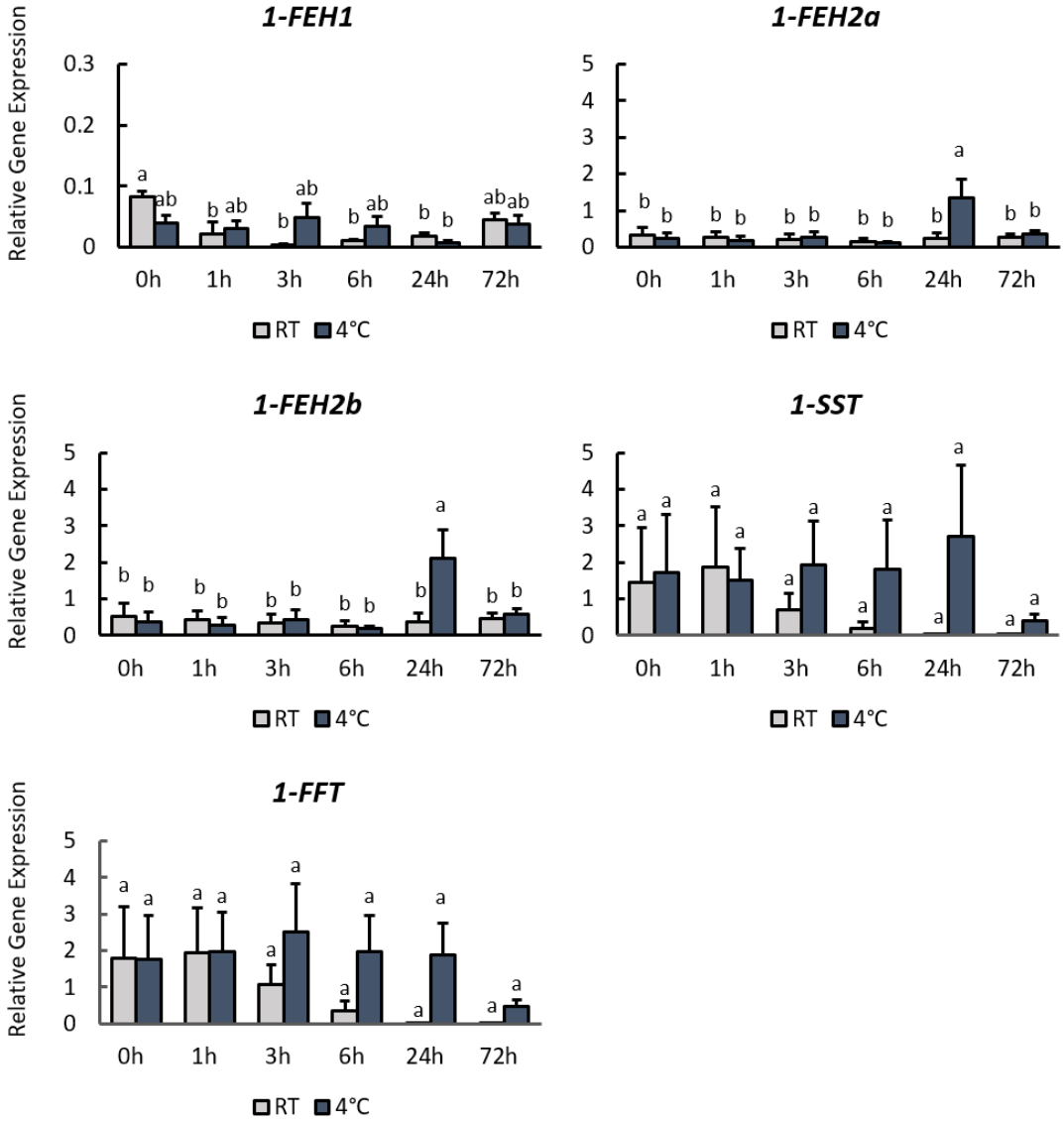

Figure 3.7 Impact of cold treatment (4°C±1) on the transcript levels of FAZYs (*1-FEH1*, *1-FEH2a*, *1-FEH2b*, *1-SST* and *1-FFT*) in taproot tissue slices of 3-month-old chicory. Taproot tissues were incubated in distilled water and transferred to a cold room (4°C±1), while controls were kept at room temperature (RT, 25°C). Transcript levels were determined by qRT-PCR and normalized against the expression of two reference genes, *Actin* and *RPL19*. Relative gene expression was calculated using the delta Ct method. The error bars represent standard deviation (n=3). The one-way ANOVA test was used to determine significance ($p<0.05$).

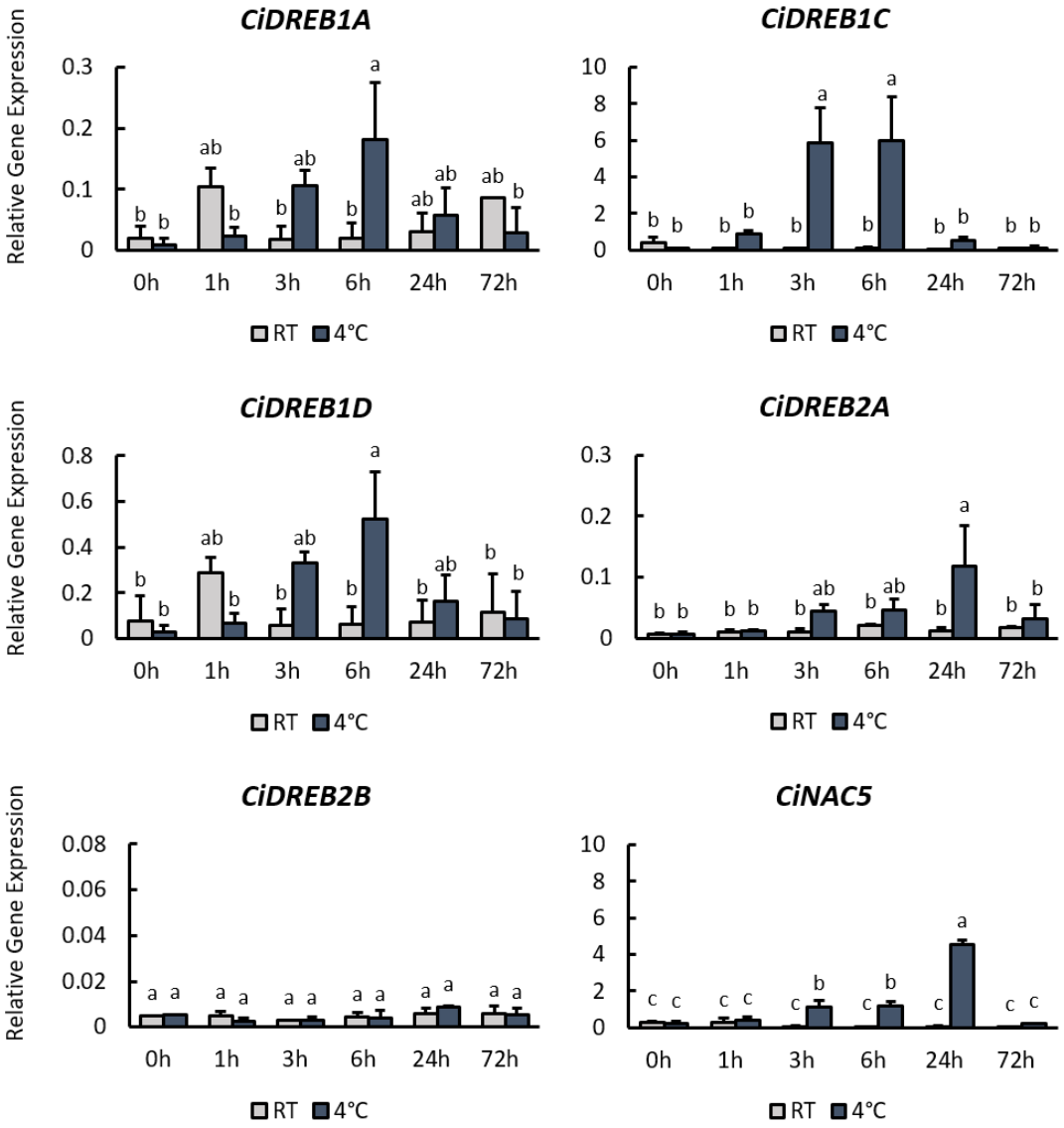

Figure 3.8 The impact of cold treatment (4°C±1) on the transcript levels of transcription factors (*CiDREB1A, CiDREB1C, CiDREB1D, CiDREB2A, CiDREB2B* and *CiNAC5*) in taproot tissue slices of 3-month-old chicory. Taproot tissues were incubated in distilled water and transferred to a cold room (4°C±1), while controls were kept at room temperature (RT, 25°C). Transcript levels were determined by qRT-PCR and normalized against the expression of two reference genes, *Actin* and *RPL19*. Relative gene expression was calculated using the delta Ct method. The error bars represent standard deviation (n=3). The one-way ANOVA test was used to determine significance ($p<0.05$).

3.2.2 In roots of 4-week-old chicory seedlings, *1-FEH* genes show different expression patterns under low temperature

To address the gene expression profile in developing chicory, I used 4-week-old seedlings to determine the transcript levels of *1-FEH* isoforms and related transcription factor candidates. At this stage, chicory started taproot development and inulin accumulation. Additionally, it is interesting to gain insight into the effects of circadian rhythms on *1-FEH* expression, since plants face dynamic environments during growth, especially changes in diurnal temperature. Under cold treatment, taproot samples were harvested every four hours within two days with 12 hours light and 12 hours darkness (Fig. 3.9A). In young seedling taproot, the cold induction of *1-FEH2b* was observed at the first hour and dramatically increased within the first 24 hours with subsequent decline (Fig. 3.9B), which corresponded to the expression pattern in the mature chicory (Fig. 3.7). Likewise, the cold induction of *1-FEH2a* was only maintained for 24 hours. In contrast, the cold induction for *1-FEH1* started after 8 hours and slowly increased along cold treatment, which showed a gradual and constant expression pattern comparing to *1-FEH2b* (Fig. 3.9B). However, there was no marked diurnal difference on gene expression of *1-FEH1*, *1-FEH2a* or *1-FEH2b*.

As sucrose produced by photosynthesis is the substrate for *1-SST* and the initial molecule for fructan synthesis, I investigated the expression of fructan synthesis genes under low temperature and diurnal variation. Interestingly, the expression of *1-FFT* moderately increased under cold treatment, which indicated a dual function of *1-FFT* in fructan composition and degradation, whereas there was no significant cold induction or diurnal fluctuation for *1-SST* (Fig. 3.9).

To analyze the expression of identified transcription factor candidates in a detailed time course, I measured their transcript levels in young chicory seedlings treated under low temperature. Cold induction of *CiDREB1A* appeared earlier in seedlings in the first hour than in mature taproot after 3 hours (Fig. 3.8 and Fig. 3.10). In both young seedling and mature taproot with cold treatments, the expression of *CiDREB1A* reached a peak early and then dropped to the level as room temperature control (Fig. 3.10). Several CiNAC transcription factor candidates were determined its expression levels under cold treatment, among which *CiNAC8* showed a comparable expression pattern as *CiDREB1A* (Fig. 3.10 and Fig. S2). The diurnal

rhythm did not show an impact on the expression of *1-FEH*, but transcription factors *CiDREB1D*, *CiDREB2A* and *CiNAC5* were upregulated under low temperature during the daytime, and the cold induction declined during the night (Fig. 3.10).

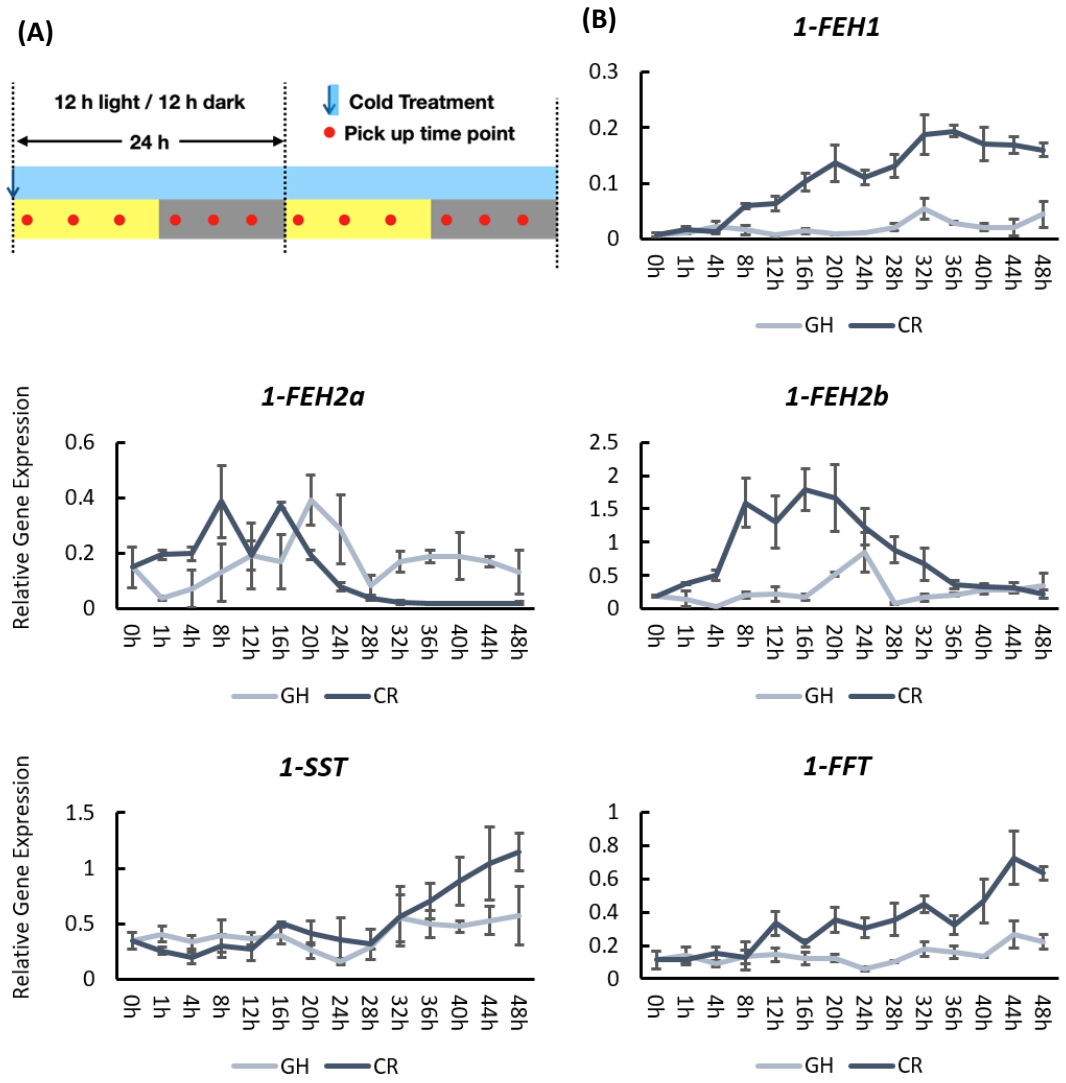

Figure 3.9 Impact of cold treatment (4°C±1) on the transcript levels of FAZYs (*1-FEH1*, *1-FEH2a*, *1-FEH2b*, *1-SST* and *1-FFT*) in taproots of 4-week-old chicory seedling. (A) Taproot samples were harvested every 4 hours after treatment. Diurnal changes with 12-hour light and 12-hour darkness conditions were indicated in yellow and gray, respectively. Seedlings were transferred to the cold room (CR, 4°C±1), while control plants were kept in the greenhouse (GH, 25°C±2). **(B)** Transcript levels were determined by qRT-PCR and normalized against the expression of two reference genes, *Actin* and *RPL19*. Relative gene expression was calculated with the delta Ct method. The error bars represent standard deviation (n = 3-4).

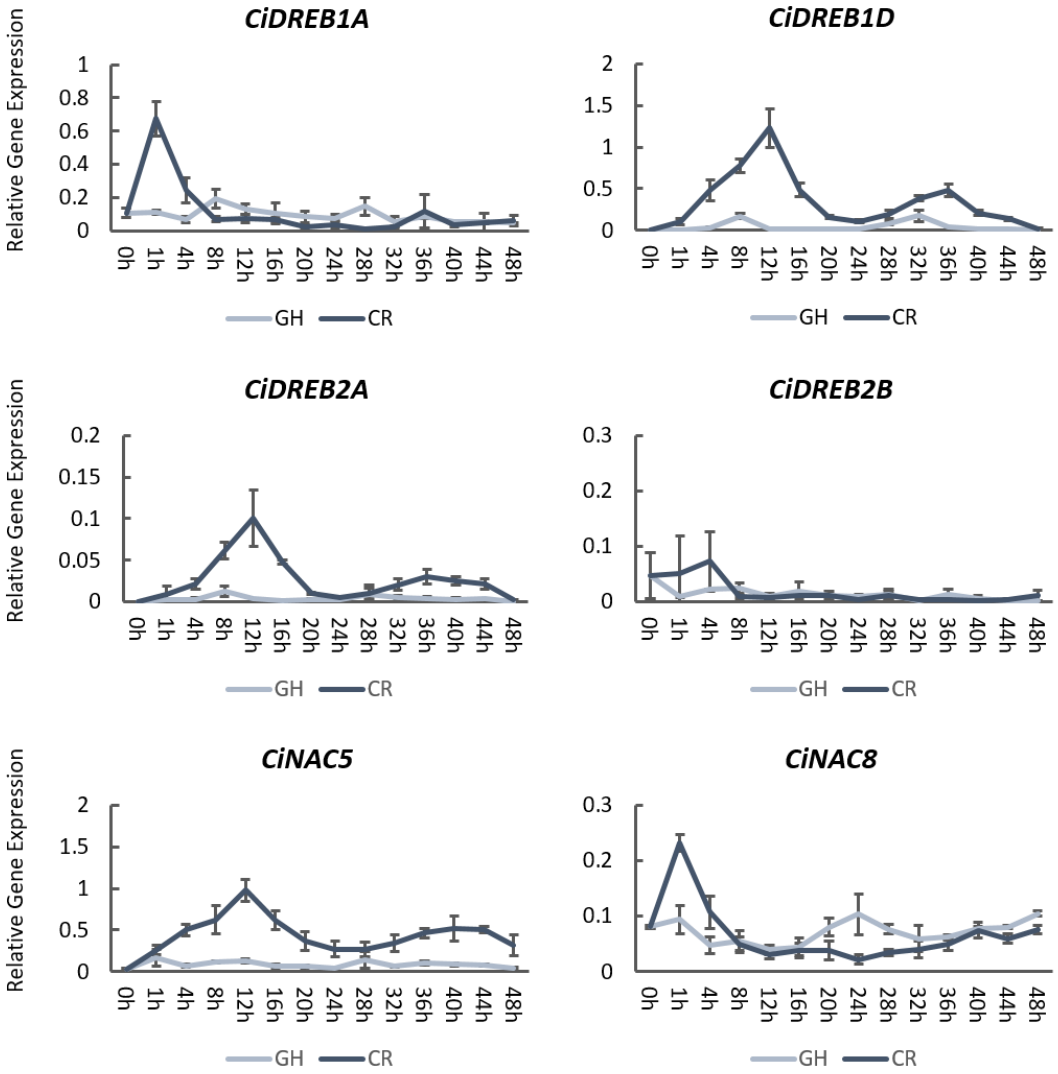

Figure 3.10 Impact of cold treatment (4°C±1) on the transcript levels of transcription factors (*CiDREB1A*, *CiDREB1D*, *CiDREB2A*, *CiDREB2B*, *CiNAC5* and *CiNAC8*) in taproots of 4-week-old chicory seedling. Seedlings were transferred to the cold room (CR, 4°C±1), while control plants were kept in the greenhouse (GH, 25°C±2). Transcript levels were determined by qRT-PCR and normalized against the expression of two reference genes, *Actin* and *RPL19*. Relative gene expression was calculated with the delta Ct method. The error bars represent standard deviation (n = 3-4).

3.3 *In vivo* promoter activation assay to confirm TF functionality for promoter of target genes

3.3.1 Establishing a homologous transient expression system using chicory protoplasts

In order to conduct *in vivo* transactivation assays in homologous plant material, I established a transient gene expression system using chicory mesophyll and root

protoplasts. In the process of protoplast isolation, I found that 4-week-old chicory seedlings were the optimal donor to generate protoplasts. At this stage, seedlings contain soft and well-expanded leaves that can be easily digested by cellulase, and the roots are grown to sizes suitable for horizontal slicing, which increases the contact surface with the enzyme solution (Fig. 3.11). Although it has been reported that gentle agitation would increase the yield of protoplast, I found that prolonging the incubation time and keeping digestion without shaking generated more intact cells. For both, mesophyll and root protoplast, a high yield was achieved by using this method. In this study, protoplasts were transfected with plasmid via PEG4000 and the transfection efficiency was visualized by GFP. The concentration of PEG is crucial for the transfection efficiency, while the type of polymerization (PEG4000, PEG6000 or PEG8000) does not show differences (Fig. 3.12).

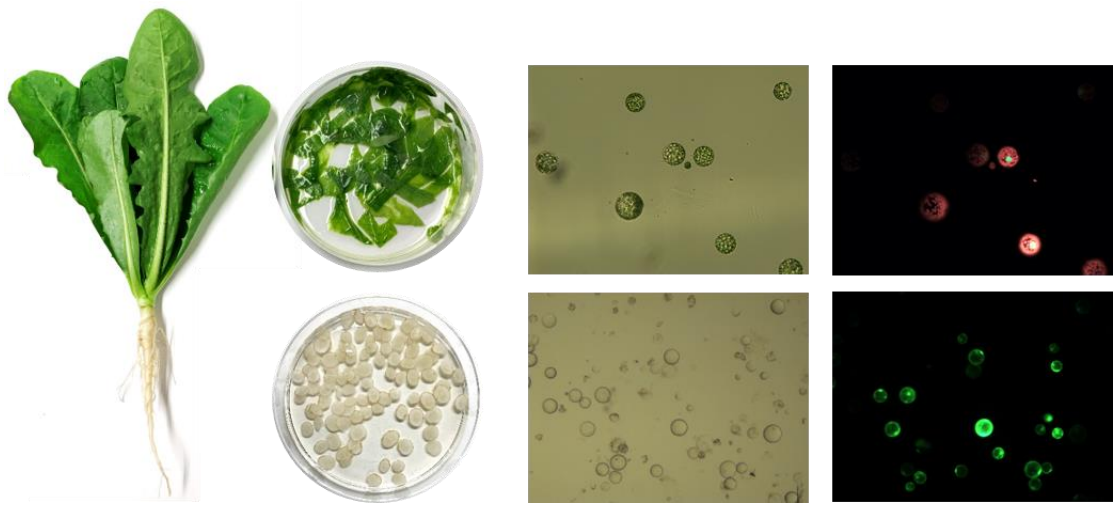

Figure 3.11 Isolation of mesophyll and root protoplasts in chicory. Leaves and roots were harvested from 4-week-old seedlings and incubated overnight in enzyme solution. Transient expression and transfection efficiency were tested via transfecting *CaMV35S:EGFP* into protoplasts

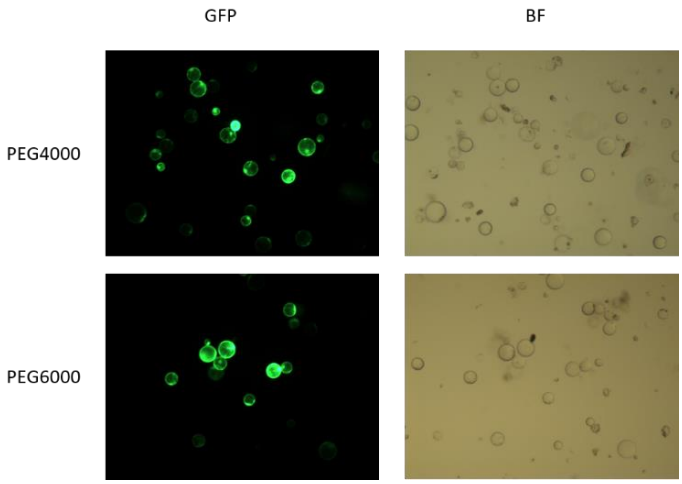

Figure 3.12 Comparison between PEG4000 and PEG6000 transfection method in chicory root protoplast. GFP signal showed the transient transformation of *CaMV35S:EGFP*.

3.3.2 CiNAC5 strongly activates the promoter of *1-FEH1*

To address the question whether CiNACs have an impact on the promoters of *1-FEH*, I performed dual luciferase assay in the well-established protoplast system. Approximate 1kb promoter sequences were cloned into the reporter construct and co-transfected with transcription factors driven by a strong promoter CaMV35S (Fig. 3.13A). In this analysis, a threshold of 2-fold-induction was set to exclude random impacts. As shown in the result, CiNAC5 activated *p1-FEH1* significantly by 8- to 9-fold, while CiNAC8 showed moderate induction on the promoter of *p1-FFT* (Fig. 3.13B). Despite the presence of NACBS, CiNAC5 or CiNAC8 do not show strong activation on *1-FEH2a* and *1-FEH2b* promoter activity.

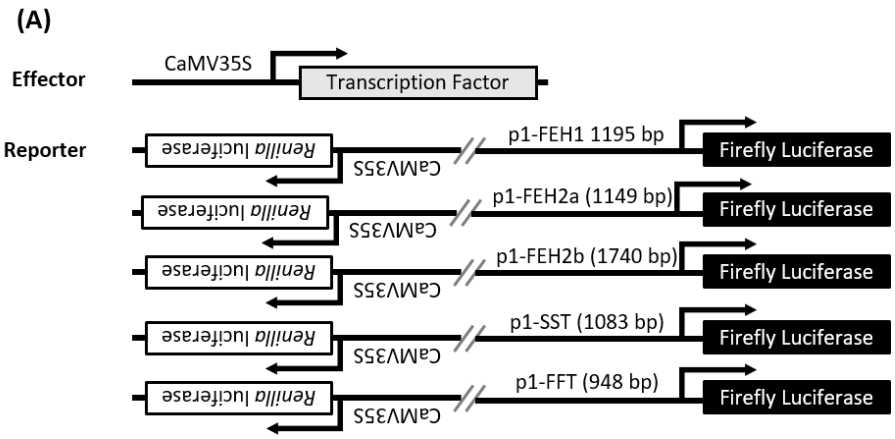

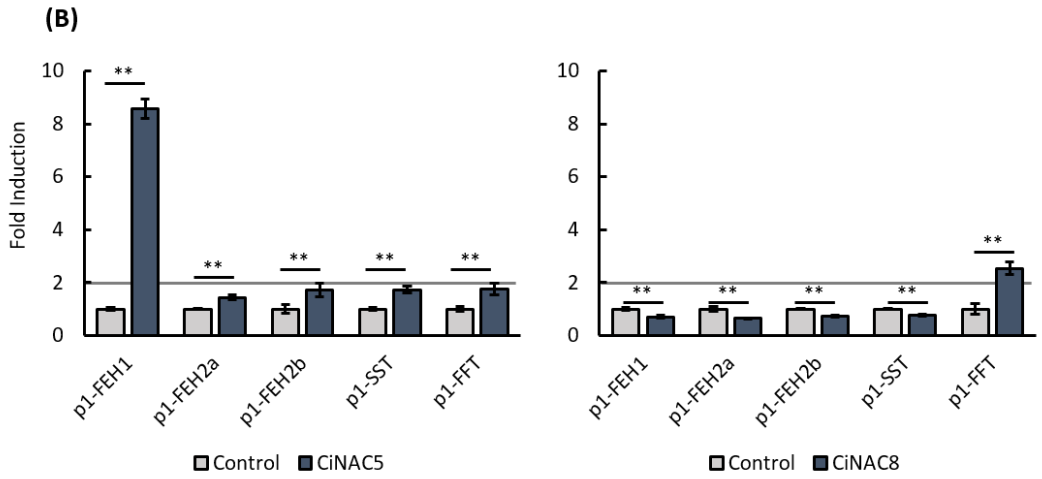

Figure 3.13 CiNAC5 and CiNAC8 activate the promoters of *1-FEH1* and *1-FFT*, respectively. (A) In the reporter construct, the 5'UTR/promoter regions of *1-FEH1* (1195 bp), *1-FEH2a* (1149 bp), *1-FEH2b* (1740 bp), *1-SST* (1083 bp) and *1-FFT* (948 bp) are individually fused upstream of a firefly luciferase gene. Transient expression was performed in chicory mesophyll protoplasts via PEG-method. Each FAZY promoter linked to a firefly luciferase reporter gene was co-transfected into cells with the effector construct (*pART7-CiNAC5* or *pART7-CiNAC8*), or with empty *pART7* vector as control. The *Renilla* luciferase was fused in reporter as a control for normalization in each transfection. **(B)** Fold induction of FAZY (*1-FEH1, 1-FEH2a, 1-FEH2b, 1-SST* and *1-FFT*) promoter activities in the presence of CiNAC5 or CiNAC8 relative to the empty vector control. Basal promoter activity is expressed as relative LUC activity (Firefly/*Renilla*). Bars indicate means ± SD of three technical replicates. Student's t-test was used to determine the significance: * $P<0.05$, ** $P<0.01$. The results were confirmed in two independent experiments.

3.3.3 Promoter deletion analysis of *1-FEH1*

In order to identify the functional NACBS on *p1-FEH1* for CiNAC5, I performed promoter deletion analysis to narrow down the range of the NACBS location. Three length of *p1-FEH1* fragments were cloned into the reporter constructs, which contained different amount of NACBS (Fig. 3.14A). The results show that the deletion of promoter does not dampen the promoter activity, indicating that region from −353 to ATG contains elements that can be activated by CiNAC5 (Fig. 3.14B). In this region, four putative NACBSs were mutated or deleted for further analysis. Single mutation on the core motif of NACBS (CGTC, located -167 upstream ATG; TACG, located -279 upstream ATG) and their double mutation maintains the same activation of *p1-FEH1* driven by CiNAC5 (Fig. 3.14C). Likewise, deletion of the complete NACBS at site -200 upstream ATG does not show impact on promoter activity. However, a relatively large fragment deletion on site -140 upstream ATG

decreased the CiNAC5 activation on *p1-FEH* to half level compared to the wild type of promoter (Fig. 3.14D).

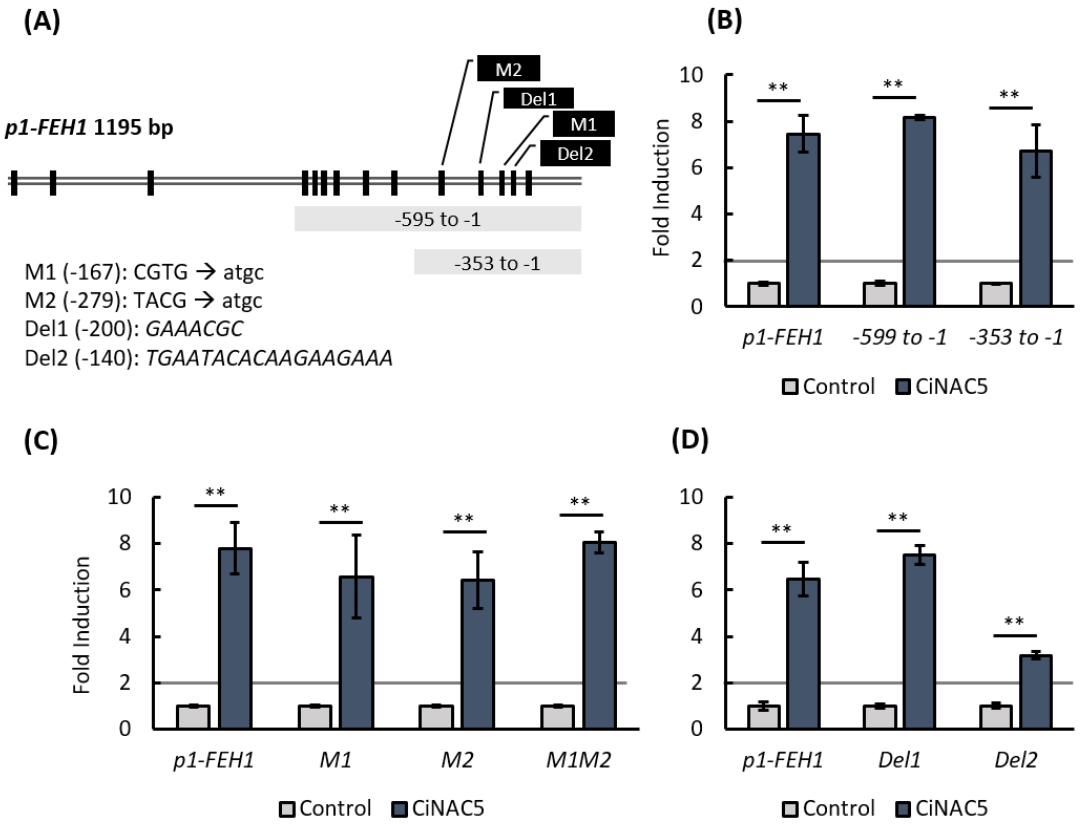

Figure 3.14 Promoters deletion analysis of *1-FEH1*. (A) Schematic of reporter constructs containing different parts of *p1-FEH1*. Nany blue bars indicate the location of putative NACBS on promoter of *1-FEH1*. Two fragments of *p1-FEH1* (595bp and 353 bp) were individually fused upstream of a firefly luciferase gene. Mutation (M) and deletion (Del) of specific NACBS on *p1-FEH1* are indicated in grey boxes. Transient expression was performed in chicory mesophyll protoplasts via PEG-method. Each promoter linked to a firefly luciferase reporter gene was co-transfected into cells with the effector construct *pART7-CiNAC5* or with empty *pART7* vector as control. The *Renilla* luciferase was fused in reporter as a control for normalization in each transfection. **(B)** Promoter activity of deletion on *p1-FEH1* in present of CiNAC5. **(C)** Promoter activity of *p1-FEH1* with NACBS mutation or **(D)** deletion in presence of CiNAC5. Basal promoter activity is expressed as relative LUC activity (Firefly/*Renilla*). The error bars indicate means ± SD of three technical replicates. Student's t-test was used to determine the significance: * $P<0.05$, ** $P<0.01$. The results were confirmed in two independent experiments.

3.3.4 Screening of R2R3-MYB transcription factors that active the promoter of *1-FEH*

In previous study (Wei, dissertation 2017), multiple R2R3-MYB transcription factors were identified in chicory that were believed to play a role in the regulation of inulin

metabolism. To investigate their function on the promoter of *1-FEH*, I performed dual luciferase assay to screen the CiMYB transcription factors. Interestingly, the impacts of CiMYB transcription factors on the promoter of *1-FEH1* were lower than 2-fold threshold. In contrast, CiMYB1/2/3/4/5/17/29/34 showed significant induction on *p1-FEH2a* and *1-FEH2b* with 2- to 15-fold (Fig. 3.15). CiMYB5 showed most remarkable activation on both *p1-FEH2a* and *1-FEH2b*, with induction of 15-fold and 10-fold, respectively.

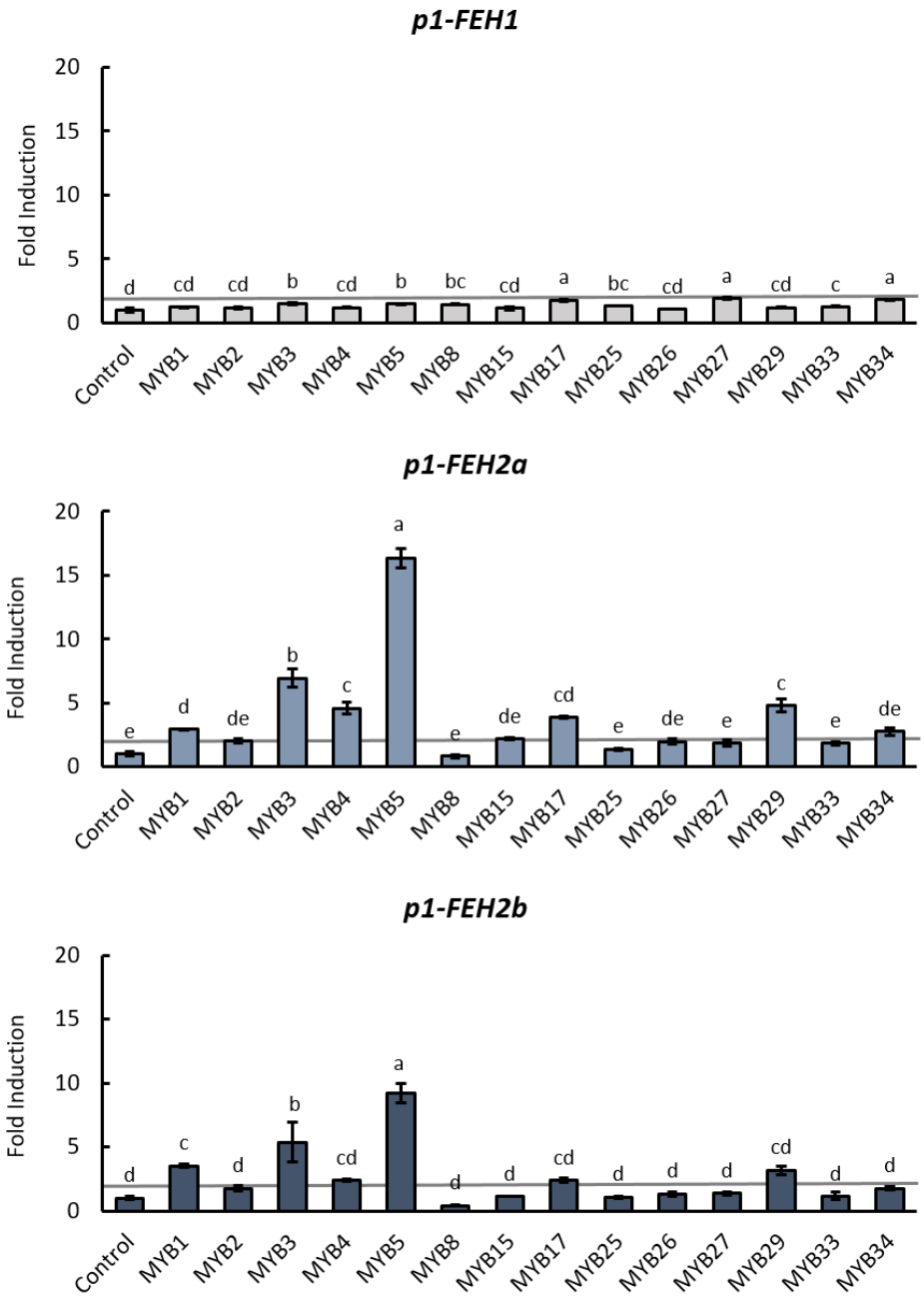

Figure 3.15 CiMYB5 activates the promoters of *1-FEH2a* and *1-FEH2b*. In the reporter construct, the 5'UTR/promoter regions of *1-FEH1* (1195 bp), *1-FEH2a* (1149 bp), *1-FEH2b* (1740 bp) are fused

upstream of a firefly luciferase gene. Transient expression was performed in chicory mesophyll protoplast via PEG-method. The promoter linked to a firefly luciferase reporter gene was co-transfected into cells with the effector construct (pART7-CiMYB), or with empty pART7 vector as control. The *Renilla* luciferase was fused in reporter as a control for normalization in each transfection. Fold induction of *1-FEH* promoter activities in the presence of CiMYB relative to the empty vector control. Basal promoter activity is expressed as relative LUC activity (Firefly/*Renilla*). The error bars indicate means ± SD of three technical replicates. One way ANOVA test was used to determine the significances: $p < 0.05$. The results were confirmed in two independent experiments.

3.3.5 CiDREB1 and CiDREB2 only activate the promoter of *1-FEH2b*

As shown in the Fig. 3.16, CiDREB1A/1C activate the promoter of *1-FEH2b* by 2-fold induction, and CiDREB2A/2B shows stronger activation on *p1-FEH2b* with 6- to 8- fold induction. Interestingly, *p1-FEH2a* is not activated by either CiDREB1 or CiDREB2, despite that it shares a high sequence similarity with *p1-FEH2b*. Although several putative DRE *cis*-elements present on *p1-FEH1*, neither CiDREB1 nor CiDREB2 show an effect on the promoter of *1-FEH1*.

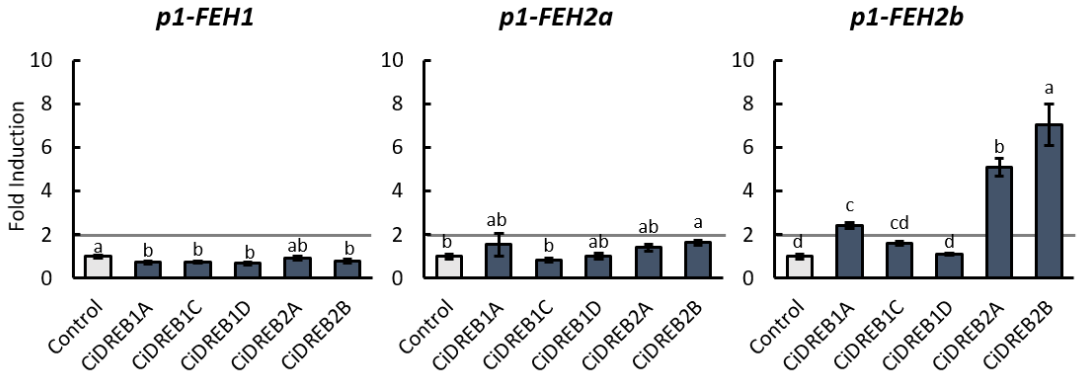

Figure 3.16 Effects of CiDREB1 and CiDREB2 on the promoters of *1-FEH1*, *1-FEH2a* and *1-FEH2b*. In the reporter construct, the 5'UTR/promoter region of *1-FEH2b* (1740 bp) are fused upstream of a firefly luciferase gene. Transient expression was performed in chicory mesophyll protoplasts via PEG-method. The promoter linked to a firefly luciferase reporter gene was co-transfected into cells with the effector construct (*pART7-CiDRERB*), or with empty *pART7* vector as control. The *Renilla* luciferase was fused in the reporter construct as a control for normalization in each transfection. Fold induction of *1-FEH2b* promoter activities in the presence of CiDREB relative to the empty vector control. Basal promoter activity is expressed as relative LUC activity (Firefly/*Renilla*). The error bars indicate means ± SD of three technical replicates. One way ANOVA test was used to determine the significances: $p < 0.05$. The results were confirmed in two independent experiments.

3.3.6 Mutation of DRE in the promoter of *1-FEH2b* abolishes the activation by CiDREB1 and CiDREB2

To investigate the difference in CiDREB activation on the promoter of *1-FEH2a* and *1-FEH2b*, I compared the promoter sequence and found a putative DRE *cis*-element on *p1-FEH2a* (AATTCGGTAG, located -136 upstream ATG) containing one base pair variance on the core-motif compared to *p1-FEH2b* (AAGTCGGTAG, located -138 upstream ATG). To explore whether this element is crucial for the function of CiDREB on *p1-FEH2b*, I generated a DRE mutation (AAtTCtGTAG at site -138) on the promoter of *1-FEH2b*, and subjected the corresponding reporter to dual luciferase assay with CiDREB. As expected, deletion or mutation of DRE on *p1-FEH2b* abrogate the activation by CiDREB2A and CiDREB2B (Fig. 3.17 and Fig. 3.18). Interestingly, mutation of DRE also interrupts the activation of *p1-FEH2b* by CiMYB5 which was reported to function as an activator on the *p1-FEH2a* and *p1-FEH2b* (Wei, dissertation 2017).

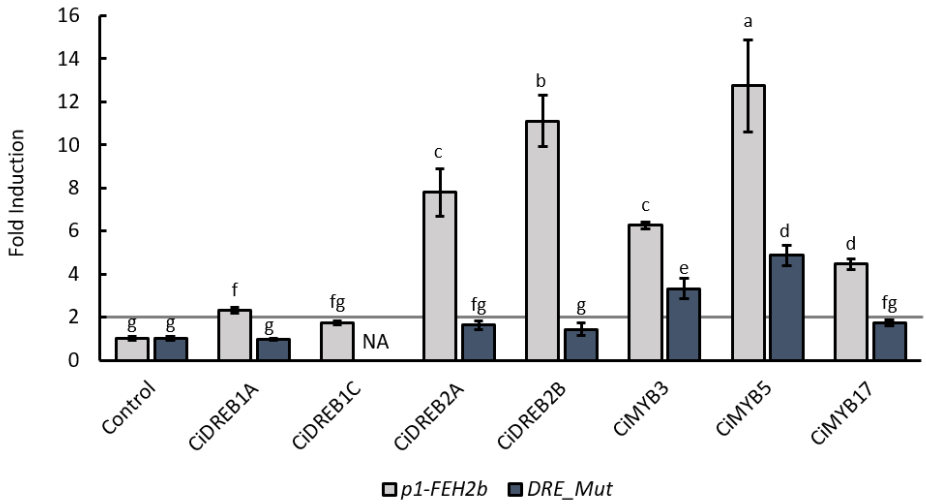

Figure 3.17 Impact of DRE mutation on *p1-FEH2b* promoter activity driven by CiDREB and CiMYB. In the reporter construct, the 5'UTR/promoter regions of *1-FEH2b* (1740 bp) were fused upstream of a firefly luciferase gene. DRE_Mut represents DRE mutation (AAtTCtGTAG at site -138) on *p1-FEH2b*. Transient expression was performed in chicory mesophyll protoplasts via PEG-method. The promoter linked to a firefly luciferase reporter gene was co-transfected into cells with the effector construct (*pART7-CiDRERB* or *pART7-CiMYB*), or with empty *pART7* vector as control. The *Renilla* luciferase was fused in the reporter construct as a control for normalization in each transfection. Fold induction of *1-FEH2b* promoter activities in the presence of CiDREB relative to the empty vector control. Basal promoter activity is expressed as relative LUC activity (Firefly/*Renilla*). The error bars

indicate means ± SD of three technical replicates. One way ANOVA test was used to determine the significances: $p < 0.05$. The results were confirmed in two independent experiments.

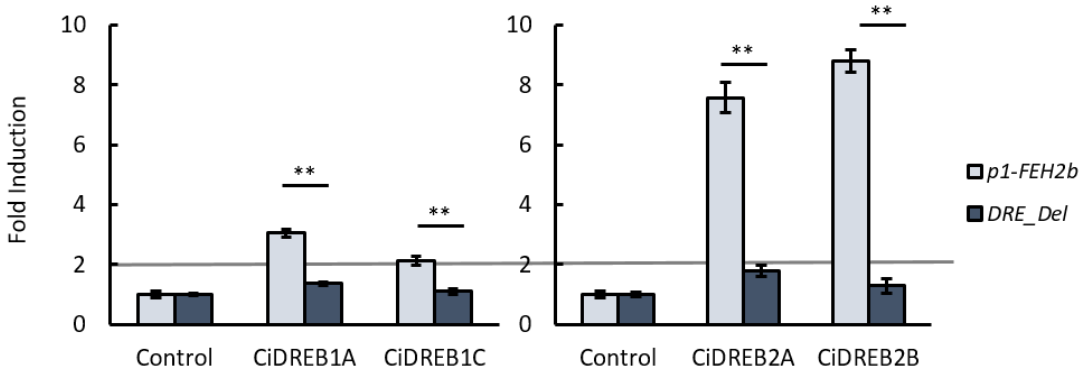

Figure 3.18 Impact of DRE deletion on *p1-FEH2b* activity driven by CiDREB1 and CiDREB2. In the reporter construct, partial promoter regions of *1-FEH2b* (-363 to -46) were fused upstream of a firefly luciferase gene. DRE_Del represents DRE deletion (at site -138) on *p1-FEH2b*. Transient expression was performed in chicory mesophyll protoplast via PEG-method. The promoter linked to a firefly luciferase reporter gene was co-transfected into cells with the effector construct (pART7-CiDRERB), or with empty pART7 vector as control. The *Renilla* luciferase was fused in reporter as a control for normalization in each transfection. Fold induction of *1-FEH2b* promoter activities in the presence of CiDREB relative to the empty vector control. Basal promoter activity is expressed as relative LUC activity (Firefly/*Renilla*). The error bars indicate means ± SD of three technical replicates.

3.3.7 CiMYB5 and CiDREB2B synergistically co-activate *p1-FEH2b*

DRE mutation on *p1-FEH2b* subsides the activation of CiMYB5, implying a connection between CiMYB and CiDREB. To explore this relationship, I conducted both two transcription factors into the dual luciferase assay. As shown in the Fig. 3.19B, CiDREB2B and CiMYB5 have 8- to 9- fold induction on *p1-FEH2b* when they are transfected individually. Co-transfection with CiDREB2B and CiMYB5 shows a rather high activation on *p1-FEH2b* by 36-fold change, indicating that two transcription factors have synergistic function. Similar result had been found between CiDREB2B and CiMYB3, which show relative high activation on p*1-FEH2b* by 20-fold.

Interestingly, CiDREB2A and CiDREB2B do not activate *p1-FEH2a*, and therefore no synergistic activation between CiDREB2 and CiMYB is observed on *p1-FEH2a* (Fig. 3.19A). Although CiMYB5 activation reduced on *p1-FEH2b* due to the DRE mutation, its activation on *p1-FEH2a* maintains at a comparable level as on *p1-FEH2b*, despite that the one base variance on the DRE core-motif.

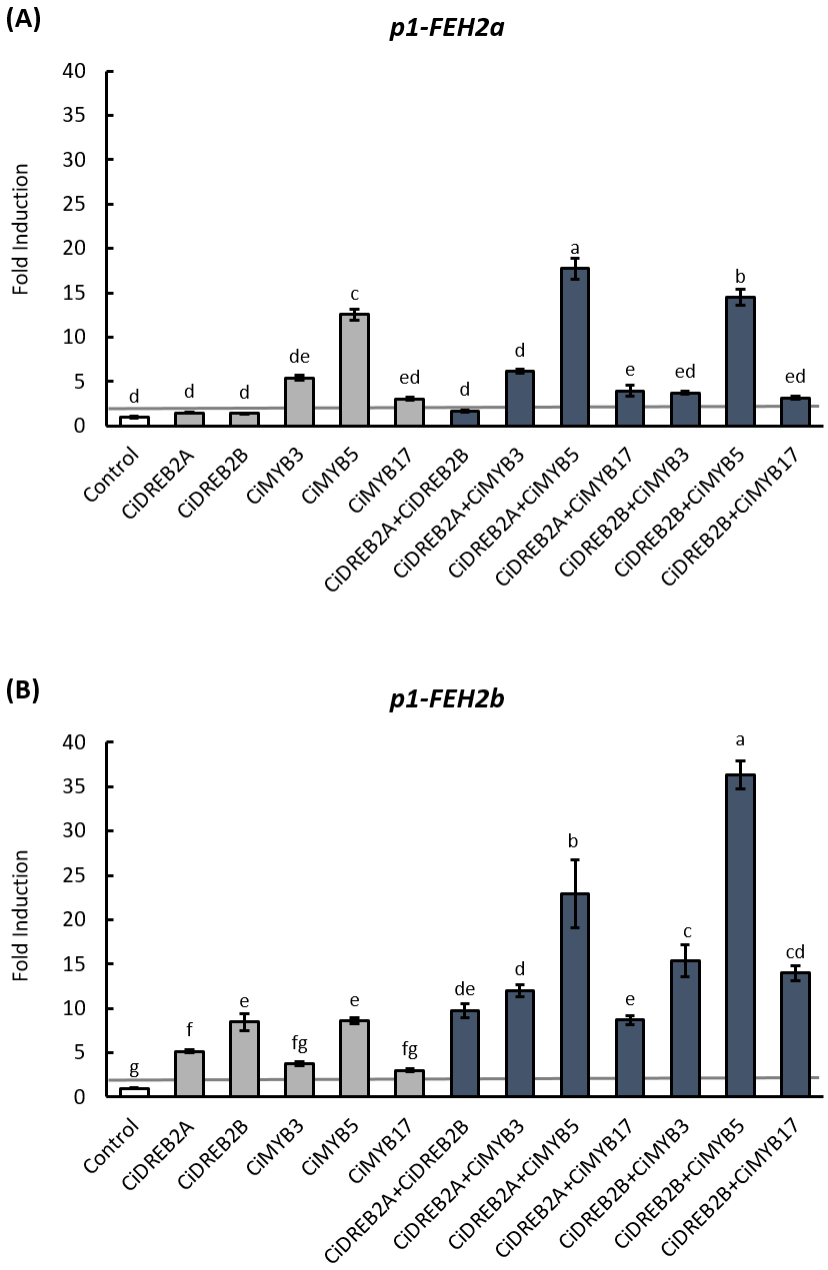

Figure 3.19 Effect of CiDREB2 and CiMYB on the promoters of *1-FEH2a* and *1-FEH2b*. In the reporter construct, the 5'UTR/promoter regions of *1-FEH2a* **(A)** or *1-FEH2b* **(B)** are fused upstream of a firefly luciferase gene. Transient expression was performed in chicory mesophyll protoplasts via PEG-method. The promoter linked to a firefly luciferase reporter gene was co-transfected into cells with the one or two effector constructs (*pART7-CiDRERB* and *pART7-CiMYB*), or with empty *pART7* vector as control. The *Renilla* luciferase was fused in reporter as a control for normalization in each transfection. Fold induction of promoter activities in the presence of CiDREB and/or CiMYB relative to the empty vector control. Basal promoter activity is expressed as relative LUC activity (Firefly/*Renilla*). The error bars indicate means ± SD of three technical replicates. One way ANOVA test was used to determine the significances: $p < 0.05$. The results were confirmed in two independent experiments.

3.3.8 CiMYB5 activates the promoter of *CiDREB2B*

Many transcription factors show the capability of self-regulation to enhance the signal when they are initially upregulated. To obtain the knowledge of the transcription factors identified in this study, I cloned the corresponding promoter sequence into the report construct and transfected with other transcription factors. Interestingly, CiMYB5 does not only show synergistic function with CiDREB2B, but also activate its promoter by around 3-fold induction. Both CiDREB2A and CiDREB2B do not have impact on its own promoter (Fig. 3.20).

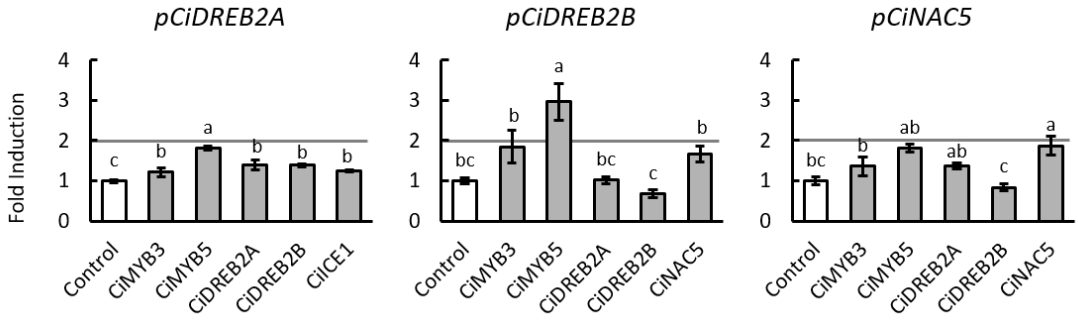

Figure 3.20 Promoter activity of *CiDREB2A*, *CiDREB2B* and *CiNAC5*. In the reporter construct, the 5'UTR/promoter regions of *CiDREB2A* (1352 bp), *CiDREB2B* (1391 bp) or *CiNAC5* (980 bp) are fused upstream of a firefly luciferase gene, respectively. Transient expression was performed in chicory mesophyll protoplasts via PEG-method. The promoter linked to a firefly luciferase reporter gene was co-transfected into cells with the one or two effector constructs (*pART7-TF*), or with empty *pART7* vector as control. The *Renilla* luciferase was fused in reporter as a control for normalization in each transfection. Fold induction of promoter activities in the presence of TF relative to the empty vector control. Basal promoter activity is expressed as relative LUC activity (Firefly/*Renilla*). The error bars indicate means ± SD of three technical replicates. One way ANOVA test was used to determine the significances: $p < 0.05$. The results were confirmed in two independent experiments.

3.4 Investigation of protein-DNA interaction between CiDREB and *p1-FEH*

3.4.1 CiDREB is expressed as insoluble protein in a prokaryotic system

Previous study in *Arabidopsis thaliana* showed that AtDREB bind to the *cis*-element DRE on the promoter of *rd29A* (Narusaka et al. 2003). In order to express and purify CiDREB proteins and determine its DNA binding capacity, I cloned the coding sequence of the transcription factors into expression vector *pETG10A* and used IPTG (Isopropyl β- d-1-thiogalactopyranoside) to induce protein expression in *E.coli* BL21 strain (Fig. 3.21). Five CiDREB proteins were successfully expressed after induction

and were abundantly present in inclusion bodies. To obtain a functional and soluble protein, purified inclusion bodies were solubilized with solubilization buffer containing 2M Urea and refolded with buffer containing 10% sucrose. I used the promoter fragment of *rd29A* as probe and performed electrophoretic mobility shift assays (EMSA) to determine the functionality of refolded CiDREB1C. Results show that the refolding buffer produced relatively low amounts but effective protein (Fig. 3.21B) and band shift indicates that CiDREB1C binds to a probe from the promoter of *rd29A* (Fig. 3.22A). Therefore, this method was used for solubilization of inclusion body to generate function transcription factor.

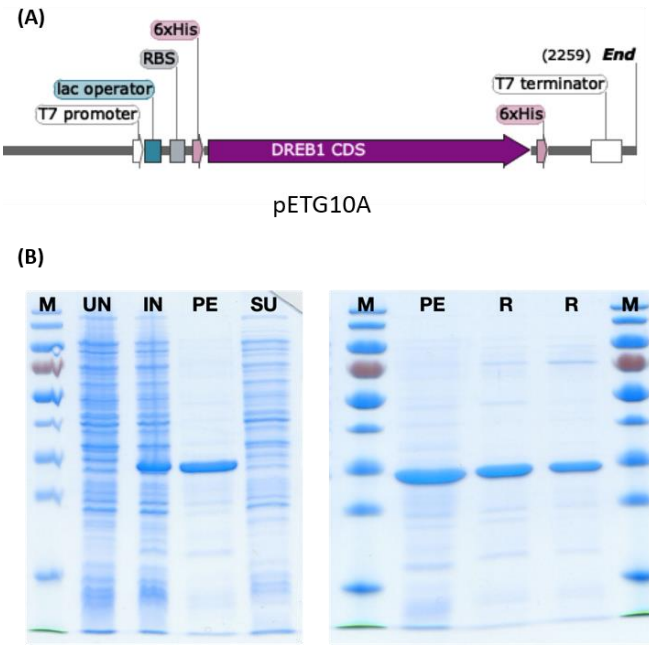

Figure 3.21 Expression analysis of recombinant CiDREB1C protein in *E. coli*. (A) Coding sequence of CiDREB1C was cloned into expression construct pETG-10A fused target protein with 6His-tag at the N-terminal.

(B) *E.coli* BL21were used for protein expression. Samples were harvested and analyzed by SDS-PAGE. UN: Un-induced; IN: Induced; PE: Pellet; SU: Supernatant; R: Re-folded protein; M: Marker.

3.4.2 CiDREB1C and CiDREB1D specifically bind to *p1-FEH2b* but not *p1-FEH2a*

CiDREB1C has the capability to bind the promoter of *rd29A* as shown in Fig. 22A. Taking the results of the dual luciferase assay into account, it is interesting to know whether the one base pair variance of DRE on *p1-FEH2a* and *p1-FEH2b* have different effect on protein-DNA binding and thus on promoter activity. To perform EMSA, 40bp promoter fragment containing the putative DRE of *1-FEH* was used as probe and labeled with CY5 at the 5'-end. I designed a DRE-null probe named as *Dummy* and used here to determine the protein specificity. As shown in Fig. 3.22B, CiDREB1C bound to the *p1-FEH2b* and showed a significant band shift. The interaction between CiDREB1C and *p1-FEH2b* vanished with the addition of

unlabeled *p1-FEH2b* or *rd29A* as competitors. Notably, unlabeled probes containing mutated DRE (*p1-FEH2a* and *Dummy*) did not compete with transcription factor binding and thus did not affect the interaction between CiDREB1C and *p1-FEH2b*. I observed band shift between CiDREB1C and *p1-FEH1* (Fig. 3.22C) although no activation found on the promoter of *1-FEH* by CiDRE1C. Similar results were also found in the case of CiDREB1D that binds to *p1-FEH1* and *p1-FEH2b* (Fig. 3.23), while neither CiDREB1C nor CiDREB1D bound to *p1-FEH2a* due to the point mutation on the DRE core-motif.

CiDREB1A bound to *rd29A*, suggesting that the DRE *cis*-element is conserved and specific for the DREB protein family. Although the activation of *p1-FEH2b* by CiDREB1A was higher than that of CiDREB1C and CiDREB1D in the dual luciferase assay, unexpectedly, *p1-FEH2b* was bound weaker to CiDERB1A than to CiDREB1C or CiDREB1D, appearing as a smear on the gel picture (Fig. 3.24).

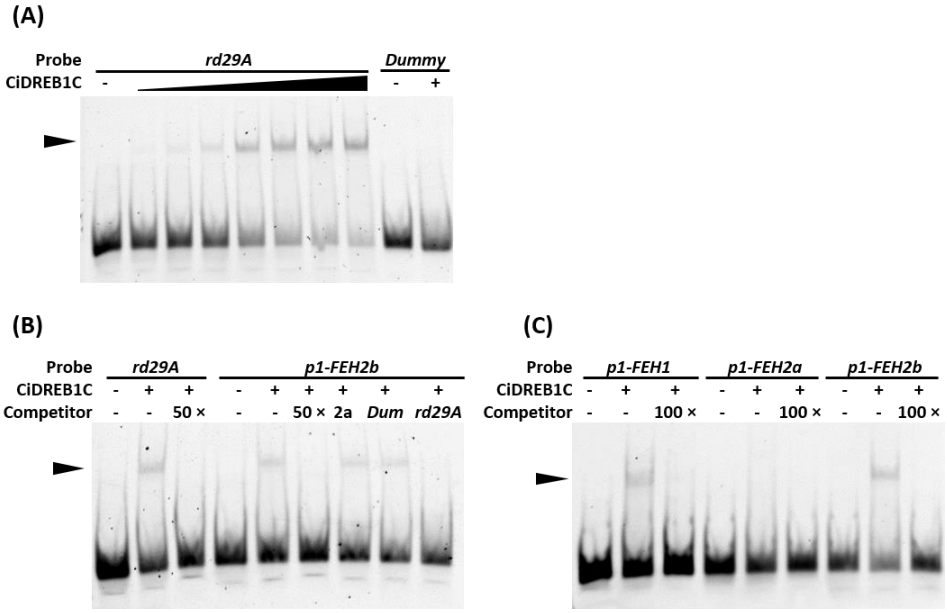

Figure 3.22 Electrophoretic mobility shift assays of CiDREB1C protein and promoter fragment of *1-FEH*. Full-length protein of CiDREB1C fussed with 6His-tag at N-terminal were used for detecting the interaction. Black arrow heads indicate the band of DNA-protein complex. 40-mer promoter fragments were labeled with CY5 at the 5'-end. 0.2 pmol labeled probes were used for visualizing the DNA fragment. 50- or 100-times unlabeled probes were used as competitors. **(A)** Binding capacity of CiDREB1C to *rd29A*. Protein were added in gradient concentration in 50 ng, 100 ng, 250 ng, 500 ng, 1000 ng, 1500 ng, 2000 ng. **(B)** 500 ng CiDREB1C protein were incubated with probes of *p1-FEH2b* with/without different competitors. Dum: *Dummy*; 2a: fragment of *p1-FEH2a*. **(C)** 1500 ng CiDREB1C protein were incubated with probes of *p1-FEH1*, *p1-FEH2a* or *p1-FEH2b*.

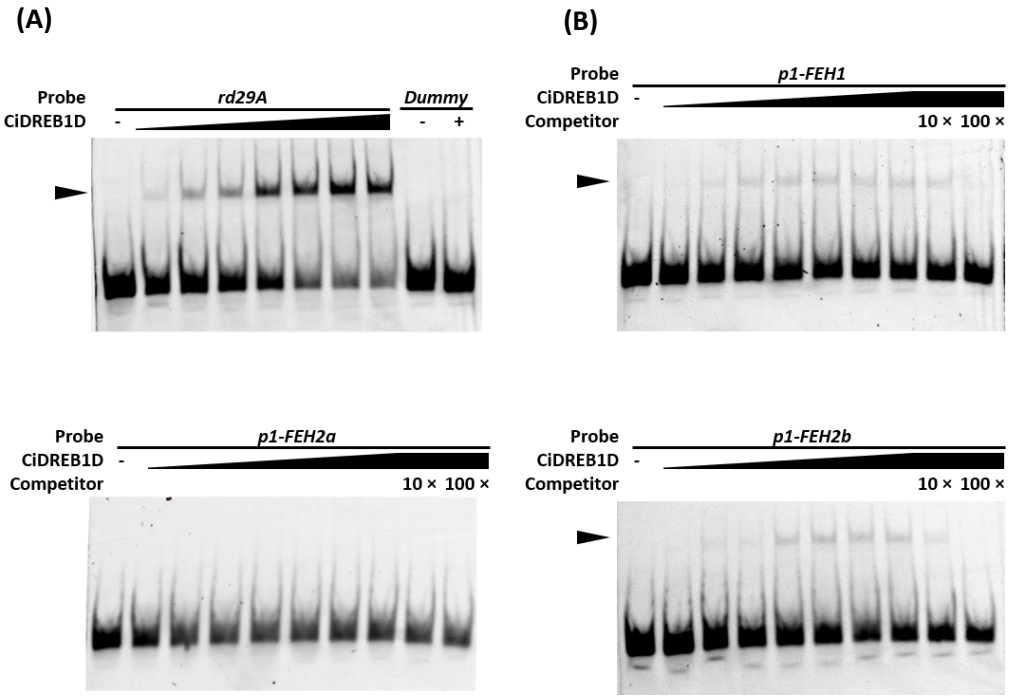

Figure 3.23 Electrophoretic mobility shift assays of CiDREB1A protein and promoter fragment of *1-FEH*. Full-length protein of CiDREB1A fussed with 6His-tag at N-terminal was used for detecting the interaction. Black arrow heads indicate the band of DNA-protein complex. 40-mer promoter fragments were labeled with CY5 at the 5'-end. 0.2 pmol labeled probes were used for visualizing the DNA fragment. 100 times unlabeled probes were used as competitors. **(A)** Binding capacity of CiDREB1A to *rd29A*. Proteins were added in gradient concentration of 50 ng, 150 ng, 300 ng, 600 ng, 1200 ng, 1800 ng, 2400 ng, respectively. **(B)** 1800 ng CiDREB1A proteins were incubated with probes of *p1-FEH* with/without competitors.

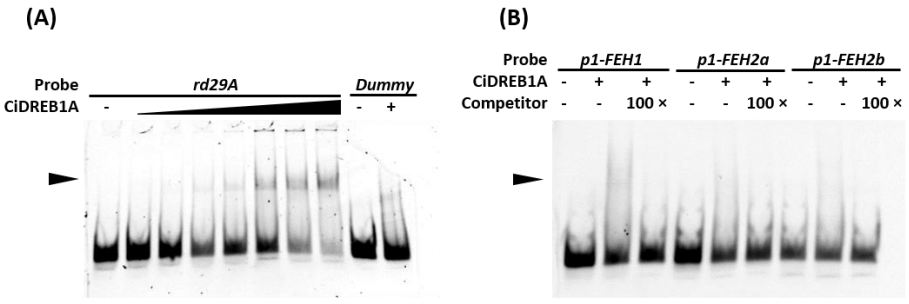

Figure 3.24 Electrophoretic mobility shift assays of CiDREB1A protein and promoter fragment of *1-FEH*. Full-length protein of CiDREB1A fussed with 6His-tag at N-terminal was used for detecting the interaction. Black arrow heads indicate the band of DNA-protein complex. 40-mer promoter fragments were labeled with CY5 at the 5'-end. 0.2 pmol labeled probes were used for visualizing the DNA fragment. 100 times unlabeled probes were used as competitors. (A) Binding capacity of CiDREB1A to *rd29A*. Proteins were added in gradient concentration of 50 ng, 150 ng, 300 ng, 600 ng, 1200 ng, 1800 ng, 2400 ng, respectively. (B) 1800 ng CiDREB1A proteins were incubated with probes of *p1-FEH* with/without competitors.

3.4.3 CiDREB2 specifically bind to *p1-FEH2b* but not *p1-FEH2a*

In dual luciferase assays, CiDREB2A and CiDREB2B induce high promoter activation of *p1-FEH2b*, demonstrating their binding capability to bind the promoter. As expected, CiDREB2B specifically bound to *p1-FEH2b* by recognizing the DRE element, while failing to bind to *p1-FEH2a* due to the mutation in the DRE core-motif. The intensity of CiDREB2B-induced band shift of *p1-FEH2b* decreased with the addition of unlabeled competitors. Furthermore, CiDREB2A resulted in reduced binding of *p1-FEH2b* and *rd29A*, which may be due to inefficient protein production (Fig. 3.25).

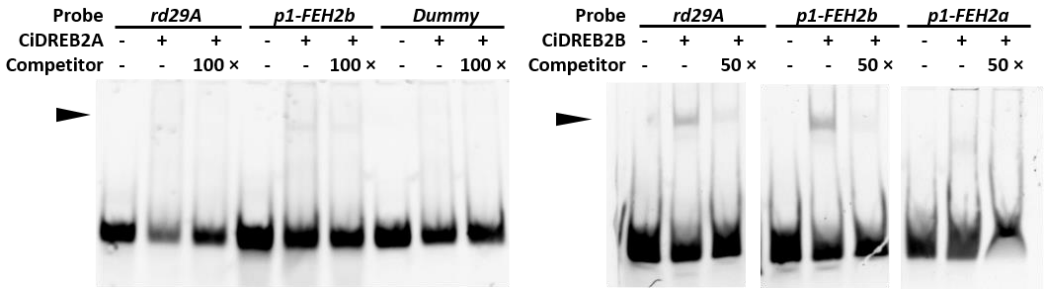

Figure 3.25 Electrophoretic mobility shift assays of CiDREB2A/CiDREB2B protein and promoter fragment of *1-FEH*. Full-length protein of CiDREB2A/CiDREB2B with 6His-tag at N-terminal was used for detecting the interaction. Black arrow heads indicate the band of DNA-protein complex. 40-mer promoter fragments were labeled with CY5 at the 5'-end. 0.2 pmol labeled probes were used for visualizing the DNA fragment. 50- or 100-times unlabeled probes were used as competitors.

3.5 Protein-protein interaction between CiDREB2B and CiMYB3/5

Promoter analysis reveals that one MYB core motif (TAACTA) located -148 bp upstream from ATG of *p1-FEH2b*, which is 4 bp from DRE. Considering the synergistic function of CiDREB2B and CiMYB5 on *p1-FEH2b*, I performed yeast-two-hybrid to investigate whether these two transcription factors interact with each other. CiMYB3 and CiMYB5 were fused with Gal4 activating domain and CiDREB2B was fused with Gal4 binding domain. Construct were transformed into competent AH109 yeast cells, which is unable to grow on media that lack essential amino acids of histidine and adenine. As a result of two-hybrid interactions, colonies are able to grow on drop out media and express Mel1 that turn blue in the presence of the chromagenic substrate X-α-Gal (5-Bromo-4-chloro-3-indolyl-α-D-galactopyranoside). GADT7-T with GBKT7-53 and with GBKT7-Lam were used as

positive and negative control in this experiment, respectively. As shown in Fig. 3.26, CiDREB2B showed protein-protein interaction with CiMYB3 and CiMYB5. However, CiDREB2A was not observed to interact with CiMYB3 or CiMYB5 (Fig. 3.26). Preliminary result of luciferase complementation assay (LCA) was corresponding to the yeast-two-hybrid results, in which a strong chemiluminescence signal were detected between fusion protein CiMYB5:Nluc and Cluc:CiDREB2B (Fig. 3.27), indicating a protein-protein interaction.

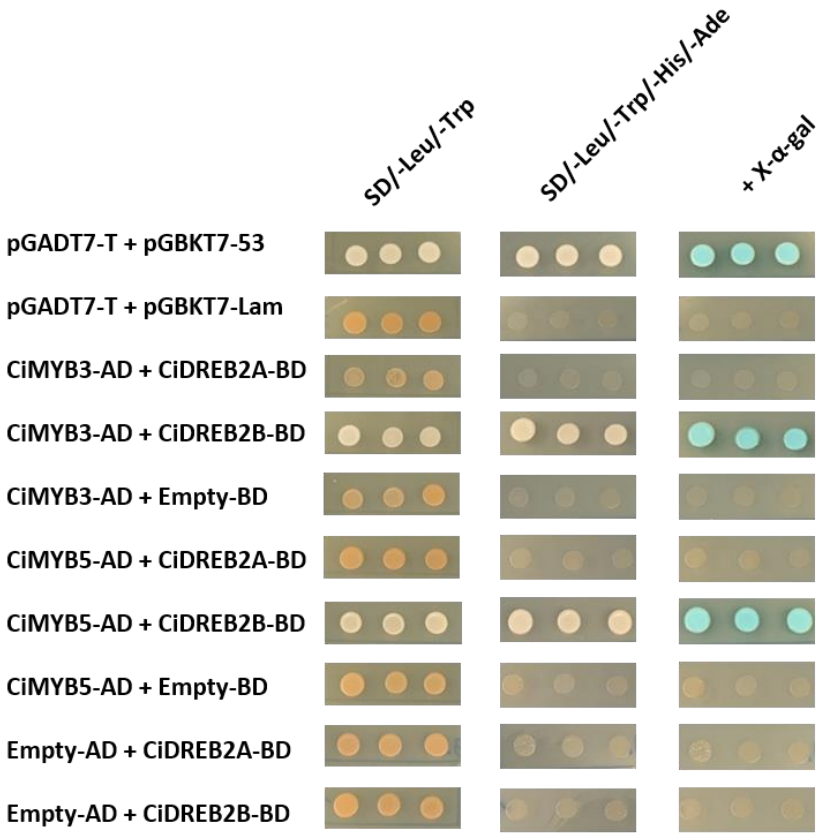

Figure 3.26 Protein-protein interaction between CiDREB and CiMYB in Y2H assays. Bait protein is expressed as a fusion with the Gal4 DNA-BD and prey protein with Gal4 AD in yeast strain AH109. SD/–Leu/–Trp dropout supplement is used to select for the bait and prey plasmids. SD/–Ade/–His/–Leu/–Trp dropout supplement is used to select for the bait and prey plasmids, and to determine the activation of the Gal-responsive *HIS3* and *ADE2* genes. X-α-gal was used to detect Gal-responsive α-galactosidase activity. pGBKT7-53 encoding the Gal4 DNA-BD fused with murine p53 and pGADT7-T encoding the Gal4 AD fused with SV40 large T-antigen were used as positive control. A negative control was performed using pGBKT7-Lam (Gal4 BD fused with lamin) and pGADT7-T.

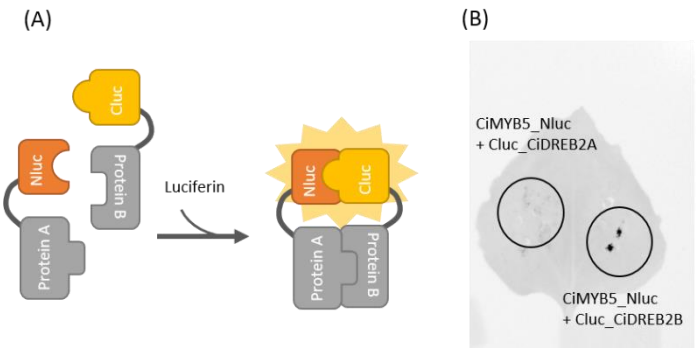

Figure 3.27 Protein-protein interaction detected by a CCD imaging system. (A) Schematic for LUC complementation resulting from NLuc (N-terminal of luciferase) and CLuc (C-termial of luciferase) fusion proteins. (B) *N. benthamiana* leaf co-infiltrated with Agrobacterium containing *CLuc:DREB2A* or *Cluc:DREB2B* and *CiMYB5:NLuc*. The luminescence images were captured using a ImageQuant™ LAS 4000 imaging system. The black circles show the range of luminescence.

3.6 Water deficiency and heat stress affect the expression of genes related to fructan metabolism

3.6.1 Heat stress (45 °C) increased *1-FEH* expression and repressed *1-SST* and *1-FFT* expression

Previous results have revealed a detailed mechanism of CiDREB2B that interact with CiMYB3/5 and co-activate the promoter of *1-FEH2b*. However, during the cold treatment of young seedling or mature taproot of chicory, CiDREB2B does not respond to low temperature. In *Arabidopsis thaliana*, DREB subgroup 2 is considered to respond to drought and heat stress, so I performed a heat treatment to investigate whether CiDREB2B responds to high temperature and consequently affect the expression of *1-FEH*. Interestingly, three isoforms of *1-FEH* were induced under 45 °C. *1-FEH2a* and *1-FEH2b* showed the heat induction at 5 hours after treatment and increase to high transcript level after 24 hours. For *1-FEH1* only a moderate up-regulation after 24 hour could be observed. In contrast, the expression of fructose biosynthesis genes *1-SST* and *1-FFT* were repressed over time under heat stress (Fig. 3.28).

Interestingly, *CiDREB2A* was upregulated by high temperature first observed after 5 hours, indicating that *CiDREB2A* responds to dynamic temperature change in both directions. The expression levels of *CiDREB2B*, *CiMYB3* and *CiMYB5* increased slightly after 5 hours and stronger induction showed after 24 hours, suggesting that the co-activation of CiDREB2B and CiMYB5 on *p1-FEH2b* is involved in the heat responding pathway.

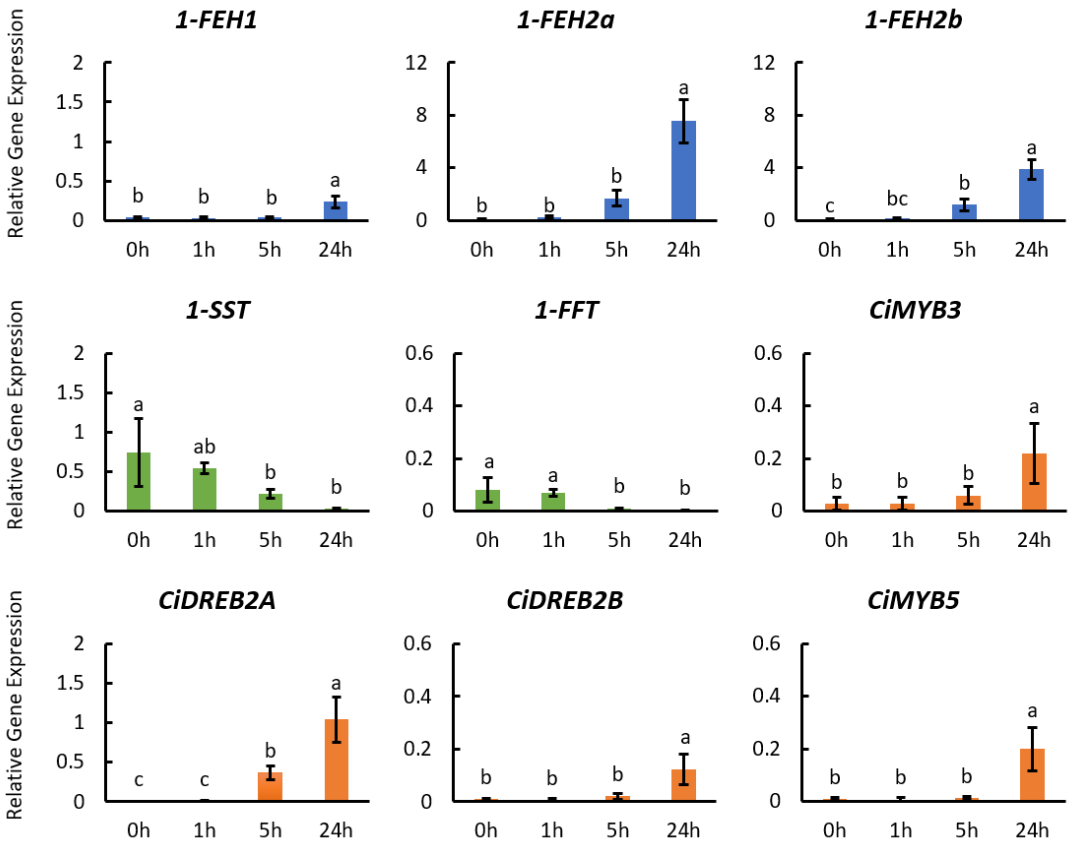

Figure 3.28 Impact of heat treatment (45°C±1) on transcript levels of FAZYs and transcription factors in taproots of 6-week-old chicory seedlings. Seedlings were transferred to incubator under 45°C±1 and taproot samples were collected at time points 0, 1, 5 and 24 hours after treatment. Transcript levels were determined by qRT-PCR and normalized against the expression of two reference genes *Actin* and *RPL19*. Relative gene expression was calculated with delta Ct method. The error bars represent standard deviation (n = 3). One way ANOVA test was used to determine the significances: $p < 0.05$.

3.6.2 Moderate heat treatment (37 °C) increased *1-FEH* expression and repressed *1-SST* and *1-FFT* expression

To further understand the effect of high temperature on genes related to fructan metabolism, I treated 6-week-old chicory seedlings at 37 °C for up to 72 hours. Corresponding to the 45 °C heat treatment, expression of *1-FEH2a* increased under 37 °C treatment and reached a peak after 48 hours (Fig. 3.29). Comparably, the heat induction of *1-FEH2b* was less pronounced, with the strongest induction after 6 hours and the transcript levels subsiding over time. Interestingly, *1-FEH1* exhibited a constant long-term expression pattern over time under 37°C treatment, which was similar to that of cold treatment. The expression *1-SST* and *1-FFT* were repressed

under 37 °C (Fig. 3.29), which was consistent with the observation in extreme heat treatment at 45 °C (Fig. 3.28).

CiDREB2A transcript level increased under 37 °C with peaking after 24 hours and gradually decreased afterwards, while *CiDREB2B* showed highest heat induction after 48 hours and maintained relatively high expression level subsequently. Expression of *CiMYB3* and *CiMYB5* increased after 6 hours and preserved along the heat treatment (Fig. 3.29). Notably, although CiNAC5 has been determined as the activator of *p1-FEH1*, its expression was repressed in the heat treatment (SFig. 3), which is contrary to the expression of *1-FEH1*.

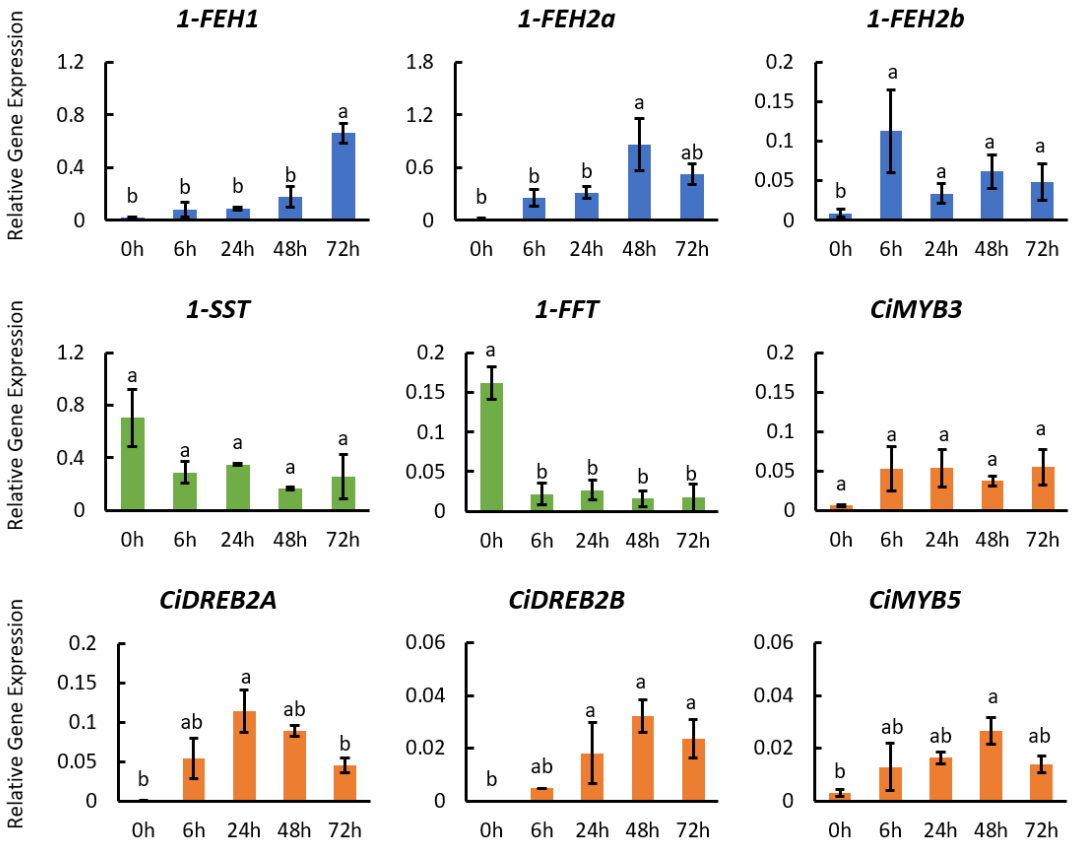

Figure 3.29 Impact of heat treatment (37°C±1) on transcript levels of FAZYs and transcription factors in taproots of 6-week-old chicory seedlings. Seedlings were transferred to incubator under 37°C±1 and taproot samples were collected at time points 0, 6, 24, 48 and 72 hour after treatment. Transcript levels were determined by qRT-PCR and normalized against the expression of two reference genes *Actin* and *RPL19*. Relative gene expression was calculated with delta Ct method. The error bars represent standard deviation (n = 3). One way ANOVA test was used to determine the significances: $p < 0.05$.

3.6.3 Water deficiency strongly increase *1-FEH1* transcript level

It has been found that fructan metabolism is related to stabilizing the cell membrane, which is affected by multiple abiotic stresses, such as drought. To understand whether water deficiency has an impact on the FAZY genes expression, a well-established hydroponic system was used to culture chicory. Seeds were germinated in a water-soaked sponge and transferred to Hoagland solution (Epstein and Bloom 2005) when the first true leaves expanded. 6 weeks after germination, Hoagland solution was drained out to simulate the water deficiency condition. Compared to PEG treatment or traditional soil-based drought treatment, the hydroponic drainage method avoids toxic side effect by chemicals and obtained instant water loss. Unlike cold treatment in which *1-FEH1* was upregulated slowly and moderately, water loss dramatically induced the expression of *1-FEH1* and further increased its level till 48 hours after treatment (Fig. 3.29). By comparison, water deficiency show less impact on *1-FEH2a* and *1-FEH2b* by inducing their expression until 24 hours and the transcript level were subsided afterwards. Transcription factors *CiDREB2A* showed an early induction by water loss after 6 hours, with its expression level gradually decreasing over time. While the expression of *CiMYB5* appeared later time point after 24 hours. Although CiNAC5 activates the promoter of *1-FEH1*, unexpectedly, water loss shows no impact on the expression of *CiNAC5* (SFig. 3) despite the strong induction on *1-FEH1*. Similarly, transcript level of *CiDREB2B* is not affected by water deficiency (Fig. 3.30).

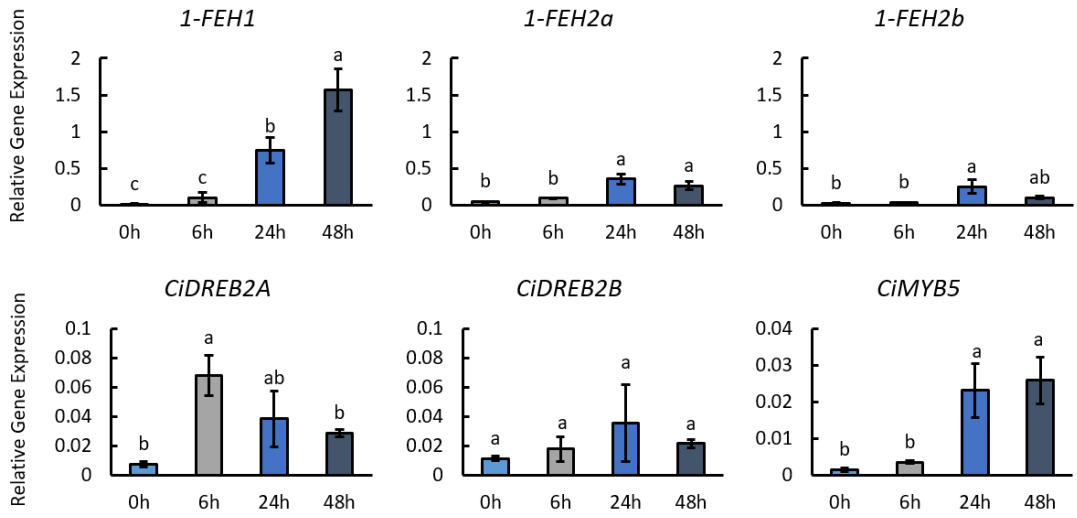

Figure 3.30 Impact of water deficiency on transcript level of 1-FEHs, CiDREB2 and CiMYB5. 6-week-old hydroponic seedlings were drained out solution and harvested at indicated time. Transcript

levels were determined by qRT-PCR and normalized against the expression of two reference genes Actin and RPL19. Relative gene expression was calculated with delta Ct method. The error bars represent standard deviation (n = 3-4). One way ANOVA test was used to determine the significances: $p < 0.05$.

3.7 CRISPR ribonucleoprotein-mediated genetic engineering in chicory: Protoplast regeneration and RNP assemble

Numerous lines of evidence have demonstrated distinct regulatory pathways governing the expression of *1-FEH1*, *1-FEH2a*, and *1-FEH2b* in response to environmental cues, suggesting that each isoform plays distinct roles in chicory. A potential approach for confirming the precise roles of these genes in inulin metabolism is to knockout the specific gene. The present chapter outlines a viable and effective methodology that employed CRISPR/Cas9 and protoplast regeneration technology to create accurate and targeted gene mutations in chicory via RNP delivery.

3.7.1 Different industrial chicory genotypes show variable capability of protoplast regeneration

To successfully obtain plants from protoplasts, the regeneration capacity of a single cell is crucial. It has been reported that the rate of protoplast regeneration is highly relevant to species and genotypes (Qi et al. 2021). In order to find the optimum genotypes of chicory for efficient protoplast regeneration, I tested the chicory commercial variety Zoom F1 and 5 components of the synthetic variety SELENITE S15C80090, S18C80026, S16C80007, S21C80004 and S15C80086. All varieties in this study yield high amount of protoplast, however cell division were only observed in Zoom, S16C80007, S15C80086 and S18C80026. S15C80086 and S18C80026 had high cell division rate, while less callus produced from microcalli. Interestingly, comparing to Zoom, S15C80086 and S18C80026 showed more asymmetric cell division in 5 days after protoplast isolation (Fig. 3.31).

Zoom showed relatively high rates of cell division and microcalli production, but significantly lower rates of callus growth from microcalli compared to other varieties. S16C80007 showed the most promising regeneration rate, which obtained the highest number of callus and regenerated plants after two months (Table 2, Fig. 3.32).

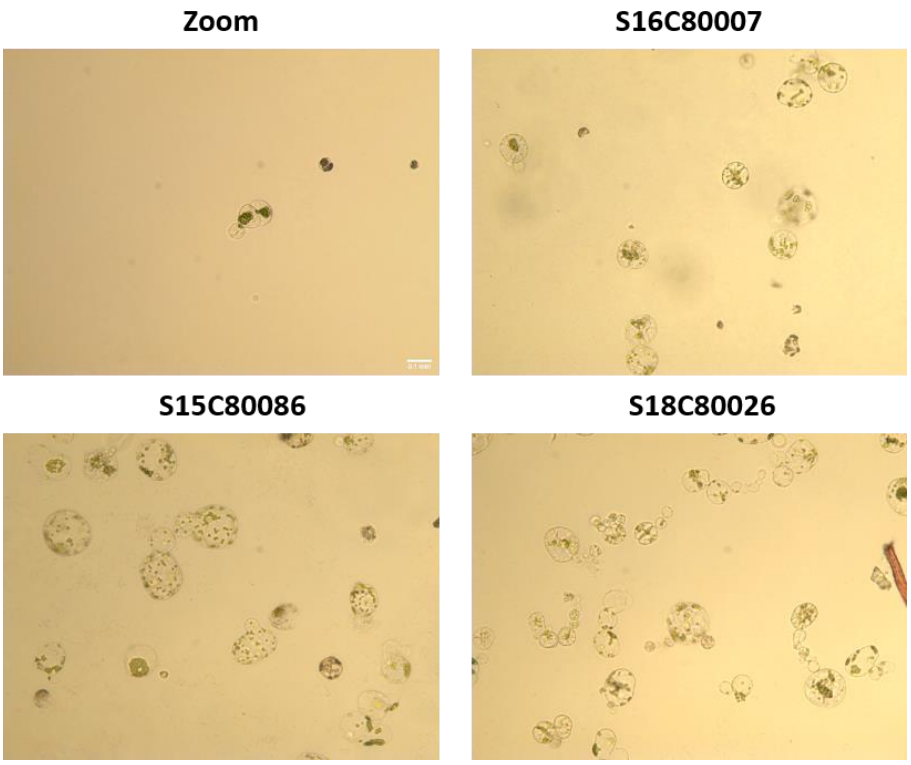

Figure 3.31 Comparison of protoplast division in different genotypes. Protoplast were culture in MC1 for 5 days after isolation. Scale bars = 100 μm

Table 2 Protoplast regeneration among genotypes

Genotypes	Protoplast Isolation	Cell division[a]	Microcalli[b]	Callus[c]	Plants
Zoom	+	39.13%	44.90%	2.13%	NA
S16C80007	+	25.98%	45.45%	62.77%	+
S21C80004	+	NA	NA	NA	NA
S15C80086	+	38.30%	+	26.60%	+
S18C80026	+	44.72%	+	22.98%	+
S15C80090	+	NA	NA	NA	NA

Data collected from two independent experiments.
[a] Percentage of dividing protoplast in 5 days after embedding.
[b] Percentage of microcalli produced from protoplast in 14 days after embedding.
[c] Percentage of callus grown from microcalli transferred to MC_3 solid medium.

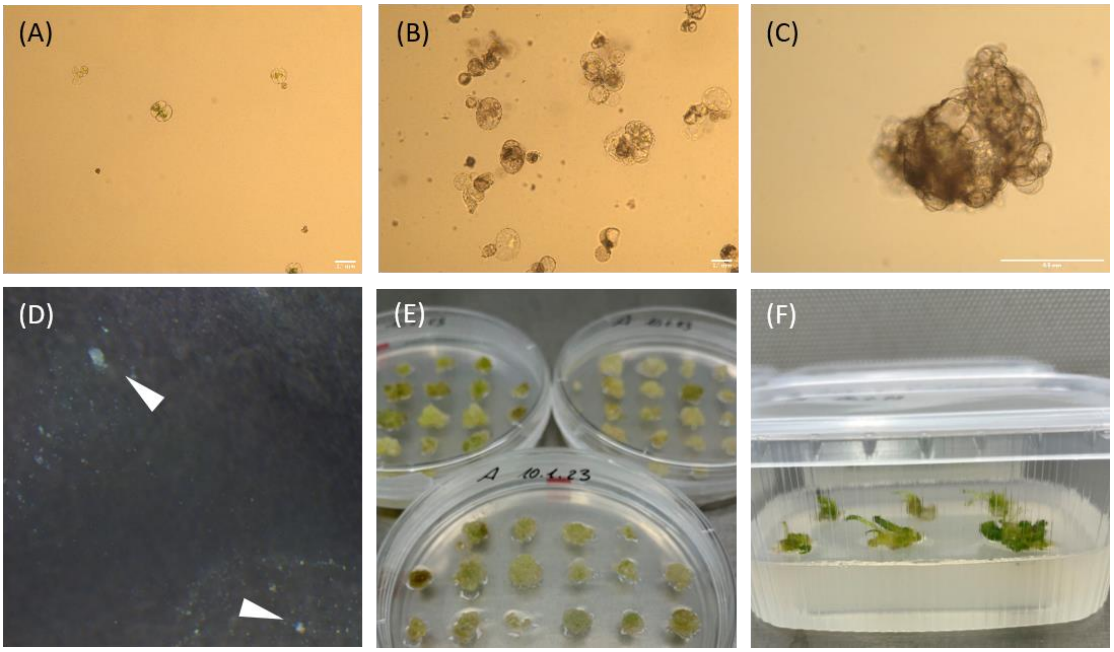

Figure 3.32 Chicory S16C80007 protoplast regeneration phases: (A) Mitotic division 5 days after protoplast embedding. (B) Microcalli after the 14 days. (C) Microcalli development after the 20 days. (D) White arrowheads: Microcalli under stereomicroscope. (E) Callus and shoot development. (F) Young regenerated plants.

3.7.2 Target design and *in vitro* cleavage of dsDNA with RNP complex

In order to devise specific single guide RNAs (sgRNAs) for the targeting of *1-FEH1* and *1-FEH2*, I adopted an approach whereby candidate sequences were initially generated using CRISPOR (Concordet and Haeussler 2018). Subsequently, to address the issue of off-target effects, the selected sequences were subjected to further refinement via the utilization of Cas-OFFinder (Bae, Park, and Kim 2014), which enabled the exclusion of sequences with high levels of off-target activity (Table S1). The candidate target, FEH1_195forw, was chosen for *1-FEH1* as it exhibited no alignment to other regions of the genome with a mismatch of less than three base pairs. Given the high level of similarity observed in the gene sequence of *1-FEH2a* and *1-FEH2b*, FEH2ab_514rev was selected as the target for both genes, owing to its minimal off-target rate. To determine the efficiency of a Cas9 ribonucleoprotein (RNP) complex on target site of DNA, selected sgRNAs were assembled *in vitro* with Cas9 protein and tested its ability to cleave double-strand DNA (dsDNA). Fragment (785 bp) of *1-FEH1* exon 3 were amplified by PCR and after column clean up, incubated with RNP containing specific sgRNA target to *1-FEH1*. Compared to control, the DNA were cleaved into two fragments (260 bp and 525 bp) in presence

of RNP (Fig. 3.33), indicating that the RNP complex was specific and effective to the target.

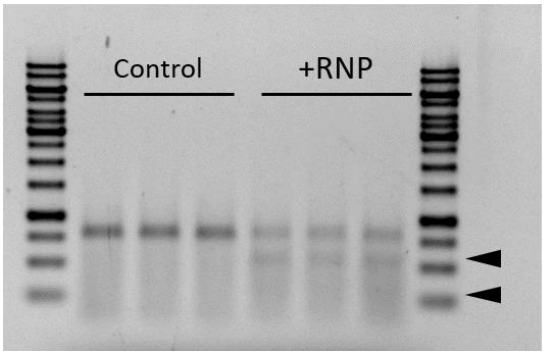

Figure 3.33 *In vitro* cleavage of 1-FEH1 exon 3 fragment by RNP. Exon 3 of *1-FEH1* were amplified by PCR and incubated with RNP. Control: Cas9 protein without sgRNA; RNP: assemble Cas9 protein and sgRNA complex.

3.7.3 RNP delivery and *in vivo* mutation detection

In order to assess the transfection efficiency of RNP complexes, GFP-tagged Cas9 proteins were employed and introduced into mesophyll protoplasts of chicory S16C80007 via PEG-method. Following a 24-hour incubation period, approximately two-thirds of the transfected cells were found to exhibit detectable GFP signal, as illustrated in the accompanying Fig. 3.34. The transfected cells were then harvested for genomic DNA extraction, and the region encompassing the target site was amplified and cloned into the pJET vector. The vectors were further transferred into E.*coli* to facilitate determination of the frequency of mutations by sanger sequencing.

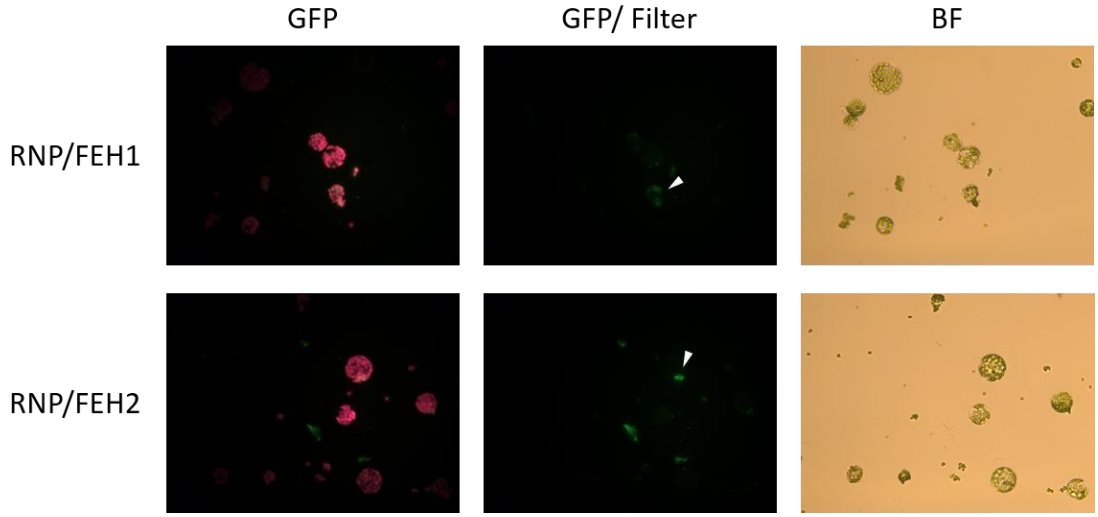

Figure 3.34 RNP transfection with GFP signal. Cas9 proteins were fused with GFP. RNP complexes were transfected into chicory mesophyll protoplast. White arrowheads indicate the GFP signal of RNP complexed in the cell. BF: bride field.

In the case of *1-FEH1*, a total of 23 E. *coli* colonies that contain pJET vector were subjected to sequencing analysis, which revealed that four of these clones displayed mutations at the targeted site (Fig. 3.35). One of the identified mutants exhibited a substitution of AC with TT on two base pairs located upstream of the protospacer adjacent motif (PAM) sequence, resulting in a single amino acid substitution from proline to serine at position 123. The remaining three mutants demonstrated a four base pair deletion within the target sequence, leading to the introduction of a premature stop codon via frameshift, and indicating overall mutation frequency of 17.39% and frameshift frequency of 13.04%. In the context of *1-FEH2a*, it was observed that mutations were present in five of the 22 clones examined. Notably, three of these mutants exhibited deletions spanning 6, 10, and 11 base pairs, respectively, whereas the remaining two mutants manifested insertions of A or T nucleotides (Fig. 3.35). It was further noted that four of the mutants resulted in frameshifts and premature stop codons, thereby giving rise to a mutation frequency of 22.72%. Among the total cloned identified, 18.18% were characterized by frameshifts. For *1-FEH2b*, four of the 27 clones were observed to contain two types of mutations resulting in frameshifts and early stop codons, with a mutation frequency of 14.81%.

```
FEH1_WT_EXON3       TGCCTGTCAGGTTCAGCCACGATCCTACCCGGGCCACGGCCCATAATTCTATATACCGGT
RNP_FEH1_13         TGCCTGTCAGGTTCAGCCACGATCCTTTCTGGGC-------------------------
RNP_FEH1_10         TGCCTGTCAGGTTCAGCCACGATC----CCGGGCCACGGCCCATAATTCTATATACCGGT
RNP_FEH1_11         TGCCTGTCAGGTTCAGCCACGATC----CCGGGCCACGGCCCATAATTCTATATACCGGT
RNP_FEH_19          TGCCTGTCAGGTTCAGCCACGATC----CCGGGCCACGGCCCATAATTCTATATACCGGT

FEH2a_WT_EXON3      TGCCACCG-GAACTTGGGAGTGCCCGGACTTTTACCCTGTGCCGTTGAACAG(N60)ATTTGAAGGGC
RNP_FEH2a_4         TGCCACCG-------GGGAGTGCCCGGACTTTTACCCTGTGCCGTTGAACAG(N60)ATTTGAAGGGC
RNP_FEH2a_19        TGCCACCG-----------GTGCCCGGACTTTTACCCTGTGCCGTTGAACAG(N60)ATTTGAAGGGC
RNP_FEH2a_22        TGCCACCG------------TGCCCGGACTTTTACCCTGTGCCGTTGAACAG(N60)ATTTGAAGGGC
RNP_FEH2a_1         TGCCACCGAGAACTTGGGAGTGCCCGGATTTTTACCCGGTGCCGTTGAACAG(N60)ATTTGAAGGGC
RNP_FEH2a_5         TGCCACCGTGAACTTGGGAGTGCCCGGACTTTTACCCTGTGCCGTTGAACAG(N60)ATTTGAAGGGC

FEH2b_WT_EXON2      TGCCACCG-GAACTTGGGAGTGCCCGGACTTTTACCCTGTGCCGTTGAACAG(N60)ATTTGAAGGCC
RNP_FEH2b_27        TGCCACCG-----TTGGGAGTGCCCGGATTTTTACCCGGTGCCGTTGAACAG(N60)ATTTGAAGGGC
RNP_FEH2b_7         TGCCACCG-----TTGGGAGTGCCCGGATTTTTACCCGGTGCCGTTGAACAG(N60)ATTTGAAGGGC
RNP_FEH2b_4         TGCCACCGAGAACTTGGGAGTGCCCGGATTTTTACCCGGTGCCGTTGAACAG(N60)ATTTGAAGGGC
RNP_FEH2b_22        TGCCACCGAGAACTTGGGAGTGCCCGGATTTTTACCCGGTGCCGTTGAACAG(N60)ATTTGAAGGGC
```

Figure 3.35 Results of sequence analysis conducted on mutations that occurred in the target region of the RNP. Transfection of the RNP complex with FEH1_195forw sgRNA and FEH2ab_514rev sgRNA was performed separately. sgRNA target sites are shown with underline; the PAM sequences (NGG) are denoted in yellow; instances of miss-match or insertion are highlighted in red; deletion events are marked in blue; and instances of stop codons are emphasized with red lettering.

4 Discussion

The extraction of inulin from the chicory taproot yields an essential commercial fructan product. The understanding of the regulatory mechanisms underlying fructan exohydrolases, which predominantly mediate inulin degradation, offers valuable insight into future directions for both breeding and genetic engineering of chicory. The initial part of this thesis elucidated the distinct expression patterns of *1-FEH1*, *1-FEH2a*, and *1-FEH2b* in young chicory seedlings and mature taproots, in response to cold stimulation. In addition to low temperature, the three isoforms of 1-FEH are also responsive to heat stress and water deficiency, thereby indicating their multifunctional roles in chicory's response to abiotic stresses, as well as the potential crosstalk between these stress pathways. Stress-related transcription factors were identified and found to be involved in different regulatory pathways of *1-FEH*. CiNAC5 is a specific regulator of *1-FEH1* under cold conditions, whereas CiDREB2A is responsive to multiple stresses and specifically regulates *1-FEH2b*. The differential regulation of *1-FEH2a* and *1-FEH2b* by CiDREB is attributed to a mutation in the DRE *cis*-element located on the promoter of *1-FEH2a*. Moreover, it was found that CiDREB2B interacts with CiMYB5, leading to a synergistic upregulation of *1-FEH2b* to be expected in response to heat stress (Fig. 4.1). The comprehension of the regulatory networks that control fructan metabolism pathways provides a fundamental knowledge for the genetic modification of transcriptional regulator expression levels via conventional and transgenic methods, with the aim of enhancing fructan accumulation or conferring abiotic stress tolerance.

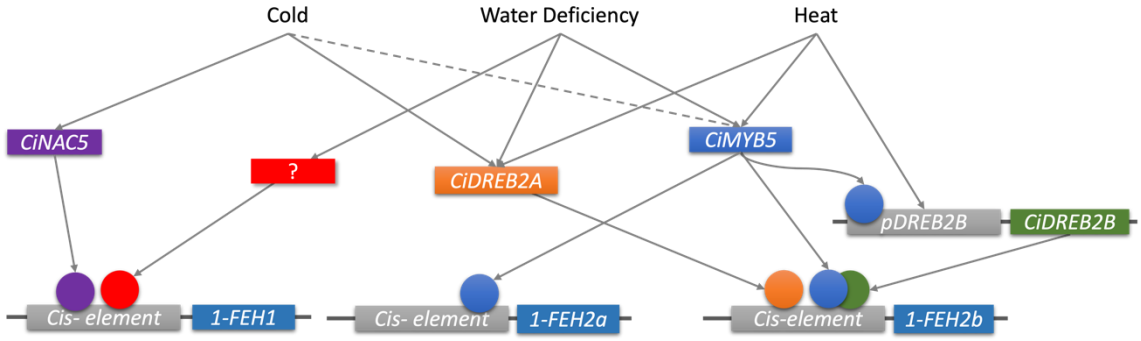

Figure 4.1 The transcriptional network of *1-FEH*s. The solid line with arrows represents the positive relationships verified in this thesis. The dashed line indicates that the cold induction of *CiMYB5* previously identified (Wei et al. 2017) but not confirmed in this thesis.

The other part of the thesis outlines a methodology to establish a reliable transient transfection protoplast system for the introduction of site-specific mutations on the genome via CRISPR ribonucleoprotein (RNP) and regeneration of plants from protoplasts. The approach resulted in a relatively high transfection efficiency and a favorable mutation rate in the transfected cells. This method represents a novel avenue for future genetic engineering of chicory and for elucidating the precise functions of genes.

4.1 Different expression patterns of *1-FEH1*, *1-FEH2a* and *1-FEH2b* response to various abiotic stresses

4.1.1 Under low temperature, *1-FEH1* was upregulated and showed long lasting activation, whereas *1-FEH2a* and *1-FEH2b* showed strong and transient cold induction

It has been well studied over the past decades that the inulin degradation in chicory was mainly due to enzyme activities of fructan 1-exohydrolases (1-FEH) during harvest season (Van Arkel et al. 2012). Earlier investigations on chicory hairy root demonstrated that the *1-FEH1* and *1-FEH2* expression responded differently to low temperature and phytohormones (Kusch et al. 2009; Wei et al. 2016). However, the detailed mechanism behind the gene expression and regulation of three isoforms remained unclear. In addition, due to the high similarity in coding sequence between *1-FEH2a* and *1-FEH2b*, researchers were not able to distinguish these two genes when they investigated *1-FEH2* transcript levels. In this study, I designed specific qRT-PCR primers for *1-FEH2a* and *1-FEH2b*, respectively. These primers ensure the specific amplification of *1-FEH2a* and *1-FEH2b*, providing a deep insight to the expression patterns of these two genes. In chicory mature taproot, *1-FEH2a* and *1-FEH2b* showed a rapid and strong cold induction after 24 hours followed by a decline. In contrast, *1-FEH1* did not display any cold induction in mature taproot sliced tissue; instead, its expression fluctuated in response to cold treatment or when maintained at room temperature. It has been shown in a previous study, that *1-FEH1* exhibited an immediate reaction upon treatment with the wounding-related phytohormone Jasmonic acid (JA) (Wei, dissertation 2017). The fluctuation of *1-FEH1* expression during the taproot slice experiment could be attributed to its heightened sensitivity to wounding, which in turn affects its response to cold regulation.

On the other hand, *1-FEH1* displayed a gradual yet consistent increase of expression in young seedlings subjected to cold treatment, in contrast to the rapid and pronounced cold induction observed in *1-FEH2a* and *1-FEH2b*. This observation is corresponding to previous results, in which *1-FEH2* was more instant cold responsive than *1-FEH1* (Kusch et al. 2009). Regarding the two *1-FEH2* genes, their expression levels declined after 24 hours, with *1-FEH2a* exhibiting a reduction in expression several hours earlier than *1-FEH2b*. It is the first observation of difference on transcript levels between *1-FEH2a* and *1-FEH2b*. In a former study, it is suggested that loss of function of *1-FEH2b* has more impact on post-harvest inulin degradation than copy number variation of its close paralog *1-FEH2a* in *Cichorium intybus* (Dauchot et al. 2015). It is intriguing to comprehend the mechanism underlying the precise regulation of inulin degradation by *1-FEH2a* and *1-FEH2b*, which will be discussed in detail in the chapter 4.3.

4.1.2 Heat stress and water deficiency induced the expression of *1-FEH*

Major abiotic stresses such as drought and high temperatures have significantly reduced crop productivity and eroded global food security, exacerbated by the effects of climate change and the increased frequency and severity of these stressors (Lamaoui et al. 2018). A previous study noted that chicory exhibited an atypical bolting pattern during a hot and dry summer, possibly due to the stress of high temperatures and drought (Dielen et al. 2005). Exposure of chicory to heat resulted in a reduction in inulin degree of polymerization (DP) and constrained the growth of its roots (Mathieu et al. 2018). This thesis provides insight into the expression pattern of FAZY genes and their potential roles in the chicory response to high temperatures. During both extreme heat shock (45 °C) and moderate heat (37 °C) treatment, the genes *1-FEH1*, *1-FEH2a*, and *1-FEH2b* were upregulated, while the fructan synthesis genes *1-SST* and *1-FFT* were repressed over time (Fig. 3.28 and Fig. 3.29). This result corresponds to the inulin degradation and fructose release observed during heat treatment, which led to bolting and flowering of non-vernalized chicory (Mathieu et al. 2020). The findings indicate that during high temperatures, upregulation of *1-FEH* expression contributes to inulin hydrolysis, which provides material and energy for the flowering process independently of vernalization. On the other hand, heat stress-induced redox imbalance and decreased photosynthetic efficiency (Zahra et al. 2023)

may accounting for the downregulation of *1-SST*, which relies on sucrose as a substrate to initiate fructan biosynthesis.

High temperature is often accompanied by subsequent drought stress, which further exacerbates the negative impact on plants. Plants tend to accumulate more water-soluble carbohydrates (WSC) in their roots under abiotic stress prior to anthesis, using osmotic adjustment mechanisms to survive. In wheat, during the grain-filling stage, while root fructan is being degraded, the high levels of sucrose, fructose, and glucose present in drought-affected plants may function as osmoregulators (Zhang et al. 2016). Previous research revealed that under drought stress conditions, growth restriction resulted in an increase in the concentration of glucose, fructose, and sucrose in the roots and leaves of young chicory plants (Van Laere et al. 2000). This thesis revealed that during dehydration treatment, the expression of *1-FEH* increased (Fig. 3.30), which could explain to the observation of increasing fructose in young chicory from previous research. It is noteworthy that in both cold and heat treatments, the expression levels *of 1-FEH2* were considerably higher than those of *1-FEH1*. However, in the case of drought treatment, *1-FEH1* expression was constant and pronounced for 48 hours, whereas *1-FEH2a* and *1-FEH2b* expression increased slightly after 24 hours and then decreased. This observation indicated that 1-FEH1 and 1-FEH2 might have distinct functions in response to various abiotic stresses. Similar expression patterns of *1-FEH1* (long-term) and *1-FEH2* (short-term) were also found after cold (Fig. 3.9) and heat treatments (Fig. 3.29) in chicory seedlings, indicating that 1-FEH1 may play a dominant role in long-term stimulations such as seasonal changes during the chicory growth phase, while 1-FEH2 exhibits transient responses to momentary environmental cues such as diurnal changes. Overall, this study provides a new perspective on the expression patterns of *1-FEH*, which is not only induced by low temperature, but also impacted by heat stress and water deficit.

4.2 Cold inducible CiNAC5 is a transcription factor that activates the expression of *1-FEH1*

4.2.1 CiNAC5 recognizes the promoter region (-353 to ATG) of *1-FEH1* and acts as a specific regulator

The plant-specific transcription factor family NAC [NAM (no apical meristem, Petunia), ATAF1–2 (Arabidopsis thaliana activating factor), and CUC2 (cup-shaped

cotyledon)] has been extensively studied, revealing their involvement in various plant response pathways such as cold, salinity, drought, and wounding (Puranik et al. 2012). While the association between NAC transcription factors and fructan metabolism has not been previously documented, the promoter analysis indicated the presence of several putative NAC binding sites (NACBS) on the promoter of *1-FEH*, suggesting that NAC may be involved in regulating *1-FEH*. Among the eight CiNAC transcription factors identified in chicory, CiNAC5 appeared to be the most promising candidate for regulating *1-FEH* according to the co-expression analysis. In chicory mature taproot tissue, *CiNAC5* had a strong cold induction after 24 hours (Fig. 3.8), whereas the cold-induced expression of *CiNAC5* in young chicory seedlings was regulated in a circadian manner (Fig. 3.10). The early induction of *CiNAC5* under cold treatment occurred prior to the expression of *1-FEH*, indicating that the transcription factor might function as an upstream regulator of *1-FEH*. The specific activation of the *1-FEH1* promoter by CiNAC5 was demonstrated through the dual luciferase assay, with no effect observed on the promoters of other FAZY genes (Fig. 3.13), which provided an explanation for the different regulatory pathways of *1-FEH1* and *1-FEH2*. Promoter deletion analysis of *1-FEH1* showed that the activation site of CiNAC5 located on the promoter region between -353 to ATG. However, the activation of CiNAC5 on *p1-FEH1* was not abolished even after mutation or deletion of putative NACBS in this region (Fig. 3.14). One potential explanation for the unsuccess of NACBS mutation or deletion to prevent CiNAC5-induced activation is that CiNAC5 may have multiple binding sites on the *1-FEH1* promoter, rendering single or double mutations of NACBS insufficient. Additionally, it is possible that CiNAC5 has unidentified binding sites that have not yet been identified on the promoter of *1-FEH1*. In this study, attempts to express CiNAC5 protein in prokaryotic system were unsuccessful, which limited the understanding of how CiNAC5 interacts with *p1-FEH1*. Therefore, it is crucial to develop a method to obtain CiNAC5 protein. Further analysis, such as yeast-one-hybrid assay or ChIP-Seq would provide insight into the CiNAC5 recognition site.

It is noteworthy that the expression pattern of *CiNAC5* during heat stress and water deficiency treatments of chicory seedlings revealed a decrease over time (Fig. S3), contradicting the expected induction of *1-FEH1* under such conditions. These

findings suggest that CiNAC5 is primarily responsive to low temperature stress and may not have a significant impact on the response to heat and drought stress.

On the other hand, *CiNAC8* showed a transient upregulation during the initial stage of cold treatment in young chicory seedlings. A 3-fold increase of activation on the promoter of *1-FFT* by CiNAC8 was demonstrated in the dual luciferase assay, which could explain the modest cold-induced expression of *1-FFT* in chicory seedlings (Fig. 3.9). This finding was consistent with a previous study (del Viso et al. 2009), which suggested that fructosyltransferase was involved in the fine-tuning of fructan accumulation that occurs during cold conditions and influence the degree of polymerization of fructan.

4.2.2 CiNAC5 as a homolog of ANAC013, ANAC016 and ANAC017 in *Arabidopsis thaliana*

The molecular phylogenetic analysis showed that CiNAC5 is evolutionarily related to ANAC013/16/17 in *Arabidopsis thaliana* (Fig. 3.6), which belong to a group of endoplasmic reticulum (ER)-bound NAC transcription factors that have been identified as primary regulators of the nuclear response to mitochondrial dysfunction (De Clercq et al. 2013; Ng et al. 2013). Among them, ANAC016 and ANAC017 have been identified as important regulators in various plant physiological processes and play crucial roles in submergence tolerance (Bui et al. 2020). Overexpression of ANAC017 has been shown to cause growth retardation, altered leaf development with decreased cell size and viability, and early leaf senescence (Meng et al. 2019). These findings suggest potential avenues for future research on CiNAC5, including investigating its response to flooding stress and its role in the development of chicory plants. Additionally, Broda et al. (2021) reported that during late senescence, ANAC017 directly controlled the transcription of ANAC016 in a feed-forward loop. In the present study, dual luciferase assay revealed that CiNAC5 activated its own promoter by approximately 2-fold, thereby generating a positive feedback loop for self-regulation in response to environmental stimuli (Fig. 3.20).

Various NAC proteins have been shown to bind to the DNA containing NAC binding site (NACBS) CGTG/A or its reverse complement T/CACG (Olsen et al. 2005). A previous study showed that the mitochondrial dysfunction motif (MDM) *cis*-element contained the imperfect inverted-repeat structure $CTTGN_5CAA/CG$, which could be

bound by ANAC013, ANAC016 and ANAC017 (De Clercq et al. 2013). This discovery suggested the possibility that the promoter region of *1-FEH1* might contain an unidentified and imperfect recognition site for CiNAC5, which could explain the lack of effect on CiNAC5 activation due to the mutation on the putative NACBS (Fig. 3.14 M1/M2). The results of a yeast-two-hybrid screening utilizing OsNAC5 as a bait revealed its interaction with other OsNAC proteins including itself, indicating that rice NAC transcription factors function as homodimers and heterodimers (Jeong et al. 2009). The detailed mechanism underlying CiNAC5 regulation of *1-FEH*, including potential cooperativity with other transcription factors and the precise recognition site, remains to be further investigated.

4.3 CiDREB1 and CiDREB2 specifically regulates *1-FEH2b* response to various stresses via binding to its promoter

4.3.1 Distinct responses of CiDREB1 and CiDREB2 to heat, cold, and drought stresses

Traditional genetic and molecular investigations have characterized C-repeat/DREB binding factors (CBFs/DREBs) as essential transcription factors involved in the process of cold acclimation (Shi, Ding and Yang 2018). Several genes are activated by both dehydration and cold temperature, and their transcript levels decrease upon stress relief, which implies the existence of common biochemical pathways that regulate these processes (Shinozaki and Yamaguchi-Shinozaki 2000). In *Arabidopsis*, such genes include *rd* (*responsive to dehydration*) and *cor* (*cold-regulated*). The DRE *cis*-element (TACCGACAT) plays an indispensable role in regulating the induction of *rd29A* in response to dehydration and cold via the ABA-independent pathway (Narusaka et al. 2003). It was initially believed that two distinct subgroups of DREB family, namely DREB1/CBF and DREB2, recognized DRE *cis*-element and acted as trans-acting factors in two distinct signal transduction pathways in response to cold and drought conditions, respectively (Liu et al. 1998). Subsequent research has indicated that the functional distinction between DREB1 and DREB2 members is less apparent than originally supposed. The transcription factors of DREB1 type are activated by major abiotic stresses, including not only cold but also high temperatures, drought, and high salinity. However, the expression patterns of orthologous genes differ considerably across different species, indicating variations in the regulatory

mechanisms (Agarwal et al. 2017). In this study, it was found that *CiDREB1A/C/D* were upregulated in response to low temperature in chicory (Fig 3.8). Among these genes, *CiDREB1D* exhibited cold-inducible expression that was regulated by circadian signal, while *CiDREB1A* showed rapid and robust upregulation at the onset of cold treatment. This observation is consistent with a previous finding in *Arabidopsis*, which demonstrated that cold stress can be categorized into two different signals and differently induce the expression of *AtDREB1* genes (Kidokoro et al. 2017). *AtDREB1B* expression in response to cold stress is primarily regulated by CALMODULIN BINDING TRANSCRIPTION ACTIVATOR3 (CAMTA3) and CAMTA5, while *AtDREB1A* expression is under the regulation of clock factors, including CIRCADIAN CLOCK ASSOCIATED1 and LATE ELONGATED HYPOCOTYL, which act as transcriptional activators specifically during the day (Kidokoro et al. 2017).

On the other hand, *DREB2* was initially thought to be activated by heat and dehydration. However, further examination of the expression of other members within this subgroup in *Arabidopsis*, as well as similar genes in other plant species, has shown that numerous *DREB2* genes are also responsive to cold stress (Lee et al. 2010). The present study shows that *CiDREB2A* exhibits responsiveness to a variety of stresses, including low and high temperature as well as dehydration. Additionally, the cold-induced expression of *CiDREB2A* was found to be regulated by circadian rhythm. On the contrary, *CiDREB2B* appears to be specifically induced by heat stress, as its expression was scarcely detectable under control, cold or drought conditions. The findings offer evidence of crosstalk between cold and heat stress, and intricate regulatory mechanisms involving DREB in response to abiotic stresses.

4.3.2 Effect of SNP on DRE *cis*-element in the promoter of *1-FEH2a* and *1-FEH2b* on their respective regulation pathways

Based on the results presented in this study, it is proposed that CiDREB1 and CiDREB2 play significant roles in the regulation of the *1-FEH2b* gene under low temperature. This notion is supported by the following observations: (1) The co-expression analysis conducted during cold treatment revealed that CiDREB1A/C/D and CiDREB2A were induced by cold stress, preceding the induction of *1-FEH2b* (Fig 3.8–3.10); (2) The dual luciferase assay demonstrated that the activation of the *1-*

FEH2b promoter by CiDREB1A/C/D and CiDREB2A resulted in a 2- to 6-fold induction rate. Notably, this effect appeared to be highly specific, as no significant activation of either the promoters of *1-FEH1* or *1-FEH2a* was observed (Fig 3.16); (3) The electrophoretic mobility shift assay (EMSA) results illustrated the binding of CiDREB1 or CiDREB2 to the promoter of *1-FEH2b* through the DRE *cis*-element (Fig. 3.22–3.25); (4) Further analysis revealed that a point mutation in the DRE sequence within the *p1-FEH2b* resulted in disruption of the protein-DNA interaction and the loss of CiDREB-mediated activation of the promoter of *1-FEH2b* (Fig. 3.17–3.18).

In a previous study, Sakuma et al. (2002) employed the EMSA method utilizing single-base substituted DRE sequences as substrates to demonstrate that the core sequence of DRE is the 6-bp A/GCCGAC sequence in *Arabidopsis*. Additionally, they found that the 4th C, 5th G, and 7th C of DRE (TACCGACAT) were crucial for highly specific interactions with the DREB proteins. An analysis of the promoter region demonstrated that a single nucleotide polymorphism (SNP) located in the core sequence of the DRE *cis*-element between *1-FEH2a* (TTCG) and *1-FEH2b* (GTCG) was the primary factor responsible for the differential promoter activity observed on *p1-FEH2a* and *p1-FEH2b* driven by CiDREBs. Notably, a single base mutation in the DRE *cis*-element of *p1-FEH2a* disrupted the DNA-protein interaction, indicating the importance of this sequence for promoter activation by CiDREBs.

4.3.3 *CiDREB2B* is co-induced with *CiMYB3* and *CiMYB5* under heat stress, which might be involved in the activation of *1-FEH2b* expression

Transcriptional regulation relies on intricate networks of protein-protein interactions. These interactions between transcription factors (TFs) are crucial for coordinating both positive and negative regulation of stress responses, enabling efficient expression of diverse downstream genes. The results of the yeast-two-hybrid and dual luciferase assay via co-transfection with two transcription factors demonstrated that CiDREB2B interacted with CiMYB3 and CiMYB5 to significantly activate the promoter of *1-FEH2b* (Fig. 3.19; Fig. 3.26). The dual luciferase assay employed a single transcription factor transfection strategy for the overexpression of CiMYB5 in chicory leaf protoplasts, which in turn, facilitated the involvement of endogenous CiDREB2B in assisting CiMYB5 to execute its complete function. This cooperative

activity resulted in the activation of *p1-FEH2b* with an induction of approximately 10-fold (Fig. 3.19B). However, the impact of CiMYB5 on *p1-FEH2b* was confined to the quantity of endogenous CiDREB2B, as its expression was infrequent in the absence of stimulation. Evidently, the activation of *p1-FEH2b* through CiMYB5 necessitates the presence of CiDREB2B, given that the mutation or deletion of the DRE *cis*-element resulted in the impairment of *p1-FEH2b* activation by CiMYB5. Simultaneous transfection of CiDREB2B and CiMYB5 surmounted the quantity restrictions imposed on both transcription factors, ultimately resulting in notable activation of *p1-FEH2b*, featuring over 35-fold induction (Fig. 3.19B). Interestingly, CiDREB2A exhibited no interaction with either CiMYB3 or CiMYB5, resulting in solely a superimposed effect without any synergistic activation on *p1-FEH2b*. Despite prior research demonstrating the upregulation of *CiMYB3* and *CiMYB5* under cold conditions (Wei et al. 2017a), the current investigation produced inconsistent results within chicory young seedling or mature taproot. Through examination of *CiDREB2B*, which correlates with *CiMYB5* and specifically responds to heat stress, it was determined that these transcription factors might play a role in the regulation of *1-FEH2b* under a high-temperature response pathway.

CiDREB2B had been validated to bind on the promoter of *1-FEH2b* via DRE. Promoter analysis illustrated the presence of a MYB-core motif located 6 bp from the DRE *cis*-element. However, the relationship between CiMYB5 and *p1-FEH2b* remains unclear, as protein expression of CiMYB5 in prokaryotic systems was not successful. According to the possible relationship between CiDREB2B/CiMYB5 and *p1-FEH2b*, three hypothetical interaction models between these transcription factors could be proposed (Fig. 4.2). (1) Both CiDREB2B and CiMYB5 directly bind to the promoter of *1-FEH2b* to activate the promoter. The interaction between CiDREB2B and CiMYB5 reinforces the DNA-protein binding and enhance transcription of *1-FEH2b*; (2) CiMYB5 does not bind to the promoter of *1-FEH2b*, instead, CiDREB2B recruits CiMYB5 and initiate the transcription of *1-FEH2b*; (3) The CiDREB2B and CiMYB5 complex involves a third transcription factor. In the absence of CiDREB2B, the formation of the TF complex is interrupted, leading to impaired activation on *p1-FEH2b*. Further investigation is required to elucidate the precise mechanism by CiMYB5 interacts with CiDREB2B and *p1-FEH2b*.

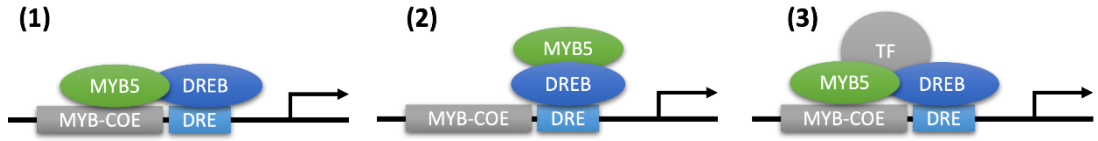

Figure 4.2 Schematic of the hypothetical relationship between CiMYB5 and CiDREB2B in regulating the promoter of *1-FEH2b*. Transcription factors were presented in circles; *cis*-elements were presented in boxes.

4.3.4 Neither CiDREBs nor CiMYBs show significant activation on *p1-FEH1*

A previous study has identified a master transcription factor, CiMYB17, which is capable of activating both fructosyltransferase and fructan exohydrolase genes to orchestrate fructan synthesis and degradation (Wei et al. 2017). According to the study, the *1-FEH1* promoter contains five copies of DTTHGGT element that can be bound by CiMYB17. Furthermore, the study found that CiMYB17 was able to activate the *1-FEH1* promoter by 6-fold in a dual luciferase assay conducted in grapevine suspension cells. In contrast to previous studies, the effect of CiMYB17 on *p1-FEH1* was found to be rather restricted in chicory protoplasts (Fig. 3.15). The results showed that all 14 CiMYB proteins tested in the dual luciferase assay have limited activation on *p1-FEH1*, in contrast to the notable activation observed for CiMYB on *p1-FEH2*. Since chicory protoplasts offer a homologous system that ensures consistent and reproducible dual luciferase assays, it might be assert that CiMYB17 does not serve as an activator of *1-FEH1*. It is probable that the prior observation of marked induction of *p1-FEH1* by CiMYB17 is an incidental effect of utilizing a heterologous system which yields considerable error bars in the results. The CiDREB protein has been observed to interact with the promoter of *1-FEH1*; however, this interaction alone does not necessarily imply that CiDREB functions as a regulator for *1-FEH1*. Notably, there has been no observation of a discernible impact of CiDREB on *p1-FEH1*. Given the specific regulation of *1-FEH1* by CiNAC5, the findings of this investigation suggest that the regulation of *1-FEH1*, *1-FEH2a*, and *1-FEH2b* occur via distinct and separate pathways.

4.4 Utilizing transgenic approaches for attaining high-yield and high-quality inulin in chicory

The improvement of both inulin yield and quality in chicory represents a primary objective for farmers and breeders. Reduction in fructan synthesis, coupled with

increase of fructan exohydrolase activity, are the principal factors responsible for the degradation of inulin polymerization (DP). Alterations to the fructan metabolism pathway present a prospective avenue for the optimization of inulin production in the field. Genetic engineering approaches can be categorized into two distinct directions: (a) the engineering of enzymes that are directly implicated in fructan metabolism, and (b) the manipulation of stress signaling and the regulation of genes responsible for fructan metabolism. For the former approach, a previous study achieved to developed to overexpress *sucrose:sucrose 1-fructosyltransferase* (*1-SST*) under the control of the CaMV35S promoter in chicory plants cv. Melci (Maroufi et al. 2018). Analysis of the findings revealed a comparatively high degree of expression of *1-SST* in the transgenic chicory plants relative to those of the wild-type plants. Nonetheless, the impact on the degree of DP was observed to be restricted. The fructan metabolism is an intricacies process involving different isoforms of fructan exohydrolases and fructan:fructan 1-fructosyltransferase, which exert an influence on the length of inulin. Mere augmentation of *1-SST* may prove inadequate in attaining the desired outcome of generating chicory plants that yield a substantial amount of inulin, in the presence of continuous inulin degradation that is impervious to inhibition. Another research pointed out that nucleotidic polymorphisms of *FEH* genes in chicory are statistically associated with enhanced resistance to post- harvest inulin depolymerization (Dauchot et al. 2014). Directing attention towards *1-FEH* genes and introducing mutations therein may exert a more substantial influence on the accumulation of inulin by hindering its degradation. This thesis presents a feasible method of inducing targeted mutations to *1-FEH* genes in chicory through RNP delivery, which obviates the need for the introduction of exogenous DNA. The on-target mutation frequency ranges from 17.39% to 22.72%. Despite progress made thus far, further analysis of transgenic plants exhibiting bi-allelic mutations is necessary, including additional genotyping of the mutant plants and the determination of the loss-functions of *1-FEH1* and *1-FEH2*.

It is noteworthy that the consequences of a complete knockout of *1-FEH* remain ambiguous, given its potential involvement in various stress-response processes in chicory, including those related to pathogen infections (Versluys et al. 2018). This thesis offers insight into the transcriptional regulators of *1-FEH*, furnishing information to potentially interrupt the regulatory pathway of *1-FEH* expression

under certain stress conditions. For instance, modifying the DRE *cis*-element on the promoter region of *1-FEH2b* to disrupt its regulation by CiDREB in response to both cold and heat stress, which is more practical for field production, as it mitigates the potential for serious side effects resulting from a complete gene knockout. Furthermore, mutation in CiNAC5 has the potential to disrupt the expression of *1-FEH1* in response to low temperatures during the harvest season, as CiNAC5 exhibits specificity in its response to cold stress and serves as a specific regulator of *1-FEH1*. The present thesis offers a potential avenue for genetic engineering in future chicory breeding, but it is essential to conduct further research and implement transgenic experiments to advance this line of inquiry.

5 Materials and Methods

5.1 Plant material

5.1.1 Chicory young seedlings

Cichorium intybus L. var. Zoom seedlings were grown on vermiculite under long-day conditions in the greenhouse. At the start of the treatment, four-week-old chicory seedlings were grown under 12 hours of light alternating with 12 hours of darkness. Cold water was poured onto the vermiculite for the cold treatment, and the seedlings were placed in a cold room (6 °C) with the same light conditions. The taproots were harvested at time points of 0, 1, 4, 8, 12, 16, 20, 24, 28, 32, 36, 40, and 48 hours after the cold treatment started. Each biological replicate contained a pool of 2-3 individual seedling roots. The taproot tissue was frozen in liquid nitrogen immediately after harvesting, ground into powder using a Mixer Mill MM 400 (Retsch), and stored at -80 °C for further experiments.

5.1.2 Chicory mature root culture

Cichorium intybus L. var. Zoom was grown in the field in the University of Heidelberg botanic garden in 2017. Three-month-old chicory was harvested from the field in November before flowering. A one-centimeter-thick cross-section of the root was taken at a position 5 cm below the hypocotyl. Root tissue was cut from the peripheral part of the root section in a 1 cm diameter using a cork borer and incubated in distilled water under cold room conditions for cold treatment, or at room temperature as a control. The root tissue was harvested at time points of 0, 1, 3, 6, 24, and 72 hours after the cold treatment started. Each biological replicate represented root tissue harvested from one independent chicory plant. The taproot tissue was frozen in liquid nitrogen immediately after harvesting, ground into powder using a Mixer Mill MM 400 (Retsch), and stored at -80 °C for further experiments.

5.1.3 Chicory hydroponic culture

Cichorium intybus L. var. Zoom seeds were sown on water-soaked sponge and incubated under darkness for three days to promote germination. After the seeds germinated, the sprouts were cultured with ½ Hoagland solution and placed in a climate chamber under long-day conditions (25 °C, 16 h day/8 h night) until the first

true leaves expanded. The seedlings were then transferred into plastic beakers and cultured with Hoagland solution for four weeks. The Hoagland solution was drained to induce water deficiency treatment. The seedling roots were harvested at time points of 0, 6, 24, and 48 hours after treatment. Each biological replicate represented an independent chicory plant. The taproot tissue was frozen in liquid nitrogen immediately after harvesting, ground into powder using a Mixer Mill MM 400 (Retsch), and stored at -80 °C for further experiments.

5.1.4 Heat treatment of chicory seedling

Cichorium intybus L. var. Zoom seedlings were grown in mixed nutrient soil under long day conditions in the greenhouse. For the heat treatment, four-week-old seedlings were placed in an incubator at 45 °C with alternating 16 hours of light and 8 hours of darkness. Root tissue was harvested 1 hour after the start of the incubation. After the soil temperature reached 45 °C, root tissue was harvested at 1 and 24 hours. For moderate heat treatment, seedlings were placed under 37 °C and harvested at 0, 6, 24, 48, and 72 hours after treatment. The humidity in the incubator was maintained at 70-80%. Each biological replicate represented an independent chicory plant. Taproot tissue was frozen in liquid nitrogen immediately after harvesting, ground into powder using a Mixer Mill MM 400 (Retsch), and stored at -80 °C for further experiments.

5.1.5 Chicory mesophyll protoplast preparation

The second pair of true leaves from 3-4-week-old chicory was chosen and cut into 1 mm leaf strips. The leaf strips were then transferred into the enzyme solution (20 mM MES, 1.5% cellulase R10, 0.4% macerozyme R10, 0.4 M mannitol, 20 mM KCl, 10 mM $CaCl_2$, 0.1% BSA, pH 5.7) and allowed to be completely submerged. The digestion was continued, without shaking, in the dark for at least 8 hours at room temperature. The enzyme solution containing protoplasts was diluted with an equal volume of W5 solution (2 mM MES, 154 mM NaCl, 125 mM $CaCl_2$, 5 mM KCl, pH 5.7) and filtered with a 100-µm nylon mesh. The flow-through was centrifuged at 150 *xg* for 2 min to collect the protoplasts in a 50-ml falcon tube. The protoplast pellet was re-suspended with W5 solution by gentle swirling and kept at room temperature, allowing the protoplast to settle at the bottom by gravity for 30 min. The W5 solution was then removed as much as possible without touching the protoplast pellet. The

protoplasts were re-suspended at 2×10^5 cell/ml in MMG solution (4 mM MES, 0.4 M mannitol, 15 mM $MgCl_2$, pH 5.7), and ready for further experiments.

5.1.6 Protoplast transfection with plasmid

10 μg of plasmids (with a 6:4 ratio of effector to reporter) were mixed with 100 μl of protoplasts in a 2-ml microfuge tube. Add 110 μl of PEG solution (50% PEG4000, 0.2 M mannitol, 100 mM $CaCl_2$), and mix completely by gently tapping the tube. The transfection mixture was incubated at room temperature for up to 15 min and then stopped by diluting with 440 μl of W5 solution and mixing well by inverting the tube. The mixture was then centrifuged at 100 *xg* for 2 min and the supernatant was removed. The protoplasts were re-suspended in 500 μl of WI solution (4 mM MES, 0.5 M mannitol, 20 mM KCl, pH 5.7) in each well of a 12-well tissue culture plate. The protoplasts were then incubated at room temperature for 20 h, re-suspended, and harvested by centrifugation at 100 *xg* for 2 min. The protoplasts pellet was mixed with 50 μl of 2× lysis buffer and vigorously vortexed. After 5 min of incubation on ice, the mixture was centrifuged at 1,000 *xg* for 2 min. LUC activity was measured with a luminometer using 20 μl of the lysate and 50 μl of LUC mix (Promega).

5.1.7 Ribonuclease (RNP) deliver in protoplast

10 μg Cas9 protein and 100 pmol sgRNA were mix in room temperature for 10 min before transfection. 20 μl RNP complex was gently mixed in 200 μl protoplast. Add 220 μl of PEG solution (50% PEG4000, 0.2 M mannitol, 100 mM $CaCl_2$), and mix completely by gently tapping the tube. The transfection mixture was incubated at room temperature for up to 15 min and then stopped by diluting with 440 μl of W5 solution and mixing well by inverting the tube. The mixture was then centrifuged at 100 *xg* for 2 min and the supernatant was removed. The protoplasts were re-suspended in 1 ml of WI solution (4 mM MES, 0.5 M mannitol, 20 mM KCl, pH 5.7) in each well of a 6-well tissue culture plate.

5.1.8 Protoplast regeneration

The method for chicory protoplast regeneration, as described in (Ref.), was modified as follows: the transfected chicory protoplasts were mixed with an equal volume of MC_2 medium containing 5 g/L low melting agarose. Then, 50 μl of the mixture was dropped into a 6-well plate, left to solidify, and 1 ml of MC_1 medium was added. The plate was incubated in a climate chamber under long-day conditions (25°C, 16 h

day/8 h night). After 5 days, the liquid medium was exchanged with MC_2, and the medium was refreshed every week until microcolonies were generated. The microcolonies were then placed on solid MC_3 media and cultured to small plants.

5.1.9 Transient transformation of tobacco leaves

Nicotiana benthamiana plants were cultivated on standardized ED-73 soil in the greenhouse under continuous light at 22-25 °C for four weeks. A single colony of *A. tumefaciens* containing the desired construct was inoculated in 4 mL LB medium with appropriate antibiotic and incubated overnight in a rotary shaker at 180 rpm at 28 °C. The OD_{600} of the cell culture was measured using a spectrophotometer. When the OD_{600} reached 1.0, the cells were harvested by centrifugation for 5 min at 4,000 rpm at room temperature. The supernatants were discarded, and bacterial cells were washed twice by re-suspending the pellets in induction medium (1/2 MS medium, 150 μM acetosyringone) and adjusting the final concentration to OD_{600}=0.8 with induction medium. The bacterial suspensions were incubated for at least 2 h at 28 °C without shaking. For the luciferase complementation assay (LCA), the bacterial suspension was pre-mixed with pNluc, pCluc, and P19 at a ratio of 1.5:1.5:1 before infiltration. A 1-mL needleless syringe was used to infiltrate the bacterial suspension into the fully expanded young leaves of *N. benthamiana*. The syringe tip was inserted into the part of the abaxial side of the leaves without major veins. After infiltration, the plants were kept in the greenhouse for 48 h with plastic cover to maintain relatively high humidity before measuring. For LCA, 1 mM D-Luciferin (Sigma) was sprayed on the leaves and kept in the dark for 5 min. Luminescence images were captured using ImageQuant LAS 4000 and further analyzed with Fiji imageJ.

5.2 Microbiological techniques

5.2.1 Bacterial and yeast strains

Specie	Strain	Usage
E. coli	DH5α	General restriction enzyme-based or gateway cloning purposes
	DB3.1	To propagate Gateway or GreenGate vector
	BL21 (DE3)	Protein expression
A. tumefaciens	GV3101	Luciferase complement assay
S. cerevisiae	AH109	Yeast two-hybrid
	Y1HGold	Yeast one-hybrid

5.2.2 Media and antibodies for bacterial and yeast cultures

Escherichia coli and *Agrobacterium tumefaciens* bacteria were grown in low salt LB (Luria-Bertani) medium (0.5% yeast extract, 1% peptone, 8.5 mM NaCl, pH 7.0; agar plates were supplemented with 2% bacto agar). For recovery after transformation, *E. coli* or *A. tumefaciens* bacteria were incubated in SOC medium (0.5% yeast extract, 2% peptone, 10 mM NaCl, 2.5 mM KCl, 10 mM $MgCl_2$, 10 mM MgSO4, 10 mM glucose, pH 7.0). To prepare competent *E. coli* and *A. tumefaciens*, SOB medium (2% tryptone, 0.5% yeast extract, 8.5 mM NaCl, 2.5 mM KCl, 10 mM $MgCl_2$, pH 7.0) was used.

Saccharomyces cerevisiae was grown in YPDA (1% yeast extract, 2% peptone, 20% (w/v) glucose, 0.005% L-adenine hemisulfate salt, pH 6.5; agar plates were supplemented with 2% bacto agar). For selecting Y1H and Y2H, SD media with amino acid dropout mixes were purchased from Takara.

5.2.3 Preparation of competent *E. coli* and *A. tumefaciens* cells

The *E. coli* or *A. tumefaciens* bacteria were inoculated from a single colony in LB medium and grown overnight in a rotary shaker at 180 rpm at 37°C or 28°C. The overnight pre-culture was then inoculated into 250 ml of SOB medium and the culture was continued with shaking until the OD_{600} reached 0.6. The culture was then chilled at 4°C for 20 minutes and the cells were harvested by centrifugation in a pre-chilled rotor at 4°C at 2500 *xg*. The supernatant was removed and the cells were re-suspended in 100 ml of Inoue buffer (86 mM $MnCl_2$, 20 mM $CaCl_2$, 250 mM, 10 mM PIPES, pH 6.7) and centrifuged as above. The supernatant was again removed and the cells were re-suspended in 20 ml of Inoue buffer and 1.5 ml of DMSO was added, and the mixture was swirled. The cells were then incubated on ice for 10 minutes and 50 µl of competent cells were aliquoted into sterile tubes and frozen in liquid nitrogen. The competent cells were stored at -80°C.

5.2.4 Transformation of *E. coli* and *A. tumefaciens* competent cells

For *E. coli* transformation, 50 µl of competent cells were thawed on ice and 100 ng of plasmid DNA was mixed with them by pipetting. The mixture was placed on ice for 30 min followed by heat-shocking at 42 °C with a water bath for 60 s. The cell was placed back on ice for 5 min and 950 µl of SOC medium was added. The cell was recovered by culturing it in a rotary shaker at 180 rpm at 37 °C for 1 h. Transformed

cells were plated on LB agar media with the appropriate antibiotic and incubated at 37 °C overnight.

For *A. tumefaciens* transformation, 50 µl of competent cells were thawed on ice for 10 min and mixed with 1 µg of plasmid DNA, then mixed by pipetting. The cells were incubated on ice for 10 min followed by snap-freezing into liquid nitrogen for 5 min. The cells were heat-shocked at a 37 °C water bath for 5 min and 950 µl of SOC medium was added before culturing the cells in a rotary shaker at 180 rpm at 28 °C for 2 h. Transformed cells were plated on LB agar media with the appropriate antibiotic and incubated at 28 °C for 2 days.

5.2.5 Yeast-two-hybrid (Y2H)

Inoculation of one colony of AH109 (less than 4 weeks old) into 3 ml of YPDA medium was cultured in a sterile 15 ml culture tube and incubated at 30°C overnight for 12 hours. The overnight culture was diluted to 1:10 in 10 ml of YPDA medium in a 50-ml Falcon tube. It was then incubated with shaking until the OD_{600} reached 0.15–0.3 (around 2 h). The cells were then centrifuged at 700 *xg* for 5 min at room temperature, and the supernatant was discarded. The pellet was re-suspended in 20 ml of fresh YPDA and incubated at 30°C until the OD_{600} reached 0.4–0.5 (around 3–5 h). The cells were then centrifuged at 700 *xg* for 5 min at room temperature, and the supernatant was discarded. Each pellet was re-suspended in 12 ml of sterile, deionized H_2O. The cells were then centrifuged at 700 $_{xg}$ for 5 minutes at room temperature, and the supernatant was discarded. Each pellet was then re-suspended in 600 µl of 1.1×TE/LiAc (1.1 mM EDTA, 11 mM Tris-Cl, 110 mM LiAC). The cell suspensions were transferred to 1.5 ml microcentrifuge tubes and centrifuged at high speed for 15 seconds. The supernatant was discarded, and each pellet was re-suspended in 240 µl of 1.1×TE/LiAc. The cells were ready to be transformed with plasmid DNA. The competent cells could be stored on ice for a few hours without significant loss in efficiency. Co-transformation of 300 ng pGADT7 and 300 ng pGBKT7 constructs with 5 µl denatured Deoxyribonucleic acid (D7656, Sigma) was performed into 50 µl competent cells. The mixture was then added with 500 µl PEG/LiAC solution [1mM EDTA, 10 mM Tris-Cl, 40% (w/v) PEG335, 100 mM LiAC] and incubated at 30 °C with gentle tapping. 20 µl DMSO was added and mixed well. The tube was then placed in a 42 °C water bath for 15 min. The yeast

cells were then centrifuged at high speed for 15 s to pellet, and the supernatant was removed. The pellet was re-suspended in 1 ml of 2×YPDA medium, centrifuged again to pellet the yeast cells, and the supernatant was discarded. The cell was re-suspended in 0.9% (w/v) NaCl solution. The selection of cells on SD/-Leu/-Trp plate was done at 30°C for 3–5 days. Inoculation of colonies on SD/-Leu/-Trp/-His/-Ade plate was done for 3-5 days. Positive colonies were then indicating the protein interaction. 4 mM X-α-Gal (16555, Merck) was dropped on the colonies, and positive colonies turned blue.

5.2.6 Preparation of glycerol stocks

Overnight cultures, which had been inoculated with a single bacterial or yeast colony, were mixed with 30% glycerol to obtain a final glycerol concentration of 15%. The cultures were then shock frozen in liquid nitrogen and subsequently stored at -80°C.

5.3 DNA and RNA techniques

5.3.1 Isolation of genomic DNA, RNA or plasmid DNA

Genomic DNA and RNA were isolated from plant tissue, and plasmid DNA was isolated from *E. coli* using kits according to the manufacturer's instructions.

Usage	**Kit**
Plant Genomic DNA isolation	innuPREP Plant DNA Kit (Analytik Jena)
Plasmid DNA for cloning	GeneJET Plasmid Miniprep Kit (Thermo Scientific)
Plasmid DNA for protoplast transformation	PureLink™ HiPure Plasmid-Midiprep-Kit (Thermo Scientific)
PCR products purification and Gel extraction	GeneJET PCR Purification kit (Thermo Scientific)
Plant RNA extraction	GeneMATRIX Universal RNA Purification Kit (EURX)

5.3.2 Determination of nucleic acid concentrations

To measure the concentration of DNA or RNA, a NanoDrop2000 Spectrophotometer (Thermo Scientific™) was used following the manufacturer's instructions. The purity of DNA and RNA was assessed by determining the ratio of absorbance at 260 nm and 280 nm. The generally accepted pure DNA has a ratio of 1.8, while pure RNA has a ratio of 2.0.

5.3.3 Polymerase chain reaction (PCR)

The DNA fragments were amplified through PCR by utilizing Phusion polymerase (Thermo Scientific™) or OneTaq polymerase (NEB) in accordance with the manufacturer's guidelines.

5.3.4 Site-directed mutagenesis

The plasmid DNA containing the desired sequence was used as a template for PCR using Phusion polymerase (Thermo Scientific™) according to the manufacturer's instructions to amplify DNA fragments. Site mutations were introduced by incorporating the desired nucleotide changes in the center of the forward primer on the 3´ ends of the mutations. The reverse primer was designed so that the 5´ ends of the two primers annealed back-to-back. After amplification, the linearized DNA was phosphorylated with T4 Polynucleotide Kinase (Thermo Scientific™) according to the manufacturer's instructions. Subsequently, the linear DNA was self-circulated with T4 DNA Ligase (Thermo Scientific™).

5.3.5 Reverse transcription

Use 1 µg of total RNA for cDNA synthesis with AMV Reverse Transcriptase (Roboklon) according to the manufacturer's instructions.

5.3.6 Quantitative real time PCR (qRT-PCR)

The transcript levels of the genes of interest were determined through qPCR using a Rotorgene Q device (Qiagen) and a 2x qPCRBIO SyGreen Mix Lo-ROX. A 12 µl reaction mixture was prepared by adding 2 µl of cDNA, 0.5 µl of forward primer (10 µM), 0.5 µl of reverse primer (10 µM), 6 µl of 2x qPCRBIO SyGreen Mix, and 3 µl of ddH2O. The cycling conditions were as follows: an initial denaturation at 95 °C for 2 min, followed by 40 cycles of denaturation at 95 °C for 5 s and annealing and extension at 62 °C for 20 s. This was followed by a melt cycle with 1 °C increments

for 5 s each from 63 °C to 95 °C. The gene expression was calculated relative to the transcript levels of two reference genes (*Actin* and *RPL19*). Standard curves for primer efficiency determination were prepared using 1:4, 1:16, 1:64, and 1:256 dilutions of cDNA samples.

5.3.7 DNA gel electrophoresis

The DNA samples were mixed with 5× DNA loading buffer [50% (w/v) glycerol, 5x TAE buffer, 1% (w/v) Orange-G] prior to gel loading. GeneRuler 1 kb DNA ladder (Thermo Scientific™) was used as the molecular weight marker. The DNA samples were separated on 1% agarose gels in 1x TAE buffer (40 mM Tris-base, 20 mM sodium acetate, 1 mM EDTA, pH 7.2) by applying a constant voltage of U=90 V. The DNA fragments were stained by incubation in a 0.0001% (w/v) ethidium bromide solution and imaged under UV-light using INTAS science imaging instruments (Göttingen, Germany)

5.3.8 DNA sequencing

The sequencing reactions of the plasmids were performed by Eurofins Genomics (München, Germany) following the instructions for sample preparation.

5.3.9 Gateway cloning

Gateway compatible attB-PCR products were amplified using gene-specific primers with attB overhangs. Entry clones were generated by conducting the BP reaction with 75 ng pDONR221 vector and an equal amount of purified PCR products with 1 µl BP ClonaseII enzyme mix in a 5 µl reaction for 1 h at 25 °C. BP reactions were optionally stopped by incubation with 0.5 µl Proteinase K for 10 min at 37 °C. For LR reactions, 75 ng entry clone and 75 ng destination vector were incubated for 1 h at 25 °C with 1 µl LR ClonaseII Enzyme mix in a total volume of 5 µl. LR reactions were stopped by incubation with 0.5 µl Proteinase K for 10 min at 37 °C.

5.3.10 GreenGate cloning

GreenGate cloning was performed with modifications according to the protocol described by Lampropoulos et al. (2013). The procedure involves using six different entry vectors containing individual elements to insert into a pGreen-IIS based destination vector. The six modules include a plant promoter, an N-terminal tag, a coding sequence, a C-terminal tag, a plant terminator, and a plant resistance cassette.

Each module contains a restriction site of Eco31I and specific overhangs to ensure the orderly assembly and correct orientation. Digestion and ligation were performed in one reaction in a PCR-tube with the following components: 1.5 µl of each of the six entry modules (A-F), 1 µl of destination vector pGGZ003, 2 µl of FastDigest buffer, 1.5 µl of 10 mM ATP, 1 µl of T4 DNA ligase (Thermo Scientific™), and 1 µl of Eco31I (FastDigest). The reaction mix was placed into a PCR thermocycler with the following cycles: 35 cycles of 37 °C for 2 min and 16 °C for 2 min, 50 °C for 5 min, 80 °C for 5 min. Finally, 5 µl of the reaction mix was transformed into ccdB-sensitive chemically competent *E. coli* cells DH5α.

5.4 Protein techniques

5.4.1 Recombined protein expression

The construct of the recombined protein was transformed into *E. coli* BL21 competent cells, and positive colonies were selected by colony PCR. A positive colony was inoculated into 10 ml of LB medium with the appropriate antibiotic and allowed to grow overnight in a shaker at 37 °C and 180 rpm. Subsequently, a 10 ml primary culture was inoculated into 1 l of LB medium with the appropriate antibiotic, and cell culture was continued under the same conditions until the OD_{600} reached 0.6-0.8. IPTG (Isopropyl β-D-1-thiogalactopyranoside) was added to the cell culture at a final concentration of 1 mM to induce protein expression, and the cells were allowed to grow for an additional 3 h in an orbital shaker. The culture was then transferred to Oakridge tubes and centrifuged at 10,000 *xg* for 20 min at 4 °C. The supernatant was discarded, and the pellet was stored at -20 °C for further use. To determine the solubility of the protein, 1 ml of the cell culture after IPTG induction was collected and centrifuged at 7,000 *xg* for 3 min at room temperature. The supernatant was discarded, and the pellet was re-suspended in 50 µl of sonication buffer (300 mM NaCl, 50 mM NaPi, pH 8). The cells were sonicated with ultrasonic baths for 10 min or until the solution became clear. After sonication, the cells were centrifuged at 13,000 *xg* for 2 min at 4 °C, and the supernatant containing soluble proteins was transferred to a new tube. The insoluble proteins remained in the pellet, which was re-suspended in 30 µl of Lipsick buffer [10mM Tris, 1 mM EDTA, 7 M Urea, 50 mM NaCl, 20% (w/v) glycerol] by vortexing. The protein sample can be further analyzed by SDS-PAGE.

5.4.2 Protein Solubilization

The cell containing the target protein was collected and the pellet was suspended in 40 mL of lysis buffer (50 mM Tris-HCl, 5 mM EDTA, 1 mM PMSF, pH 8.5) in a 50 ml beaker. The mixture was vortexed until no pellet was visible. The cell suspension was sonicated with a sonotrode for 10 min with short pulses of 1 s followed by a gap of 1 s. Low temperature was maintained during sonication using an ice bath. The cell suspension was then centrifuged at 20,000 *xg* for 20 min at 4 °C. The supernatant was discarded and the pellet was re-suspended in 40 ml of wash buffer A (50 mM Tris-HCl, 5 mM EDTA, 1 mM PMSF, pH 8.5) by vortexing. Sonication and centrifugation were repeated as mentioned above. The resulting pellet was washed by suspending it in 25 mL of wash buffer B (50 mM Tris-HCl, pH 8.5). The suspension was then centrifuged at 20,000 xg for 20 minutes at 4 °C and the wash step with wash buffer B was repeated. The final pellet (purified inclusion body) was re-suspended in 2 mL of ddH2O and used for solubilization and refolding. Buffer C (50 mM Tris-HCl, 5 mM EDTA, 1 mM PMSF, 2 M urea, pH 12) was added into the inclusion body and mixed well by vortexing. The mixture was allowed to incubate at room temperature for at least 1 hour with 3-6 times vortexing during the incubation. The solubilized protein sample was centrifuged at 20,000 *xg* for 30 minutes at 4 °C. Protein refolding was done by slowly dripping 1 ml of solubilized protein into 9 ml of cool refolding buffer [50 mM Tris-HCl, 1 mM EDTA, 10% (w/v) sucrose, 1 mM PMSF, pH 7.5]. Once all the solubilized protein was added, the refolding process was kept on ice overnight. The refolded protein sample was centrifuged at 20,000 *xg* for 30 minutes at 4 °C to remove protein aggregates. The protein's solvent and concentration can be replaced and adjusted by an Amicon® Ultra-15 Centrifugal Filter according to the manufacturer's instructions.

5.4.3 SDS-polyacrylamid gel electrophoresis (SDS-PAGE)

The protein samples were mixed with 4× ROTI®Load 1 (Roth) and boiled for 5 min at 95°C before being loaded onto SDS-polyacrylamide gels. The molecular weight markers used were PageRuler Prestained Protein Ladder (Thermo Scientific™). The protein samples were separated in running buffer [25 mM Tris-base, 200 mM glycine, 0.1% (w/v) SDS, pH 8.6] by discontinuous SDS-PAGE applying a constant voltage of U = 100 V in stacking gels and U = 180 V in resolving gels. The stacking gels were composed of 3 ml water, 1.25 ml stacking gel buffer [0.5 M Tris-base pH 6.9,

0.4% (w/v) SDS], 0.75 ml acrylamide-mix (30% acrylamide/ bisacrylamide mix, 37.5:1, SERVA), 60 µl 10% APS, and 8 µl TEMED. The resolving gels were composed of 3.5 ml water, 2.5 ml resolving gel buffer [1.5 M tris-base pH 8.8, 0.4% (w/v) SDS], 4.4 ml acrylamide-mix (30% acrylamide/ bisacrylamide mix, 37.5:1, SERVA), 45 µl 10% APS, and 10 µl TEMED.

5.4.4 Coomassie staining

To visualize proteins in SDS polyacrylamide gels, the gels were incubated for 30 min at room temperature in Coomassie staining solution [0.2% (w/v) Coomassie Blue G250, 45% (w/v) methanol, 10% (w/v) glacial acetic acid] and then de-stained for 15 min in de-staining solution [10% (w/v) acetic acid]. Excess dye was removed and the gels were completely de-stained by incubating them overnight in deionized water.

5.5 Protein-DNA interaction techniques

5.5.1 Dual luciferase assay (DLA)

To generate effectors, the full length of transcription factors was cloned into the pART vector via Gateway cloning. The transcription factors were expressed under the CaMV35S promoter. To generate reporters, the promoter sequence of genes was cloned into the pRlucFluc vector, followed by the firefly luciferase coding sequence. As a normalization control, pRlucFluc contained the CaMV35S driven *Renilla* luciferase coding sequence in an opposite reading orientation to firefly luciferase. Transient promoter assays were carried out in chicory mesophyll protoplasts by co-transformation of effector and reporter plasmids in ratio 6:4. All transfection experiments were independently repeated two to three times. Luciferase activities were measured by the Dual-Luciferase® Reporter Assay System (Promega) and detected by a microplate reader (BMG LABTECH). Mean values of firefly and *Renilla* luciferase ratios were reported as relative luciferase activity with error bars indicating standard deviation (SD).

5.5.2 Electrophoretic mobility shift assay (EMSA)

Labeled oligonucleotides were modified at the 5'- end with Cyanine 5 (CY5) and were ordered from Eurofins. The oligonucleotides were dissolved in annealing buffer (10 mM Tris, 50 mM NaCl, 1 mM EDTA, pH 7.5) and equimolar concentrations of the oligonucleotides were mixed in a PCR tube. The thermocycler was used with the

following thermal profile: 95°C for 2 min; cool down to 25°C over 45 min; cool to 4°C. The annealed probe (0.2 pmol) was used to bind with 500 ng protein in binding buffer [25 mM HEPES, 50 mM KCl, 0.5 mM EDTA, 0.5 mM DTT, 5% (w/v) glycerol, 1 mg/mL BSA] in a 10 µl total volume for 30 min on ice. The reaction was stopped by adding 2 µl of 6× loading buffer [10 mM Tris-HCl, 0.15% (w/v) orange G, 60% (w/v) glycerol, 60 mM EDTA]. Samples were applied to a 6% (w/v) non-denaturing polyacrylamide gel in 0.5× TBE buffer. Electrophoresis was performed at 120V for 35 min on ice, and the gel shift was recorded using ImageQuant LAS 4000. For competitor assays, non-labeled oligonucleotides were pre-incubated with the protein prior to adding the CY5-labeled probes.

5.6 Vectors

Vector	Resistance	Application
pJET1.2	Ampicillin	Blunt end cloning of PCR products
pDONR221	Kanamycin	Gateway entry vector
pART7	Ampicillin	Gateway destination vector, in planta protein expression
pRlucFluc	Ampicillin	Gateway destination vector, promoter driven firefly luciferase expression; CaMV35S promoter driven Renilla luciferase expression
pETG10A	Ampicillin	His-tag; Protein expression vector in prokaryotic system
pAbAi	Ampicillin	Yeast reporter vector, used in Y1H to identify DNA-binding proteins
pGBKT7	Kanamycin	Yeast expression vector (Tryptophan marker) fused to a GAL4 BD
pGADT7	Ampicillin	Yeast expression vector (Leucine marker) fused to a GAL4 AD
pNluc	Kanamycin	pCAMBIA1300 for LCA, N-terminal fragment of luciferase
pCluc	Kanamycin	pCAMBIA1300 for LCA, C-terminal fragment of luciferase

5.7 Primer list

Oligonucleotides were ordered at Eurofins MWG Operon (Ebersberg, Germany), dissolved to a concentration of 100 µM and stored at -20°C.

5.7.1 Primers used for qRT-PCR

Gene	Description	Sequence (5'-3')
RPL19	RPL19_for	CTGCCAGCGTCCTCAAGTG
	RPL19_for	CATTGGGATCAAGCCAAACCT
Actin	Actin_for	CCAAATCCAGCTCATCAGTCG
	Actin_rev	TCTTTCGGCTCCGATGGTGAT

1-FEH2a	qFEH2a_1_for	GGGTTCCTGAAACTGATTCTCAAGC
	qFEH2a_1_rev	CCGCCTGAGAAGCAGCAATC
1-FEH2b	qFEH2b_1_for	GGTTCCTGAAACTGATGCTCCAGA
	qFEH2b_1_rev	CATCCGCCTGTGAAGCAGTAATG
1-FEH1	qFEH1_for	GGCTTCACAGGCTGATGTAGAA
	qFEH1_rev	GCCGAACTTCCCACTGATAGAA
1-SST	1-SST_F	CCAACAACCATCAGGGAGGAG
	1-SST_R	AGCAACGGAGCTGTGAACGT
1-FFT	1-FFT_F	CGGCTACGCAGTTGGACATAG
	1-FFT_R	CTCGTGGTGCAACCGTATTCA
CiDREB1A	qDREB1A_F	GGTTGAGTCCTCTTCCTCTTCT
	qDREB1A_R	CGGCTTCAAGAACTCCAAACTAT
CiDREB1C	qDREB1C_2_for	GGAGTTGCCGGAAATTCAGTT
	qDREB1C_rev	CATCCGTGTAGTTGTCAAACCCC
CiDREB1D	qDREB1D_F	CGGAGGATGAGATTGAGACTGTG
	qDREB1D_R	CATCCACATAGTTGACATACCCTAC
CiDREB2A	qDREB2A_F	AACCCAGATGATGCTACTTATGAG
	qDREB2A_R	CGGCTTCAAGAACTCCAAACTAT
CiDREB2B	qDREB2B_F	TCCAGATTCACAAACGGTCA
	qDREB2B_R	TTAAACCAGGTGCGTTAGGG
CiMYB3	MYB3_F	GCTGCCTGAAATGCCACAAC
	MYB3_R	AATCCCATCATATCAAACCCTCCT
CiMYB5	MYB5_F	GGACACGATGCGGTATCTTTGG
	MYB5_R	TGGTGGTGGAGGAGGAGGAA
CiNAC1	qCiNAC1_F	CGAAAGAGAAGTTCAAAGTGAAGC
	qCiNAC1_R	GAAGTCGTTGTAGTATTGGCTTTGA
CiNAC2	qCiNAC2_F	GACACGTCGGAATCGGGTCCT
	qCiNAC2_R	ATCTGGAAGGGCTTTGGTGTGTA
CiNAC3	qCiNAC3_F	ACCACCGCCAACACCACAA
	qCiNAC3_R	TATGTTCGACTGAAAGTAACTCGG
CiNAC4	qCiNAC4_F	CAGGACCCGATTACCAACAACAAT
	qCiNAC4_R	CGTGTGCATGAAGCTCTGTGAA
CiNAC5	qCiNAC5_F	CGTCATGTTCATAAGCGACTTGC
	qCiNAC5_R	AACTGATACTGTCCAGCCACTCAT
CiNAC6	qCiNAC6_F	CAAAGGCAAACGCAAAGGCAAA
	qCiNAC6_R	TCTCTTCGTGTTCATCCGTCTCA
CiNAC7	qCiNAC7_F	TCATGGCTGGTATTCCAAGAACTG
	qCiNAC7_R	CTGCTCTCTTCACCTTCATCTGC
CiNAC8	qCiNAC8_F	ACCGACGAAGAGCTGGTAAA
	qCiNAC8_R	TGGACTCAATCACCGACAAA

5.7.2 Primers used for promoter amplification

Promoter	Description	Sequence (5'-3')
p1-FEH1	-1195_F	CCGGTAGATTACGTTATTATGAAC
	-595_F	TTCATGCATCCGTCCAAA
	-353_F	TGGACAAACACCGAACCTCA
	R	ATTGTTCAGTGTCGATCT
p1-FEH2a	F	CCGCAGACCTCTATCCATATATTAGTTC
	R	ATGATGAGTGTGTGTGTTTGGGGA
p1-FEH2b	F	TAACAGAATGGACCCAATTATTCG
	R	TGAGGAGAATGGGTGTTATGGA
pDREB2A	F	CATGTTATGCAGCGAGCTTT
	R	GCGCCGCAAATCAATATCTA
pDREB2B	F	CTGTCCGTCTCCTCCATACGv
	R	ATGCAGCAAATCAAAAGCTACTT
pNAC5	F	GAATGTCCCCACCAAACAAC
	R	ATTCAGGGATGGGGGAGTTA

5.7.3 Primer used for generating mutation

Name	Back to back	Sequence (5'-3')
pFEH1_DEL1	F	AATCATTGTGGGTGAGACTA
	R	CATCTTATATTGGAAAAAGGAAAC
pFEH1_DEL2	F	TATTCACTATAAATACTAGCCATG
	R	AAACGAATTTTGATTACTCCC
pFEH1_M1	F	GAGGGAGTAATCAAAATTCG
	R	gcatGATGGACTAGTCTCACCC
pFEH1_M2	F	CCTTATTTTTTATGCTTATGAGTG
	R	gcatCCAAGTTTAGCAATTAGCATA
pFEH2b_DRE	Del_F	GATACTATTTGTCTCAAAGTCTA
	Mut_F	AAtTCtGTAGATACTATTTGT
	R	ATGTTAGTTATTGCCCCTTG

5.7.4 Primers used for sequencing

Vector	Description	Sequence (5'-3')
pDONR201	M13uni-21	TGTAAAACGACGGCCAGT
	M13rev-29	CAGGAAACAGCTATGACC

pART7	35S_F	CTATCCTTCGCAAGACCCTT
	OCS_R	GGCGGTAAGGGAGCTA
pGADT7	Gal4AD	TACCACTACAATGGATG
pGBDT7	Gal4BD	TCATCGGAAGAGAGTAG
pAbAi	pAbAi_F	CATCTCGAAAAAGGGTTTGCCATTA
	pAbAi_R	CATCTCGAAAAAGGGTTTGCCATTA
pRLUC_Fluc	LUC_R	GGATAGAATGGCGCCGG

5.7.5 Oligonucleotides used for EMSA

Name	Sequence (5'-3')
rd29A (+)	ATGGAATAAATATCATACCGACATCAGTTTGAAAGAAAAG
rd29A (-)	CTTTTCTTTCAAACTGATGTCGGTATGATATTTATTCCAT
pFEH1 (+)	TTCATTGGCCTTAATGTCGGACGAAATTATATATCTTTTA
pFEH1 (-)	TAAAAGATATATAATTTCGTCCGACATTAAGGCCAATGAA
pFEH1-2 (+)	GATGAAACGCAATCATTGTGGGTGAGACTAGTCCATCCGT
pFEH1-2 (-)	ACGGATGGACTAGTCTCACCCACAATGATTGCGTTTCATC
pFEH2a (+)	CAATAACTAACATAATTCGGTAGATACTATTTGTCTCAAA
pFEH2a (-)	TTTGAGACAAATAGTATCTACCGAATTATGTTAGTTATTG
pFEH2b (+)	CAATAACTAACATAAGTCGGTAGATACTATTTGTCTCAAA
pFEH2b (-)	TTTGAGACAAATAGTATCTACCGACTTATGTTAGTTATTG
DRE_Mutant (+)	CAATAACTAACATGCACTAACTAATACTATTTGTCTCAAA
DRE_Mutant (-)	TTTGAGACAAATAGTATTAGTTAGTGCATGTTAGTTATTG

5.7.6 Primer used for CRISPR/Cas9

Name	Sequence (5'-3')
U-F	CTCCGTTTTACCTGTGGAATCG
gR-R	CGGAGGAAAATTCCATCCAC
Pps-R	TTCAGAGGTCTCTACCGACTAGTCACGCGTATGGAATCGGCAGCAAA
Pgs-L	AGCGTGGGTCTCGCTCGACGCGTATCCATCCACTCCAAGC
SP-L1	GCGGTGTCATCTATGTTACTAG
SP-R	TGCAATAACTTCGTATAGGCT
Cas9-f	CTGACGCTAACCTCGACAAG
Cas9-r	CCGATCTAGTAACATAGATGACACC

6 Supplementary Materials

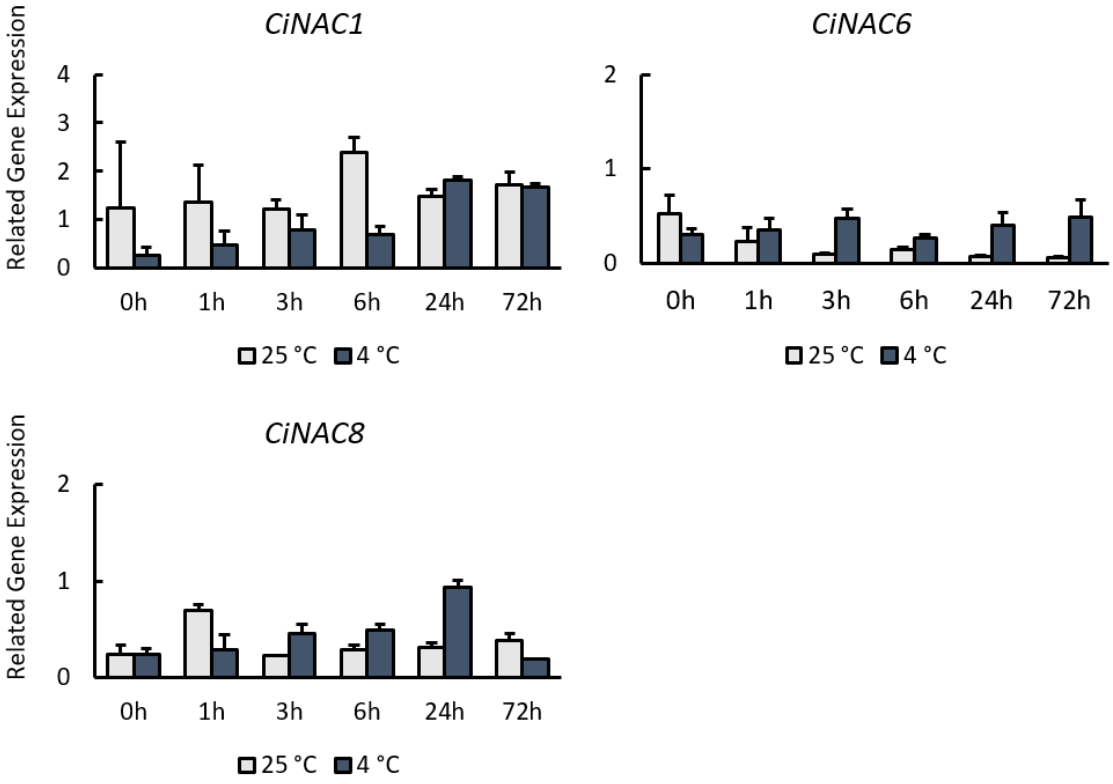

Figure S1 Impact of cold treatment (4°C±1) on transcript levels of transcription factors (CiNAC1, CiNAC6 and CiNAC8) in taproots of 3-month-old chicory. Taproot tissue were incubated in distilled water and transferred to cold room (4°C±1), while control were kept room temperature (RT, 25 °C). Transcript levels were determined by qPCR and normalized against the expression of two reference genes Actin and RPL19. Relative gene expression were calculated with delta Ct method. The error bars represent standard deviation (n = 3).

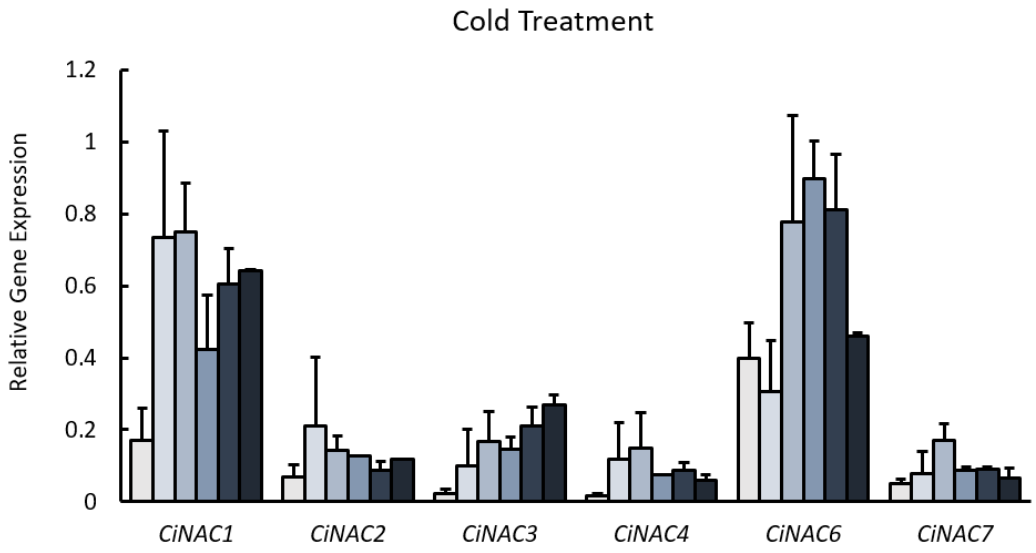

Figure S2 Impact of cold treatment (4°C±1) on transcript levels of transcription factors (CiNAC1-4 and CiNAC6-7) in taproots of 4-week-old chicory seedling. Seedlings were transferred to cold room (CR, 4°C±1). Taproot samples were harvested every 4 hour after treatment. Transcript levels were determined by qPCR and normalized against the expression of two reference genes Actin and RPL19. Relative gene expression were calculated with delta Ct method. The error bars represent standard deviation (n = 3-4).

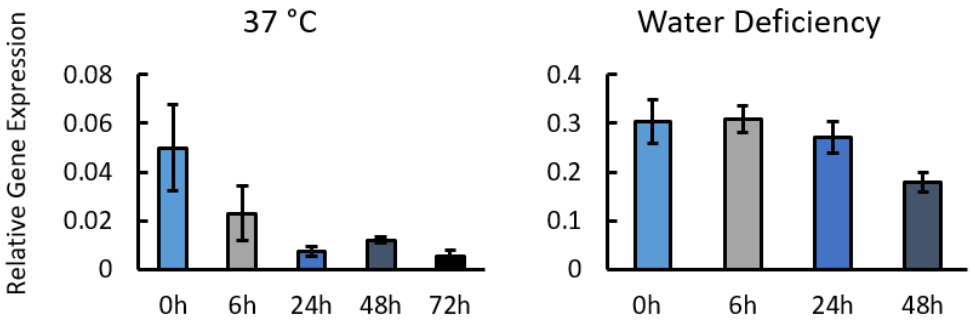

Figure S3 Transcript levels of CiNAC5 under heat treatment (37°C) and water deficiency treatment in taproots of 4-week-old chicory seedling. Soil grown seedlings were transferred to 37°C incubator for indicated time. For water deficiency, hydroponic seedlings were drained out solution and harvested at indicated time. Transcript levels were determined by qPCR and normalized against the expression of two reference genes Actin and RPL19. Relative gene expression were calculated with delta Ct method. The error bars represent standard deviation (n = 3-4).

Table S1 Off-target search of sgRNA								
		On	Miss match					
sgRNA	Target Name	target	1 bp	2 bp	3 bp	4 bp	5 bp	Sum
GGATCGTGGCTGAACCTGAC	FEH1_167rev	1	0	1	3	26	452	482
GACATCAATGGCTGCCTGTC	FEH1_173forw	1	0	1	2	32	285	320
CCGTGGCCCGGGTAGGATCG	FEH1_181rev	1	0	0	0	144	652	796
AGAATTATGGGCCGTGGCCC	FEH1_192rev	1	0	0	2	23	313	338
GTTCAGCCACGATCCTACCC	***FEH1_195forw***	***1***	***0***	***0***	***0***	***10***	***170***	***180***
CCACGATCCTACCCGGGCCA	FEH1_201forw	1	0	0	0	134	445	579
CAATAGTCAGGTTCAGAACC	FEH1_256forw	1	0	0	2	44	718	764
AGCTTTAATGTCATCGACGG	FEH1_328rev	1	0	0	6	47	505	558
CCAGCTTTAATGTCATCGAC	FEH1_330rev	1	0	0	0	31	625	656
ACAATTCCGTGATCCATCAA	FEH1_373forw	1	0	0	6	85	695	786
TCCGTGATCCATCAACGGCT	FEH1_378forw	1	0	0	5	12	212	229
ATCAACGGCTTGGATGGGTC	FEH1_388forw	1	1	4	205	144	701	1055
ACGGCTTGGATGGGTCCGGA	FEH1_392forw	1	0	1	1	34	439	475
TGCCCCAGAGTGGACCGTAA	FEH1_47rev	1	0	0	0	10	106	116
TTGCCCCAGAGTGGACCGTA	FEH1_48rev	1	0	0	2	9	119	130
ACAACCCTTACGGTCCACTC	FEH1_63forw	1	0	0	2	11	320	333
AACCCTTACGGTCCACTCTG	FEH1_65forw	1	0	0	1	19	306	326
TCTGAATGATGTGATAATGC	FEH2a_107forw	1	0	1	12	108	1365	1486
TAATGAAAGCAGGATTTGAA	FEH2a_630forw	2	0	0	18	240	2624	2882
TCATCATTCTGGAAACTGGT	FEH2a_64forw	1	0	1	4	84	1238	1327
CATCATTCTGGAAACTGGTC	FEH2a_65forw	1	0	3	4	53	584	644
CCGGAAGTACGTTGGATTTG	FEH2a_726forw	2	0	0	0	35	576	611
CAGAAGGGTTTTGTGGGCGT	FEH2a_802forw	1	1	0	3	99	642	745
CCGACCCGTTCCTTCGTGAA	FEH2ab_300forw	2	0	1	0	17	212	230
GCCAGGCGGTGCTCGGGTCA	FEH2ab_362rev	2	0	0	0	3	93	96
GGCCGAGCCAGGCGGTGCTC	FEH2ab_368rev	1	1	0	1	18	219	239
GGGCCGAGCCAGGCGGTGCT	FEH2ab_369rev	1	1	0	2	11	164	178
GCCGTCGGGGCCGAGCCAGG	FEH2ab_376rev	1	1	0	1	22	155	179
TACGCCGTCGGGGCCGAGCC	FEH2ab_379rev	1	1	0	0	2	41	44
TCCGTGACCCGAGCACCGCC	FEH2ab_381forw	2	0	0	0	9	136	145
GACCCGAGCACCGCCTGGCT	FEH2ab_386forw	1	1	0	0	10	320	331
AGACCGTGACAACAACGGTA	FEH2ab_442forw	2	0	0	5	27	384	416
CGGGCACTCCCAAGTTCCGG	***FEH2ab_514rev***	***2***	***0***	***0***	***0***	***24***	***102***	***126***
GGCGGATGCCACCGGAACTT	FEH2ab_526forw	1	0	1	0	12	174	187
ACGGCACAGGGTAAAAGTCC	FEH2ab_533rev	1	0	1	0	10	125	136
AACGGCACAGGGTAAAAGTC	FEH2ab_534rev	1	0	1	2	18	286	307
CACCGGAACTTGGGAGTGCC	FEH2ab_535forw	2	0	0	1	16	125	142
GTGAGACATGTAATGAAAGC	FEH2ab_620forw	3	0	0	6	108	913	1027
CCACGCCGTATCATACGACT	FEH2b_106forw	2	0	0	0	9	129	138

7 List of Abbreviations

1-FEH	fructan 1-exohydrolase
1-FFT	fructan: fructan 1-fructosyltransferase
1-SST	sucrose: sucrose 1-fructosyltransferase
6-SFT	sucrose: fructan 6-fructosyltransferase
6G-FFT	fructan: fructan 6G-fructosyltransferase
ABA	abscisic acid
ACC	1-aminocyclopropane-1-carboxylic acid
AP2	APETALA2
CAMTA	CALMODULIN BINDINGTRANSCRIPTION ACTIVATOR3
Cas	CRISPR-associated protein
CBF	C-repeat binding factors
ChIP	chromatin immunoprecipitation
COR	cold-regulated
CRISPR	Clustered Regularly Interspaced Short Palindromic Repeats
crRNA	CRISPR RNA
CRT	C-repeat
DAPI	4', 6-diamino-2-phenylindole, dihydrochloride
DLA	Dual luciferase assay
DP	degree of polymerization
DRE	Dehydration Response Element
DREB	Dehydration Responsive Element-Binding protein
DSB	double-strand break
dsDNA	double-strand DNA
EGFP	Enhanced green fluorescent protein
EMSA	Electrophoretic mobility shift assay
ERF	ethylene-responsive element binding factors
FAZY	fructan active enzyme
FDCA	2,5-furandi-carboxylic acid
HDR	homology-directed repair
IPTG	Isopropyl β- d-1-thiogalactopyranoside
LCA	luciferase complementation assay

LFS	LATE FLOWERING SEMI-DWARF
mDP	mean degree of polymerization
NAC	No apical meristem (NAM), Arabidopsis transcription activation factor (ATAF), Cup-shaped cotyledon (CUC)
NACBS	NAC Binding Site
NHEJ	nonhomologous end joining
PAM	protospacer adjacent motif
PEG	polyethylene glycol
PPC2	protein phosphatases 2C
qRT-PCR	quantitative real-time PCR
RAV	Related to ABI3/VP
RNP	ribonucleoprotein
ROS	reactive oxygen species
Seq	sequencing
sgRNA	single guide RNA
SUSIBA	sugar signaling in barley
TAL	transcription activator-like
TF	transcription factor
tracrRNA	*tans*-activating crRNA
WSC	water-soluble carbohydrates
X-α-Gal	5-Bromo-4-chloro-3-indolyl-α-D-galactopyranoside
ZFN	Zinc finger nucleases

8 References

Abeynayake SW, Etzerodt TP, Jonavičienė K, Byrne S, Asp T, Boelt B (2015) Fructan Metabolism and Changes in Fructan Composition during Cold Acclimation in Perennial Ryegrass. *Frontiers in Plant Science* 6 (5): 1–13.

Afinjuomo F, Abdella S, Youssef SH, Song Y, Garg S (2021) Inulin and Its Application in Drug Delivery. *Pharmaceuticals* 14 (855):1–37.

Agarwal M, Hao Y, Kapoor A, Dong CH, Fujii H, Zheng X, Zhu JK (2006) A R2R3 Type MYB Transcription Factor Is Involved in the Cold Regulation of CBF Genes and in Acquired Freezing Tolerance. *Journal of Biological Chemistry* 281 (49): 37636–37645.

Agarwal PK, Gupta K, Lopato S, Agarwal P (2017) Dehydration Responsive Element Binding Transcription Factors and Their Applications for the Engineering of Stress Tolerance. *Journal of Experimental Botany* 68 (9): 2135–2148.

Akalın AS, Karagözlü C, Ünal G (2008) Rheological Properties of Reduced-Fat and Low-Fat Ice Cream Containing Whey Protein Isolate and Inulin. *European Food Research and Technology* 227 (3): 889–895.

Amitai G, Sorek R (2016) CRISPR-Cas Adaptation: Insights into the Mechanism of Action. *Nature Reviews Microbiology* 14 (2): 67–76.

Bae S, Park J, Kim JS (2014) Cas-OFFinder: A Fast and Versatile Algorithm That Searches for Potential off-Target Sites of Cas9 RNA-Guided Endonucleases. *Bioinformatics* 30 (10): 1473–1475.

Barcaccia G, Ghedina A, Lucchin M (2016) Current Advances in Genomics and Breeding of Leaf Chicory (*Cichorium Intybus* L.). *Agriculture* 6 (50): 1–24.

Barreto R, Nieto-Sotelo J, Cassab GI (2010) Influence of Plant Growth Regulators and Water Stress on Ramet Induction, Rosette Engrossment, and Fructan Accumulation in *Agave tequilana* Weber Var. Azul. *Plant Cell, Tissue and Organ Culture* 103 (1): 93–101.

Bernard G, Gagneul D, Alves Dos Santos H, Etienne A, Hilbert JL, Rambaud C (2019) Efficient Genome Editing Using CRISPR/Cas9 Technology in Chicory. *International Journal of Molecular Sciences* 20 (1155) 1–18.

Bolouri-Moghaddam MR, le Roy K, Xiang L, Rolland F, Van den Ende W (2010) Sugar Signalling and Antioxidant Network Connections in Plant Cells. *FEBS Journal*. 277 (2010): 2022–2037

Broda M, Khan K, O'Leary B, Pružinská A, Lee CP, Millar AH, Van Aken O (2021) Increased Expression of ANAC017 Primes for Accelerated Senescence. *Plant Physiology* 186 (4): 2205–2221.

Brouns S, Matthijs J, Lundgren M, Westra E, Slijkhuis R, Snijders A, Dickman M, Makarova K, Koonin E, Van Der Oost J (2008) Small CRISPR RNAs Guide Antiviral Defense in Prokaryotes. *Science* 321 (5891): 960–964.

Bui LT, Shukla V, Giorgi F, Trivellini A, Perata P, Licausi F, Giuntoli B (2020) Differential Submergence Tolerance between Juvenile and Adult *Arabidopsis* Plants Involves the ANAC017 Transcription Factor. *Plant Journal* 104 (4): 979–994.

Cadalen T, Mörchen M, Blassiau C, Clabaut A, Scheer I, Hilbert JL, Hendriks T, Quillet MC (2010) Development of SSR Markers and Construction of a Consensus Genetic Map for Chicory (*Cichorium Intybus* L.). *Molecular Breeding* 25 (4): 699–722.

Chen C, Zhang K, Khurshid M, Li J, He M, Georgiev MI, Zhang X, Zhou M (2019) MYB Transcription Repressors Regulate Plant Secondary Metabolism. *Critical Reviews in Plant Sciences* 38 (3): 1–12.

Chen C, Chen Z (2000) Isolation and Characterization of Two Pathogen-and Salicylic Acid-Induced Genes Encoding WRKY DNA-Binding Proteins from Tobacco. *Plant Molecular Biology* 42: 387–396.

Chen D, Chai S, McIntyre CL, Xue GP (2018) Overexpression of a Predominantly Root-Expressed NAC Transcription Factor in Wheat Roots Enhances Root Length, Biomass and Drought Tolerance. *Plant Cell Reports* 37 (2): 225–237.

Chen K, Wang Y, Zhang R, Zhang H, and Gao C (2019) CRISPR / Cas Genome Editing and Precision Plant Breeding in Agriculture. *Annual Reviews of Plant Biology* 70: 667–700.

Cichota R, McAuliffe R, Lee J, Minnee E, Martin K, Brown HE, Moot DJ, Snow VO (2020) Forage Chicory Model: Development and Evaluation. *Field Crops Research* 246 (2020): 10763.

Cimini S, Locato V, Vergauwen R, Paradiso A, Cecchini C, Vandenpoel L, Verspreet J, Courtin C, D'Egidio MG, Van den Ende W, De Gara L (2015) Fructan Biosynthesis and Degradation as Part of Plant Metabolism Controlling Sugar Fluxes during Durum Wheat Kernel Maturation. *Frontiers in Plant Science* 6 (2): 1–10.

Ciolkowski I, Wanke D, Birkenbihl RP, Somssich IE (2008) Studies on DNA-Binding Selectivity of WRKY Transcription Factors Lend Structural Clues into WRKY-Domain Function. *Plant Molecular Biology* 68: 81–92.

Concordet JP, Haeussler M (2018) CRISPOR: Intuitive Guide Selection for CRISPR/Cas9 Genome Editing Experiments and Screens. *Nucleic Acids Research* 46: W242–245.

Dauchot N, Raulier P, Maudoux O, Notté C, Bertin P, Draye X, Van Cutsem P (2014) Mutations in Chicory FEH Genes Are Statistically Associated with Enhanced Resistance to Post-Harvest Inulin Depolymerization. *Theoretical and Applied Genetics* 127 (1): 125–135.

Dauchot N, Raulier P, Maudoux O, Notté C, Draye X, Van Cutsem P (2015) Loss of Function of 1-FEH IIb Has More Impact on Post-Harvest Inulin Degradation in *Cichorium Intybus* than Copy Number Variation of Its Close Paralog 1-FEH IIa. *Frontiers in Plant Science* 6 (6): 455.

Deltcheva E, Chylinski K, Sharma CM, Gonzales K, Chao Y, Pirzada ZA, Eckert MR, Vogel J, Charpentier E (2011) CRISPR RNA Maturation by

Trans-Encoded Small RNA and Host Factor RNase III. *Nature* 471 (7340): 602–607.

del Viso F, Puebla A, Fusari C, Casabuono A, Couto A, Pontis H, Hopp H, Heinz R (2009) Molecular Characterization of a Putative Sucrose:Fructan 6-Fructosyltransferase (6-SFT) of the Cold-Resistant Patagonian Grass Bromus pictus Associated With Fructan Accumulation Under Low Temperatures. Plant and Cell Physiology 50 (3): 489–503.

De Clercq I, Vermeirssen V, Van Aken O, Vandepoele K, Murcha M, Law S, Inzé A, Ng S, Ivanova A, Rombaut D, Van De Cotte B, Jaspers P, Van De Peer Y, Kangasjävi J, Whelan J, Van Breusegem F (2013) The Membrane-Bound NAC Transcription Factor ANAC013 Functions in Mitochondrial Retrograde Regulation of the Oxidative Stress Response in *Arabidopsis*. *Plant Cell* 25 (9): 3472–3490.

De Roover J, Van Laere A, De Winter M, Timmermans J, Van den Ende W (1999a) Purification and Properties of a Second Fructan Exohydrolase from the Roots of *Cichorium Intybus*. *Physiologia plantarum* 106: 28–34.

De Roover J, Van Laere A, Van den Ende W (1999b) Effect of Defoliation on Fructan Pattern and Fructan Metabolizing Enzymes in Young Chicory Plants (*Cichorium Intybus*). *Physiologia plantarum* 106: 158–163.

De Roover J, Vandenbranden K, Van Laere A, Van den Ende W (2000) Drought Induces Fructan Synthesis and 1-SST (Sucrose: Sucrose Fructosyltransferase) in Roots and Leaves of Chicory Seedlings (*Cichorium Intybus* L.). *Planta* 210: 808–814.

Dielen V, Notté C, Lutts S, Debavelaere V, Van Herck JC, Kinet JM (2005) Bolting Control by Low Temperatures in Root Chicory (*Cichorium intybus* var. *sativum*). *Field Crops Research* 94 (2005): 76–85.

Du H, Zhang L, Liu L, Tang XF, Yang WJ, Wu YM, Huang YB, and Tang YX (2009) Biochemical and Molecular Characterization of Plant MYB Transcription Factor Family. *Biochemistry (Moscow)* 74 (1): 1–11.

Dubos C, Stracke R, Grotewold E, Weisshaar B, Martin C, Lepiniec L (2010) MYB Transcription Factors in *Arabidopsis*. *Trends in Plant Science* 15 (10): 573–581.

Epstein E and Bloom AJ (2005) Mineral Nutrition of Plants: Principles and Perspectives, 2nd ed. Sinauer Associates, Sunderland, MA.

Feng K, Hou XL, Xing GM, Liu JX, Duan AQ, Xu ZS, Li MY, Zhuang J, Xiong AS (2020) Advances in AP2/ERF Super-Family Transcription Factors in Plant. *Critical Reviews in Biotechnology* 40 (6): 750-776.

Fuchs P, Bohle F, Lichtenauer S, Ugalde JM, Araujo EF, Mansuroglu B, Ruberti C, Wagner S, Müller-Schüssele SJ, Meyer AJ, Schwarzländer M (2022) Reductive Stress Triggers ANAC017-Mediated Retrograde Signaling to Safeguard the Endoplasmic Reticulum by Boosting Mitochondrial Respiratory Capacity. *Plant Cell* 34 (4): 1375–1395.

Gao H, Gadlage MJ, Lafitte HR, Lenderts B, Yang M, Schroder M, Farrell J, et al. (2020) Superior Field Performance of Waxy Corn Engineered Using CRISPR–Cas9. *Nature Biotechnology* 38 (5): 579–581.

Gasperl A, Morvan-Bertrand A, Prud'Homme MP, Van Der Graaff E, Roitsch T (2016) Exogenous Classic Phytohormones Have Limited Regulatory Effects on Fructan and Primary Carbohydrate Metabolism in Perennial Ryegrass (Lolium Perenne L.). *Frontiers in Plant Science* 6 (1): 1251.

Gilmour SJ, Zarka DG, Stockinger EJ, Salazar MP, Houghton JM, Thomashow MF (1998) Low Temperature Regulation of the *Arabidopsis* CBF Family of AP2 Transcriptional Activators as an Early Step in Cold-Induced COR Gene Expression. *Plant Journal* 16 (4): 433–442.

Guven M, Yasar K, Karaca OB, Hayaloglu AA (2005) The Effect of Inulin as a Fat Replacer on the Quality of Set-Type Low-Fat Yogurt Manufacture. *International Journal of Dairy Technology* 58 (3): 180–184.

Haafl D, Abou-Mandour AA, Blaschek W, Franz G, Czygan FC (1991) The Influence of Phytohormones on Growth, Organ Differentiation and Fructan Production in Callus of Symphytum Officinale L. *Plant Cell Reports* 10: 421–424.

He Y, Zhao J, Feng D, Huang Z, Liang J, Zheng Y, Cheng J, Ying J, Wang Z (2020) RNA-Seq Study Reveals AP2-Domain-Containing Signalling Regulators Involved in Initial Imbibition of Seed Germination in Rice. *Rice Science* 27 (4): 302–314.

Heler R, Marraffini LA, Bikard D (2014) Adapting to New Threats: The Generation of Memory by CRISPR-Cas Immune Systems. *Molecular Microbiology* 93 (1): 1–9.

Hendry G (1993) Evolutionary Origins and Natural Functions of Fructans – a Climatological, Biogeographic and Mechanistic Appraisal. *New Phytologist* 123 (1): 3–14.

Heo JB, Lee YS, Chung CH (2021) Conversion of Inulin-Rich Raw Plant Biomass to 2,5-Furandicarboxylic Acid (FDCA): Progress and Challenge towards Biorenewable Plastics. *Biotechnology Advances* 53:107838

Hiraki H, Uemura M, Kawamura Y (2019) Calcium Signaling-Linked CBF/DREB1 Gene Expression Was Induced Depending on the Temperature Fluctuation in the Field: Views from the Natural Condition of Cold Acclimation. *Plant and Cell Physiology* 60 (2): 303–317.

Hou J, Huang X, Sun W, Du C, Wang C, Xie Y, Ma Y, Ma D (2018) Accumulation of Water-Soluble Carbohydrates and Gene Expression in Wheat Stems Correlates with Drought Resistance. *Journal of Plant Physiology* 231 (12): 182–91.

Hou X, Zhang H, Liu S, Wang X, Zhang Y, Meng Y, Luo D, Chen R (2020) The NAC Transcription Factor CaNAC064 Is a Regulator of Cold Stress Tolerance in Peppers. *Plant Science* 291 (11): 110346.

Jeong JS, Park YT, Jung H, Park SH, Kim JK (2009) Rice NAC Proteins Act as Homodimers and Heterodimers. *Plant Biotechnology Reports* 3 (2): 127–134.

Jiang CK, Rao GY (2020) Insights into the Diversification and Evolution of R2R3-MYB Transcription Factors in Plants. *Plant Physiology* 183 (2): 637–655.

Jin Y, Fei M, Rosenquist S, Jin L, Gohil S, Sandström C, Olsson H, et al. (2017) A Dual-Promoter Gene Orchestrates the Sucrose-Coordinated Synthesis of Starch and Fructan in Barley. *Molecular Plant* 10 (12): 1556–1570.

Jinek M, Chylinski K, Fonfara I, Hauer M, Doudna J, Charpentier E (2012) A Programmable Dual-RNA-Guided DNA Endonuclease in Adaptive Bacterial Immunity. *SCIENCE* 337 (6096): 816–821.

Jung C, Seo JS, Han SW, Koo YJ, Kim CH, Song SI, Nahm BH, Choi DY, Cheong JJ (2008) Overexpression of *AtMYB44* Enhances Stomatal Closure to Confer Abiotic Stress Tolerance in Transgenic *Arabidopsis*. *Plant Physiology* 146 (2): 623–635.

Jurczyk B, Pociecha E, Janowiak F, Dziurka M, Kościk I, Rapacz M (2021) Changes in Ethylene, Aba and Sugars Regulate Freezing Tolerance under Low-temperature Waterlogging in *Lolium Perenne*. *International Journal of Molecular Sciences* 22 (6700): 1–22.

Kawakami A, Yoshida M (2012) Graminan Breakdown by Fructan Exohydrolase Induced in Winter Wheat Inoculated with Snow Mold. *Journal of Plant Physiology* 169 (3): 294–302.

Kidokoro S, Yoneda K, Takasaki H, Takahashi F, Shinozaki K, Yamaguchi-Shinozaki K (2017) Different Cold-Signaling Pathways Function in the Responses to Rapid and Gradual Decreases in Temperature. *The Plant Cell* 29 (4): 760–774.

Kooiker M, Drenth J, Glassop D, McIntyre CL, Xue GP (2013) TaMYB13-1, a R2R3 MYB Transcription Factor, Regulates the Fructan Synthetic Pathway and Contributes to Enhanced Fructan Accumulation in Bread Wheat. *Journal of Experimental Botany* 64 (12): 3681–3696.

Kusch U, Greiner S, Steininger H, Meyer A, Corbière-Divialle H, Harms K, Rausch T (2009) Dissecting the Regulation of Fructan Metabolism in Chicory (*Cichorium Intybus*) Hairy Roots. *New Phytologist* 184 (1): 127–40.

Kusch U, Harms K, Rausch T, Greiner S (2009) Inhibitors of Plant Invertases Do Not Affect the Structurally Related Enzymes of Fructan Metabolism. *New Phytologist* 181 (3): 601–612.

Kusnandar AS, Itoh JI, Sato Y, Honda E, Hibara K, Kyozuka J, Naramoto S (2022) NARROW and DWARF LEAF 1, the Ortholog of *Arabidopsis* ENHANCER of SHOOT REGENERATION1/DORNRÖSCHEN, Mediates Leaf Development and Maintenance of the Shoot Apical Meristem in *Oryza Sativa* L. *Plant and Cell Physiology* 63 (2): 265–278.

Lamaoui M, Jemo M, Datla R, Bekkaoui F (2018) Heat and Drought Stresses in Crops and Approaches for Their Mitigation. *Frontiers in Chemistry* 6 (26):1–14.

Lampropoulos A, Sutikovic Z, Wenzl C, Maegele I, Lohmann J, Forner J (2013) GreenGate - A Novel, Versatile, and Efficient Cloning System for Plant Transgenesis. *PLoS ONE* 8 (12): 83043.

Lee JW, Lee YS, Chung CH (2022) Sustainable Production of DMF and EMF Using Inulin-Rich Raw Plant Biomass: Perspective towards Biorenewable Fuel. *Journal of Cleaner Production* 348 (2022): 131359.

Lee S, Kang J, Park HJ, Kim MD, Bae MS, Choi H, Kim SY (2010) DREB2C Interacts with ABF2, a BZIP Protein Regulating Abscisic Acid-Responsive Gene Expression, and Its Overexpression Affects Abscisic Acid Sensitivity. *Plant Physiology* 153 (2): 716–727.

Leenay R, Maksimchuk K, Slotkowski R, Agrawal R, Gomaa A, Briner A, Barrangou R, and Beisel C (2016) Identifying and Visualizing Functional PAM Diversity across CRISPR-Cas Systems. *Molecular Cell* 62 (1): 137–47.

Li J, Chen F, Li Y, Li P, Wang Y, Mi G, Yuan L (2019) ZmRAP2.7, an AP2 Transcription Factor, Is Involved in Maize Brace Roots Development. *Frontiers in Plant Science* 10 (820): 1–11.

Li M, Li X, Zhou X, Wu P, Fang M, Pan X, Lin Q, Luo W, Wu G, and Li H (2016) Reassessment of the Four Yield-Related Genes *Gn1a*, *DEP1*, *GS*3, and *IPA1* in Rice Using a CRISPR/Cas9 System. *Frontiers in Plant Science* 7 (377): 1–13.

Liang M, Chen D, Lin M, Zheng Q, Huang Z, Lin Z, Zhao G (2014) Isolation and Characterization of Two DREB1 Genes Encoding Dehydration-Responsive Element Binding Proteins in Chicory (*Cichorium Intybus*). *Plant Growth Regulation* 73 (1): 45–55.

Lieber M (2010) The Mechanism of Double-Strand DNA Break Repair by the Nonhomologous DNA End-Joining Pathway. *Annual Review of Biochemistry* 79: 181–211.

Lin CS, Hsu CT, Yang LH, Lee LY, Fu JY, Cheng QW, Wu FH (2018) Application of Protoplast Technology to CRISPR/Cas9 Mutagenesis: From Single-Cell Mutation Detection to Mutant Plant Regeneration. *Plant Biotechnology Journal* 16 (7): 1295–1310.

Liu Q, Kasuga M, Sakuma Y, Abe H, Miura S, Yamaguchi-Shinozaki K, Shinozaki K (1998) Two Transcription Factors, DREB1 and DREB2, with an EREBP/AP2 DNA Binding Domain Separate Two Cellular Signal Transduction Pathways in Drought-and Low-Temperature-Responsive Gene Expression, Respectively, in *Arabidopsis*. *The Plant Cell* 10 (8): 1391–1406.

Liu Y, Dang P, Liu L, He C (2019) Cold Acclimation by the CBF–COR Pathway in a Changing Climate: Lessons from *Arabidopsis* Thaliana. *Plant Cell Reports* 38 (5): 511–519.

Livingston III D, Henson C (1998) Apoplastic Sugars, Fructans, Fructan Exohydrolase, and Invertase in Winter Oat: Responses to Second-Phase Cold Hardening. *Plant Physiol* 116: 403–408.

Magome H, Yamaguchi S, Hanada A, Kamiya Y, Oda K (2004) Dwarf and Delayed-Flowering 1, a Novel *Arabidopsis* Mutant Deficient in Gibberellin Biosynthesis Because of Overexpression of a Putative AP2 Transcription Factor. *Plant Journal* 37 (5): 720–729.

Makarova K, Wolf Y, Alkhnbashi O, Costa F, Shah S, Saunders S, Barrangou R (2015) An Updated Evolutionary Classification of CRISPR-Cas Systems. *Nature Reviews Microbiology* 13 (11): 722–736.

Mallikarjuna G, Mallikarjuna K, Reddy M, Kaul T (2011) Expression of OsDREB2A Transcription Factor Confers Enhanced Dehydration and Salt Stress Tolerance in Rice (*Oryza Sativa* L.). *Biotechnology Letters* 33 (8): 1689–1697.

Mancilla-Margalli N, Lopez M (2006) Water-Soluble Carbohydrates and Fructan Structure Patterns from Agave and Dasylirion Species. *Journal of Agricultural and Food Chemistry* 54 (20): 7832–7839.

Maroufi A, Karimi M, Mehdikhanlou K, De Loose M (2018) Inulin Chain Length Modification Using a Transgenic Approach Opening New Perspectives for Chicory. *3 Biotech* 8 (349): 1–8.

Márquez-López R, Loyola-Vargas V, Santiago-García P (2022) Interaction between Fructan Metabolism and Plant Growth Regulators. *Planta* 255 (49): 1–14.

Mathieu AS, Périlleux C, Jacquemin G, Renard ME, Lutts S, Quinet M (2020) Impact of Vernalization and Heat on Flowering Induction, Development and Fertility in Root Chicory (*Cichorium intybus* L. var. *sativum*). *Journal of Plant Physiology* 254: 153272.

Mathieu AS, Tinel C, Dailly H, Quinet M, Lutts S (2018) Impact of High Temperature on Sucrose Translocation, Sugar Content and Inulin Yield in Cichorium Intybus L. Var. Sativum. *Plant and Soil* 432 (1–2): 273–288.

McVey M, Khodaverdian V, Meyer D, Cerqueira P, Heyer WD (2016) Eukaryotic DNA Polymerases in Homologous Recombination. *Annual Review of Genetics* 23 (50) 393–421.

Meng X, Li L, De Clercq I, Narsai R, Xu Y, Hartmann A, Claros D, et al. (2019) ANAC017 Coordinates Organellar Functions and Stress Responses by Reprogramming Retrograde Signaling. *Plant Physiology* 180 (1): 634–653.

Michiels A, Van Laere A, Van den Ende W, Tucker M (2004) Expression Analysis of a Chicory Fructan 1-Exohydrolase Gene Reveals Complex Regulation by Cold. *Journal of Experimental Botany* 55 (401): 1325–1333.

Mizoi J, Ohori T, Moriwaki T, Kidokoro S, Todaka D, Maruyama K, Kusakabe K, Osakabe Y, Shinozaki K, Yamaguchi-Shinozaki K (2013) GmDREB2A;2, a Canonical DEHYDRATION-RESPONSIVE ELEMENT-BINDING PROTEIN2-Type Transcription Factor in Soybean, Is Posttranslationally Regulated and Mediates DEHYDRATION-RESPONSIVE ELEMENT-Dependent Gene Expression. *Plant Physiology* 161 (1): 346–361.

Mizoi J, Shinozaki K, Yamaguchi-Shinozaki K (2012) AP2/ERF Family Transcription Factors in Plant Abiotic Stress Responses. *Biochimica et Biophysica Acta - Gene Regulatory Mechanisms* 1819 (2): 86–96.

Mohammadi F, Naghavi M, Peighambari S, Khosravi Dehaghi N, Khaldari I, Bravi E, Marconi O, Perretti G (2021) Abscisic Acid Crosstalk with Auxin and Ethylene in Biosynthesis and Degradation of Inulin-Type Fructans in Chicory. *Plant Biology* 23 (4): 636–642.

Nagaraj V, Riedl R, Boller T, Wiemken A, Meyer A (2001). Light and Sugar Regulation of the Barley Sucrose: Fructan 6-Fructosyltransferase Promoter. *Journal of Plant Physiology* 158:1601–1607.

Nakano T, Suzuki K, Fujimura T, Shinshi H (2006) Genome-Wide Analysis of the ERF Gene Family in *Arabidopsis* and Rice. *Plant Physiology* 140 (2): 411–432.

Nakashima K, Tran LS, Van Nguyen D, Fujita M, Maruyama K, Todaka D, Ito Y, Hayashi N, Shinozaki K, Yamaguchi-Shinozaki K (2007) Functional Analysis of a NAC-Type Transcription Factor OsNAC6 Involved in Abiotic and Biotic Stress-Responsive Gene Expression in Rice. *Plant Journal* 51 (4): 617–630.

Narusaka Y, Nakashima K, Shinwari Z, Sakuma Y, Furihata T, Abe H, Narusaka M, Shinozaki K, Yamaguchi-Shinozaki K (2003) Interaction between Two Cis-Acting Elements, ABRE and DRE, in ABA-Dependent Expression of *Arabidopsis rd29A* Gene in Response to Dehydration and High-Salinity Stresses. *The Plant Journal* 34 (2): 137–148.

Nekrasov V, Wang C, Win J, Lanz C, Weigel D, Kamoun S (2017) Rapid Generation of a Transgene-Free Powdery Mildew Resistant Tomato by Genome Deletion. *Scientific Reports* 7 (482): 1–6.

Nemati F, Ghanati F, Gavlighi H, Sharifi M (2018) Fructan Dynamics and Antioxidant Capacity of 4-Day-Old Seedlings of Wheat (*Triticum Aestivum*) Cultivars during Drought Stress and Recovery. *Functional Plant Biology* 45 (5): 1000–1008.

Ng S, Ivanova A, Duncan O, Law S, Van Aken O, De Clercq I, Wang Y (2013) A Membrane-Bound NAC Transcription Factor, ANAC017, Mediates Mitochondrial Retrograde Signaling in *Arabidopsis*. *The Plant Cell* 25 (9): 3450–3471.

Ning W, Nobel P (1998) Phloem Transport of Fructans in the Crassulacean Acid Metabolism Species *Agave deserti*. *Plant Physiology* 116: 709–714.

Nizioł-Łukaszewska Z, Bujak T, Wasilewski T, Szmuc E (2019) Inulin as an Effectiveness and Safe Ingredient in Cosmetics. *Polish Journal of Chemical Technology* 21 (1): 44–49.

Nwafor I, Shale K, Achilonu M. 2017. Chemical Composition and Nutritive Benefits of Chicory (Cichorium Intybus) as an Ideal Complementary and/or Alternative Livestock Feed Supplement. *The Scientific World Journal* 2017 (7343928): 1–11.

Oh SK, Baek KH, Park J, Yi S, Yu S, Kamoun S, and Choi D (2008) Capsicum Annuum WRKY Protein CaWRKY1 Is a Negative Regulator of Pathogen Defense. *New Phytologist* 177 (4): 977–989.

Ohanenye I, Alamar M, Thompson A, Terry L (2019) Fructans Redistribution Prior to Sprouting in Stored Onion Bulbs Is a Potential Marker for Dormancy Break. *Postharvest Biology and Technology* 149 (2019): 221–234.

Olsen A, Ernst H, Leggio L, Skriver K (2005) DNA-Binding Specificity and Molecular Functions of NAC Transcription Factors. *Plant Science* 169 (2005): 785–797.

Park SI, Kwon H, Cho M, Song J, Kim BG, Baek JH, Kim S, et al. (2021) The *Oserf115*/*Ap2erebp110* Transcription Factor Is Involved in the Multiple Stress Tolerance to Heat and Drought in Rice Plants. *International Journal of Molecular Sciences* 22 (7181): 1–23.

Patella A, Scariolo F, Palumbo F, Barcaccia G (2019) Genetic Structure of Cultivated Varieties of Radicchio (*Cichorium Intybus* L.): A Comparison between F1 Hybrids and Synthetics. *Plants* 8 (213): 1–16.

Pérez-López A, Simpson J (2020) The Sweet Taste of Adapting to the Desert: Fructan Metabolism in Agave Species. *Frontiers in Plant Science* 11 (324): 1–5.

Puranik S, Sahu P, Srivastava P, Prasad M (2012) NAC Proteins: Regulation and Role in Stress Tolerance. *Trends in Plant Science* 17 (6): 369–381.

Qin F, Kakimoto M, Sakuma Y, Maruyama K, Osakabe Y, Tran LS, Shinozaki K, Yamaguchi-Shinozaki K (2007) Regulation and Functional Analysis of *ZmDREB2A* in Response to Drought and Heat Stresses in *Zea Mays* L. *The Plant Journal* 50 (2007): 54–69.

Ran F, Hsu P, Wright J, Agarwala V, Scott D, Zhang F (2013) Genome Engineering Using the CRISPR-Cas9 System. *Nature Protocols* 8 (11): 2281–2308.

Redondo-Cuenca A, Herrera-Vázquez S, Condezo-Hoyos L, Gómez-Ordóñez E, Rupérez P (2021) Inulin Extraction from Common Inulin-Containing Plant Sources. *Industrial Crops and Products* 170 (2021): 113726.

Rigui A , Carvalho V, Wendt dos Santos A, Morvan-Bertrand A, Prud'homme MP, Machado de Carvalho A, Gaspar M (2019) Fructan and Antioxidant Metabolisms in Plants of Lolium Perenne under Drought Are Modulated by Exogenous Nitric Oxide. *Plant Physiology and Biochemistry* 145 (2019): 205–215.

Rushton P, Somssich I, Ringler P, Shen Q (2010) WRKY Transcription Factors. *Trends in Plant Science* 15 (5): 247–258.

Sakuma Y, Liu Q, Dubouzet J, Abe H, Yamaguchi-Shinozaki K, Shinozaki K (2002) DNA-Binding Specificity of the ERF/AP2 Domain of *Arabidopsis* DREBs, Transcription Factors Involved in Dehydration- and Cold-Inducible Gene Expression. *Biochemical and Biophysical Research Communications* 290 (3): 998–1009.

Salinas C, Handford M, Pauly M, Dupree P, Cardemil L (2016) Structural Modifications of Fructans in *Aloe Barbadensis* Miller (Aloe Vera) Grown under Water Stress. *PLoS ONE* 11 (7): 1–24.

Shan Q, Wang Y, Li J, Zhang Y, Chen K, Liang Z, Zhang K (2013) Targeted Genome Modification of Crop Plants Using a CRISPR-Cas System. *Nature Biotechnology* 31 (8): 686–688.

Shi J, Gao H, Wang H, Lafitte H, Archibald R, Yang M, Hakimi S, Mo H, Habben J (2017) ARGOS8 Variants Generated by CRISPR-Cas9 Improve Maize Grain Yield under Field Drought Stress Conditions. *Plant Biotechnology Journal* 15 (2): 207–216.

Shi Y, Ding Y, Yang S (2018) Molecular Regulation of CBF Signaling in Cold Acclimation. *Trends in Plant Science* 23 (7): 623–637.

Shim Y, Lim C, Seong G, Choi Y, Kang K, Paek NC (2022) The AP2/ERF Transcription Factor LATE FLOWERING SEMI-DWARF Suppresses Long-Day-Dependent Repression of Flowering. *Plant Cell and Environment* 45 (8): 2446–2459.

Shinozaki K, Yamaguchi-Shinozaki K (2000) Molecular Responses to Dehydration and Low Temperature: Differences and Cross-Talk between Two Stress Signaling Pathways. *Current Opinion in Plant Biology* 3 (3): 217–223.

Shmakov S, Abudayyeh O, Makarova K, Wolf Y, Gootenberg J, Semenova E, Minakhin L (2015) Discovery and Functional Characterization of Diverse Class 2 CRISPR-Cas Systems. *Molecular Cell* 60 (3): 385–397.

Shoaib M, Shehzad A, Omar M, Rakha A, Raza H, Sharif H, Shakeel A, Ansari A, Niazi S (2016) Inulin: Properties, Health Benefits and Food Applications. *Carbohydrate Polymers* 147 (2016): 444–454.

Silva T, Vilhalva D, Moraes M, Figueiredo-Ribeiro R (2015) Anatomy and Fructan Distribution in Vegetative Organs of Dimerostemma Vestitum (Asteraceae) from the Campos Rupestres. *Anais Da Academia Brasileira de Ciencias* 87 (2): 797–812.

Singh RS, Singh T, Hassan M, Larroche C (2022) Biofuels from Inulin-Rich Feedstocks: A Comprehensive Review. *Bioresource Technology* 346 (2022): 126606.

Su J, Hu C, Yan C, Jin Y, Chen Z, Guan Q, Wang Y (2015) Expression of Barley SUSIBA2 Transcription Factor Yields High-Starch Low-Methane Rice. *Nature* 523 (7562): 602–606.

Sun C, Palmqvist S, Olsson H, Borén M, Ahlandsberg S, Jansson C (2003) A Novel WRKY Transcription Factor, SUSIBA2, Participates in Sugar Signaling in Barley by Binding to the Sugar-Responsive Elements of the Iso1 Promoter. *Plant Cell* 15 (9): 2076–2092.

Sun X, Zong Y, Yang S, Wang L, Gao J, Wang Y, Liu B, Zhang H (2020) A Fructan: The Fructan 1-Fructosyl-Transferase Gene from Helianthus Tuberosus Increased the PEG-Simulated Drought Stress Tolerance of Tobacco. *Hereditas* 157 (14): 1–8.

Tarkowski Ł, Van den Ende W (2015) Cold Tolerance Triggered by Soluble Sugars: A Multifaceted Countermeasure. *Frontiers in Plant Science* 6 (203): 1–7.

Tawfick M, Xie H, Zhao C, Shao P, Farag M (2022) Inulin Fructans in Diet: Role in Gut Homeostasis, Immunity, Health Outcomes and Potential Therapeutics. *International Journal of Biological Macromolecules* 208 (2022): 948–961.

Tran LS, Nakashima K, Sakuma Y, Simpson S, Fujita Y, Maruyama K, Fujita M, Seki M, Shinozaki K, Yamaguchi-Shinozaki K (2004) Isolation and Functional Analysis of *Arabidopsis* Stress-Inducible NAC Transcription Factors That Bind to a Drought-Responsive Cis-Element in the Early Responsive to Dehydration Stress 1 Promoter. *The Plant Cell* 16 (9): 2481–2498.

Tripodo G, Mandracchia D (2019) Inulin as a Multifaceted (Active)Substance and Its Chemical Functionalization: From Plant Extraction to Applications in Pharmacy, Cosmetics and Food. *European Journal of Pharmaceutics and Biopharmaceutics* 141 (2019): 21–36.

Valluru R, Lammens W, Claupein W, Van den Ende W (2008) Freezing Tolerance by Vesicle-Mediated Fructan Transport. *Trends in Plant Science* 13 (8): 409–414.

Van Arkel J, Vergauwen R, Sévenier R, Hakkert JC, Van Laere A, Bouwmeester HJ, Koops AJ, Van Der Meer IM (2012) Sink Filling, Inulin Metabolizing Enzymes and Carbohydrate Status in Field Grown Chicory (*Cichorium Intybus* L.). *Journal of Plant Physiology* 169 (15): 1520–1529.

Van den Ende W, Michiels A, Van Wonterghem D, Clerens SP, De Roover J (2001) Defoliation Induces Fructan 1-Exohydrolase II in Witloof Chicory Roots. Cloning and Purification of Two Isoforms, Fructan 1-Exohydrolase IIa and Fructan 1-Exohydrolase IIb. Mass Fingerprint of the Fructan 1-Exohydrolase II Enzymes 1. *Plant Physiology* 126:1186–1195.

Van den Ende W, Michiels A, De Roover J, Verhaert, Van Laere A (2000) Cloning and Functional Analysis of Chicory Root Fructan 1-Exohydrolase I (1-FEH I): A Vacuolar Enzyme Derived from a Cell-Wall Invertase Ancestor? Mass Fingerprint of the 1-FEH I Enzyme. *The Plant Journal* 24 (4): 447–456.

Van Laere A, Van den Ende W (2002) Inulin Metabolism in Dicots: Chicory as a Model System. *Plant, Cell and Environment* 25 (6): 803–813.

Van Rensburg H, Takács Z, Freynschlag F, Öner E, Jonak C, Van den Ende W (2020) Fructans Prime ROS Dynamics and Botrytis Cinerea Resistance in *Arabidopsis*. *Antioxidants* 9 (805): 1–22.

Versluys M, Kirtel O, Öner E, Van den Ende W (2018) The Fructan Syndrome: Evolutionary Aspects and Common Themes among Plants and Microbes. *Plant Cell and Environment* 41 (1): 16–38.

Versluys M, Öner E, Van den Ende W (2022) Fructan Oligosaccharide Priming Alters Apoplastic Sugar Dynamics and Improves Resistance against Botrytis Cinerea in Chicory. *Journal of Experimental Botany* 73.

Wang X, Niu Y, Zheng Y (2021) Multiple Functions of Myb Transcription Factors in Abiotic Stress Responses. *International Journal of Molecular Sciences* 22 (6125): 1–4.

Wang Y, Cheng X, Shan Q, Zhang Y, Liu J, Gao C, Qiu JL (2014) Simultaneous Editing of Three Homoeoalleles in Hexaploid Bread Wheat Confers Heritable Resistance to Powdery Mildew. *Nature Biotechnology* 32 (9): 947–951.

Wang Y, Du F, Wang J, Wang K, Tian C, Qi X, Lu F, Liu X, Ye X, Jiao Y (2022) Improving Bread Wheat Yield through Modulating an Unselected AP2/ERF Gene. *Nature Plants* 8 (8): 930–939.

Wie H, Zhao H, Su T, Bausewein A, Greiner S, Harms K, Rausch T (2017a) Chicory R2R3-MYB Transcription Factors CiMYB5 and CiMYB3 Regulate Fructan 1-Exohydrolase Expression in Response to Abiotic Stress and Hormonal Cues. *Journal of Experimental Botany* 68 (15): 4323–4338.

Wei H, Bausewein A, Greiner S, Dauchot N, Harms K, Rausch T (2017b) CiMYB17, a Stress-Induced Chicory R2R3-MYB Transcription Factor, Activates Promoters of Genes Involved in Fructan Synthesis and Degradation. *New Phytologist* 215 (1): 281–298.

Wie H, Bausewein A, Steininger H, Su T, Zhao H, Harms K, Greiner S, Rausch T (2016) Linking Expression of Fructan Active Enzymes, Cell Wall Invertases and Sucrose Transporters with Fructan Profiles in Growing Taproot of Chicory (Cichorium Intybus): Impact of Hormonal and Environmental Cues. *Frontiers in Plant Science* 7 (1806): 1–15.

Woo J, Kim J, Kwon S, Corvalán C, Cho S, Kim H, Kim SG, Kim ST, Choe S, Kim JS (2015) DNA-Free Genome Editing in Plants with Preassembled CRISPR-Cas9 Ribonucleoproteins. *Nature Biotechnology* 33 (11): 1162–1164.

Xie Z, Yang C, Liu S, Li M, Gu L, Peng X, Zhang Z (2022) Identification of AP2/ERF Transcription Factors in *Tetrastigma hemsleyanum* Revealed the Specific Roles of ERF46 under Cold Stress. *Frontiers in Plant Science* 13 (936602): 1–14.

Xu R, Yang Y, Qin R, Li H, Qiu C, Li L, Wei P, Yang J (2016) Rapid Improvement of Grain Weight via Highly Efficient CRISPR/Cas9-Mediated Multiplex Genome Editing in Rice. *Journal of Genetics and Genomics* 43 (2016) 529–532.

Xu Y, Zhang W, Ju C, Li Y, Yang J, Zhang J (2016) Involvement of Abscisic Acid in Fructan Hydrolysis and Starch Biosynthesis in Wheat under Soil Drying. *Plant Growth Regulation* 80 (3): 265–279.

Xu Z, Gong B, Wang C, Xue F, Zhang H, Ji W (2015) Wheat NAC Transcription Factor TaNAC29 Is Involved in Response to Salt Stress. *Plant Physiology and Biochemistry* 96 (11): 356–363.

Xue GP, Kooiker M, Drenth J, McIntyre C (2011) TaMYB13 Is a Transcriptional Activator of Fructosyltransferase Genes Involved in β-2,6-Linked Fructan Synthesis in Wheat. *Plant Journal* 68 (5): 857–870.

Yang A, Dai X, Zhang WH (2012) A R2R3-Type MYB Gene, OsMYB2, Is Involved in Salt, Cold, and Dehydration Tolerance in Rice. *Journal of Experimental Botany* 63 (7): 2541–2556.

Yang J, Zhang J, Wang Z, Zhu Q, Liu L (2004) Activities of Fructan- and Sucrose-Metabolizing Enzymes in Wheat Stems Subjected to Water Stress during Grain Filling. *Planta* 220 (2): 331–343.

Yoshida M (2021) Fructan Structure and Metabolism in Overwintering Plants. *Plants* 10 (933): 1–11.

Yu Y, Yu M, Zhang S, Song T, Zhang M, Zhou H, Wang Y, Xiang J, Zhang X (2022) Transcriptomic Identification of Wheat AP2/ERF Transcription Factors and Functional Characterization of *TaERF-6-3A* in Response to Drought and Salinity Stresses. *International Journal of Molecular Sciences* 23 (3272): 1–9.

Zahra N, Hafeez M, Ghaffar A, Kausar A, Zeidi M, Siddique K, Farooq M (2023) Plant Photosynthesis under Heat Stress: Effects and Management. *Environmental and Experimental Botany* 206 (2023): 105178.

Zhai Y, Fan Z, Cui Y, Gu X, Chen S, Ma H (2022) APETALA2/Ethylene Responsive Factor in Fruit Ripening: Roles, Interactions and Expression Regulation. *Frontiers in Plant Science* 13:979348.

Zhang J, Dell B, Ma W, Vergauwen R, Zhang X, Oteri T, Foreman A, Laird D, Van den Ende W (2016) Contributions of Root WSC during Grain Filling in Wheat under Drought. *Frontiers in Plant Science* 7 (904): 1–11.

Zhang J, Xu Y, Chen W, Dell B, Vergauwen R, Biddulph B, Khan N, Luo H, Appels R, Van den Ende W (2015) A Wheat 1-FEH W3 Variant Underlies Enzyme Activity for Stem WSC Remobilization to Grain under Drought. *New Phytologist* 205 (1): 293–305.

Zhang P, Liu Y, Li M, Ma J, Wang C, Su J, Yang D (2020) Abscisic Acid Associated with Key Enzymes and Genes Involving in Dynamic Flux of Water Soluble Carbohydrates in Wheat Peduncle under Terminal Drought Stress. *Plant Physiology and Biochemistry* 151 (6): 719–728.

Zhang Y, Iaffaldano B, Qi Y (2021) CRISPR Ribonucleoprotein-Mediated Genetic Engineering in Plants. *Plant Communications* 2 (100168): 1–13.

Zhang Z, Dong J, Ji C, Wu Y, Messing J (2019) NAC-Type Transcription Factors Regulate Accumulation of Starch and Protein in Maize Seeds. *Proceedings of the National Academy of Sciences of the United States of America* 166 (23): 1–6.

Zhao Y, Antoniou-kourounioti R, Calder G, Dean C, Howard M (2020) Temperature-Dependent Growth Contributes to Long-Term Cold Sensing. *Nature* 583:825–829.

9 Acknowledgements

I would like to express my heartfelt gratitude to all the people who have supported me in completing this thesis. Without their guidance, encouragement, and help, this would not have been possible.

First and foremost, I would like to extend my sincerest thanks to my supervisor and mentor, Prof. Dr. Thomas Rausch, who recruited me as a PhD student and provided me with invaluable supports throughout my research. He gave me the freedom to pursue my research interests and provided cares and attentions when I needed it the most. I am deeply grateful for his unwavering supports and guidance. I would also like to acknowledge the supports of the Thesis Advisory Committee (TAC) members, Prof. Dr. Rüdiger Hell, Prof. Dr. Michael Wink and Dr. Steffen Greiner, with the annual meetings and the valuable advices, shaping the direction of my research and thesis.

I would also like to express my gratitude to all the members from AG Rausch and AG Greb for their help in the experiments. Special thanks to Dr. Steffen Greiner for his scientific and mental supports. He helped me revise my thesis and provided invaluable insights and encouragement. My heartfelt thanks to Cornelia Walter for her exceptional assistances with plant tissue culture, and Dr. Hongbin Wei for laying the foundation of my project with his previous work. I would also like to thank my good friends, Dr. Roland Gromes, Dr. Ketja Machemer-Noonan and Dr. Wan Zhang for the friendships and supports throughout my research journey. Kiara Käufer, my best lab mate, offered me tremendous companionship and encouragement.

Lastly, I would like to thank my parents and other family members for the countless supports. Especially my husband, Justus Hesse-Zhong, who is my best friend and favorite person in the world. I cannot thank him enough for being there for me. He has always taken care of me and given me support and endless love.